Tuttle SG, Pfützner CJ, Loegel TN, Fisher BT, Leska IA, and Hinnant KM. 2019. In-Situ Burn Testing of California Crude Oils. Naval Research Laboratory. (Bureau of Safety and Environmental Enforcement Project #1085)

Bureau of Safety and Environmental Enforcement (BSEE) Report: In-Situ Burn Testing of California Crude Oils

Steven G. Tuttle, Christopher J. Pfützner, Thomas N. Loegel, Brian T. Fisher, Iwona A. Leska, Katherine M. Hinnant

REPORT DOCUMENTATION PAGE

Form Approved
OMB No. 0704-0188

1. REPORT DATE *(DD-MM-YYYY)*	**2. REPORT TYPE**	**3. DATES COVERED** *(From -To)*
	Memorandum Report	10/01/2016 – 04/01/2019

4. TITLE AND SUBTITLE
In-Situ Burn Testing of California Crude Oils

5a. CONTRACT NUMBER
0040301894

5b. GRANT NUMBER
E16PG00038

5c. PROGRAM ELEMENT NUMBER

6. AUTHOR(S)
Steven G. Tuttle, Christopher J. Pfützner, Thomas N. Loegel, Brian T. Fisher, Iwona A. Leska, Katherine M. Hinnant

5d. PROJECT NUMBER
61-4817-075

5e. TASK NUMBER

5f. WORK UNIT NUMBER
4817

7. PERFORMING ORGANIZATION NAME(S) AND ADDRESS(ES)

Naval Research Laboratory
4555 Overlook Avenue, SW
Washington, DC , 20375-5320

8. PERFORMING ORGANIZATION REPORT NUMBER
NRL/MR/6180-14-XXXX

9. SPONSORING / MONITORING AGENCY NAME(S) AND ADDRESS(ES)

Bureau of Safety & Environmental Enforcement
45600 Woodland Road, VAE-AMD
Sterling VA 20166

10. SPONSOR/MONITOR'S ACRONYM(S)
MIS-NONDOD

11. SPONSOR/MONITOR'S REPORT NUMBER(S)

12. DISTRIBUTION / AVAILABILITY STATEMENT

Approved for public release; distribution is unlimited.

13. SUPPLEMENTARY NOTES

14. ABSTRACT

In situ burning (ISB) is a well-established method to rapidly dispose of crude oil during an oil spill at sea. Oil is mechanically or chemically herded into thick slicks and ignited. Since each oil has distinct chemical and physical properties, each will emulsify differently from wave turbulence and weather from evaporation and photochemical reaction. Oil spill responders need to understand how much emulsification and weathering an oil can undergo and still be ignited for ISB to be a practical remediation strategy. Two experimental platforms have been developed and a range of chemical analytics have been applied to examine the ignition, flammability, heat release rates, and their dependence on oil constituents for a selection of California crude oils.

15. SUBJECT TERMS
Crude oil, spray, atomization, combustion, flame, phase Doppler interferometry, flow-blurring atomizer

16. SECURITY CLASSIFICATION OF:			**17. LIMITATION OF ABSTRACT**	**18. NUMBER OF PAGES**	**19a. NAME OF RESPONSIBLE PERSON**
a. REPORT	**b. ABSTRACT**	**c. THIS PAGE**	Unlimited Unclassified		**19b. TELEPHONE NUMBER** *(include area code)*
UNCLASSIFIED	UNCLASSIFIED	UNCLASSIFIED			

Standard Form 298 (Rev. 8-98)
Prescribed by ANSI Std. Z39.18

Naval Research Laboratory
Washington, DC 20375-5320

IN-SITU BURN TESTING OF CALIFORNIA CRUDE OILS

Steven G. Tuttle
Christopher J. Pfützner
Thomas N. Loegel
Brian T. Fisher
Katherine M. Hinnant

Navy Technology Center for Safety and Survivability
Chemistry Division

Iwona A. Leska

Nova Research, Inc.

This study was funded by the U.S. Department of the Interior, Bureau of Safety and Environmental Enforcement through Interagency Agreement E16PG00038 with the Naval Research Laboratory.

CONTENTS

FIGURES

TABLES

EXECUTIVE SUMMARY

Two experimental platforms have been developed and chemical analytics have been applied to examine the ignition, flammability, heat release rates, and their dependence on oil constituents for a selection of California crude oils that were extracted from the Santa Barbara Channel. The first experimental platform, designed to simulate the thermal characteristics of a slick on the ocean, was an actively cooled, 1 m^2, square pan to examine ignition behavior at near-realistic geometric scales. A 76 m-long coil of copper tubing rested in water under a 10 mm-thick layer of crude oil. The coolant temperature was constantly cooled by a 10 kW circulating chiller. Thermocouples in the water and at the oil-water interface measured temperature while heat flux gages measured the radiative heat flux from the flames. Ignition was carried out directly or by igniting a liter of gelled diesel fuel on the surface. The ignition method, actively cooled water pool, and burn environment provided a conservative ignitability test to determine the feasibility of in situ burning for any particular crude oil. The second experimental platform, designed to mimic realistic ignition conditions on a cone calorimeter platform, was an actively cooled, 10 cm diameter, 10 mm deep pan to measure ignition behavior, burn efficiency, and heat release rate and their dependence on weathering and emulsification. The pan was surrounded by a water jacket to provide active cooling to mimic heat transfer to ocean water. The cone calorimeter architecture provided a controlled environment to determine how much heat must be transferred to an emulsified oil slick for it to adequately break and release flammable vapors before ignition. Two suites of chemical analytics were performed in association with the flammability testing. The first was saturate-aromatic-resin-asphaltene (SARA) separation to determine the fraction and characteristics of the base crude oil constituents. The SARA analysis provides a comparative characterization of crude oil chemistry that provides insight into the weathering, emulsification, ignition, and burn behavior. The second tests were mass spectrometry analysis of the crude oil residuals from the burn pan tests to determine the residual constituents. These characterize the chemistry of the residual crude oil and provide insight into how weathering and combustion changed the mass distribution of the oil and the potential biological and ecological impacts that the residual crude may have at the surface, in the water column, and at the shore.

The combination of the ignition tests and chemical analysis has revealed that crude oils that previous studies suggested were non-flammable can be ignited and burned. A careful examination of the ignition methods of this and previous studies, as well as anecdotal evidence from oil spills, reveals that field methods for slick ignition have produced much larger surface heat transfer rates than those used in laboratory ignition tests. This discrepancy suggests that both more realistic conditions and standardized fire ignition testing methods should be routinely applied to determine oil ignitability.

IN-SITU BURN TESTING OF CALIFORNIA CRUDE OILS

INTRODUCTION

In situ burning (ISB) has become an accepted oil spill response method by many government agencies to dispose of crude oil slicks before they drift into sensitive coastal ecosystems and fisheries [1]. There are a number of difficulties with executing ISB. The first challenge is to mechanically move or chemically herd the oil into a sufficiently thick slick that the heat transfer to the ocean will not slow or stop hydrocarbon evaporation and extinguish the flames. Another challenge is driven by either surface wave shear on the surface or by water-column shear as benthic spills rise to the surface that mixes the crude oil with seawater and forms emulsions of the two that are difficult or impractical to ignite. A final challenge of ISB occurs at the end of a burn, when residues remain that are light enough to float but too heavy to ignite easily.

Crude oil undergoes a number of changes once it has spilled and interacts with the marine environment. As it spreads across the ocean surface, the increased surface area accelerates the evaporation of lightweight hydrocarbons by evaporative weathering [2], exposure to sunlight and air drives photochemical reactions [3,4] that oxidizes compounds such as thiols (photochemical weathering), microbes begin to digest hydrocarbons at the interface of seawater and the slick or oil micelles [5-10], and wave turbulence emulsifies the crude oil with saltwater [11]. All of these processes change the oil's physical, thermodynamic, and chemical properties. The emulsified crude and heavier fractions require additional thermal energy to break and evaporate, respectively, prior to ignition.

S.L. Ross Environmental Research, Ltd. conducted a number of tests on the suitability of ISB for California and other crude oils, which were then reported by McCourt *et al.* [12-15]. They determined a weathering rate correlation and the emulsion stability by using standard methods [16]. Burn tests were conducted in a wave tank with water temperatures maintained at 20 °C. 2.5 L of oil or emulsion rested on the water and was contained by a 40 cm-diameter steel ring to form a 2 cm-thick slick. Gelled gasoline (40 to 50 g) accelerated the ignition process. From their tests, they concluded that heavy crude oils, such as Santa Ynez, were non-flammable if emulsified, while others were non-flammable if weathered and emulsified.

From the description by McCourt *et al.* [12-15], there were aspects of the testing that merited deeper examination and a repetition of some of the experiments. First, we were concerned with the changes of the crude oil properties since these oils were last studied by McCourt *et al.* [12-15] and cataloged by Jokuty *et al.* [17] during the 1990s. We were also concerned that there was no metric used to indicate emulsion stability, since crude oil emulsions, in general, will begin separate almost immediately, depending on the emulsification process and will separate eventually given enough time. Finally, we considered that the slick size and accelerant quantity was not representative of practical ISB conditions. In practice, it is assumed that the minimum acceptable oil slick thickness for ignition is 10 mm [18], while the slick size can be 5 m or more in diameter. Furthermore, the current practice is to use 4 L of gelled diesel fuel to ignite a slick, which is approximately 4 kg of accelerant, or two orders of magnitude greater than that used by McCourt *et al.* [12-15] in their studies. If we assume that the accelerant and slick have a similar thickness, then a 4 L accelerant pool area is 0.40 m^2 and has a nominal diameter of 70 cm, which was much larger than the 40 cm oil slick reported by McCourt *et al.* [12-15].

The work by Garo *et al.* [19] showed that the heat flux to the surface of a pool fire was nominally proportional to the square root of the diameter ($\dot{q}" \propto d^{1/2}$). Applying this relationship to compare the accelerant combustion heat fluxes, the heat flux from the McCourt *et al.* [12-15] accelerant quantities was 32% of that produced by the nominal 4 L accelerant pool used in practice. Since the heat flux back to the

slick was what drove ignition and continued combustion, such a large difference suggests that the pool fire tests should be repeated with both larger slick areas and greater volumes of accelerant to establish whether an oil can be ignited or not.

OBJECTIVE

The objective of this work was to determine the ignition and burning behavior of neat, weathered, and emulsified variants of several California crude oils from the Santa Barbara Channel to determine applicability and window of opportunity of *in-situ* burning for oil spill response planning by using both a practical pool fire experiment and cone calorimetry. Conduct Saturate-Aromatic-Resin-Asphaltene (SARA) and other chemical analysis of the oils to determine their constituents and chemical "fingerprint" for future matching of potential surfactants to break emulsions to improve ignitability. The pool fire experiments determined the ignitability in practical conditions while cone calorimetry provided comparative ignition, heat release rates, and burn efficiencies for a range of crude oil blends in controlled laboratory conditions [20].

APPROACH

This section describes three different experimental methods used in this effort as well as details of the crude oils and methods to emulsify and weather the crude oils. All of the five crude oils examined in this study were from offshore wells along the Santa Barbara Channel from the coast of California, as shown in Table 1. They range from lightweight crude, such as Carpinteria, to heavy crude, such as Santa Ynez.

Crude Oils and Sample Preparation

The final test matrix called for each oil to be tested at six different conditions. First, the oil was tested neat, as extracted from the barrels. Then, the neat, fresh oil was emulsified with 40% substitute ocean water [21]. Each oil was then weathered for 48 hours and tested neat and then emulsified with 20%, 40%, and then 60% substitute ocean water. The ignition and burn test suite was composed of three replicates of six oil conditions for each of the five crude oils, for a maximum total of ninety separate tests.

1. Fresh-neat
2. Fresh-emulsified by 40% synthetic ocean water
3. Weathered 48 hours-neat
4. Weathered 48 hours-emulsified by 20% synthetic ocean water
5. Weathered 48 hours-emulsified by 40% synthetic ocean water
6. Weathered 48 hours-emulsified by 60% synthetic ocean water

Table 1 lists the crude oils with their respective properties and sources used in this study. Some of the properties were from the oil catalogue written by Jokuty *et al.* [17]. We also measured the API to quantify how the oil changed since the original data were compiled and to better understand our results. For some of the oils, there were no appreciable changes, but for the Santa Clara and Point Arguello, the properties have changed significantly, which further motivated us to re-examine their ISB behavior. It should be noted that the Santa Clara contains an emulsion breaker and heavy oil flow improver, Nalco Flow 12021A. According to the safety documentation, it is a flow improver and contains a hydrocarbon volatiles. Carpinteria also contains an emulsion breaker, TerraChem EB596, which contains similar components to Flow 12021A.

Table 1-Crude oils tested in this investigation and their properties as reported by [1]Jokuty *et al.*[17] and measured by the [2]authors. All were from the Santa Barbara Channel, California.

Crude Oil, Field	Nom.	API[1] (°)	Visc-osity[1] (cP) @ 15 °C	Asphalt-ene[1] (%mass)	API[2] (°)	API[2] (°) 48 hr	Visc-osity[2] (cP) @ 15 °C	Platforms
Santa Ynez, Hondo Monterey	SY	19.6	735	12	19.4	14.1	1,140	Heritage, Harmony, Hondo
Sockeye	SK	19.8	550	13	20.0	15.6	924	Gail
Santa Clara	SC	22.1	304	13	33.4	22.3	30	Grace
Point Arguello	PA	21.4	533	16	16.2	14.5	14,500	Hidalgo, Harvest, Hermosa
Carpinteria	CA	22.9	164	9	24.0	17.0	132	Hogan, Houchin, Henry

We designed the cone calorimetry and the pan fire experiments to mimic ocean conditions along the Santa Barbara channel during the month of August, when ocean temperatures, air temperatures, and hours of cloudless sunlight would be at the maximum. Such conditions maximize evaporative, photochemical, and biological weathering to provide a conservative baseline to compare ignition and flammability behavior. Weather and ocean data was compiled and averaged (Table 2) from NOAA buoy data that were posted online [22]. From these data, we determined the underlying water temperature and conditions for weathering and burn testing.

Table 2-Averages for the month of August as compiled from buoy 46053 in the Santa Barbara Channel.

Wind Speed (m/s)	Wind Direction (°)	Water Temp. (°C)	Salinity (g/Kg)	Current Speed (m/s)	Current Direction (°)
4.4	226	19.7	33	0.16	147

Emulsification

Crude oil was emulsified by placing the neat crude oil, substitute ocean water, and a commercial surfactant (Span® 85) in a vessel and mixing it using a high-shear mixer for laboratory experiments and a drill press and high-shear paint mixer for the pan tests. The surfactant fraction was 2% by volume, unless otherwise noted. The components were mixed until the emulsion could remain stable for two hours. This follows a similar process used in previous work [20,23,24]. Only 2% of the surfactant was used in an effort to minimize its influence on the ignition chemistry and evaporative thermodynamics. No other characteristic quantities of the emulsion were measured.

Though here are conventions for measuring emulsion behavior in the literature [17,25], they are used with 1:20 oil-water mixtures and the water content, viscosity, and dynamic (or complex) modulus is measured to determine the emulsion stability. The method appears to be designed to determine how well an oil will emulsify and disperse into the water column as opposed to measuring how a crude oil-seawater

emulsion behaves at the ocean surface. The critical behavior of the undispersed crude oil at the surface is how it will continue to emulsify as it evaporatively, photochemically, and biologically weathers.

In this study, we examined the ignition behavior of a largely intact slick with much larger oil fractions than 20:1. In such conditions, we suspected that the micelle size distribution and thermal stability over time are critical emulsion properties that influence crude oil ignition and combustion and that these can be related to the polarity, viscosity, and chemical constituents of the crude oil in question. Constant wave motion, dispersants, and microbial-formed surfactants work together to form emulsions in actual spills but it is not clear how these influence both the micelle size distribution and emulsion static or thermal stability. At this time, we have not developed measurement methods that relate the aforementioned oil and emulsion properties to ISB ignition behavior.

Weathering

Realistic crude oil weathering was impossible to completely replicate in a laboratory without the same influence of wind, temperature, humidity, sunlight, and biology on the crude oil. Instead, we focused on the evaporative weathering process, which can be easily replicated in a laboratory. Initial weathering mass loss predictions were made using the NOAA-supplied ADIOS software for a period of 48 hours from the time of an oil spill in a field setting [26]. Though ADIOS is an industry-accepted tool, we were concerned that the changes in the oil properties (see Table 1) made an accurate prediction impossible. Therefore, we wished to experimentally establish a weathering relationship.

We followed the laboratory procedure described in Jokuty *et al.* [17]. We filled 139-mm-diameter petri dishes with 20 g of crude oil and placed them in a ventilated, temperature-controlled hood. Initial measurements of the petri dish oil, and then subsequent measurements, tracked the mass loss over time. Air speed and temperature were measured with a thermoanemometer (Cole-Parmer EW-20250-16, Digi-Sense Hot Wire Thermoanemometer with NIST-Traceable Calibration). Average air speed was (0.2 ± 0.05) m/s and temperature remained around (22 ± 1) °C. We were concerned with replicating the wind speed, but we noticed that the weathering correlations in Jokuty *et al.* [17] accounted for the temperature but not the wind speed, suggesting that it was a negligible factor in the weathering process, which corresponds with the data presented by Fingas [2]. Such weathering does not produce any of the photochemical changes that occur when oil is exposed to ultraviolet radiation [4] that may influence emulsification. Photochemical reactions frequently form oxide groups on some hydrocarbon molecules, which make them more polar and thus more likely to act as surfactants.

Figure 1shows the weathering data for the five crude oils over a little more than three days, with the associated polynomial-logarithmic fits. The ADIOS predictions were close for the Carpinteria, Santa Ynez, and especially the Point Arguello, which was nearly coincident with the corresponding data. In contrast, the ADIOS predictions were very different for the Santa Clara and the Sockeye. Because we only examined a single temperature, we used a logarithmic, polynomial curve fit of the form:

$$\delta \mathrm{m} = \mathrm{a}_3(\ln(t))^3 + \mathrm{a}_2(\ln(t))^2 + \mathrm{a}_1 \ln(t) + \mathrm{a}_0 \quad (1)$$

where δm is the normalized mass loss, a_n is the polynomial coefficient, and t is time in units of hours. The corresponding weathering mass loss fractions used in this study, to replicate 48 hours of weathering, is shown in Table 3.

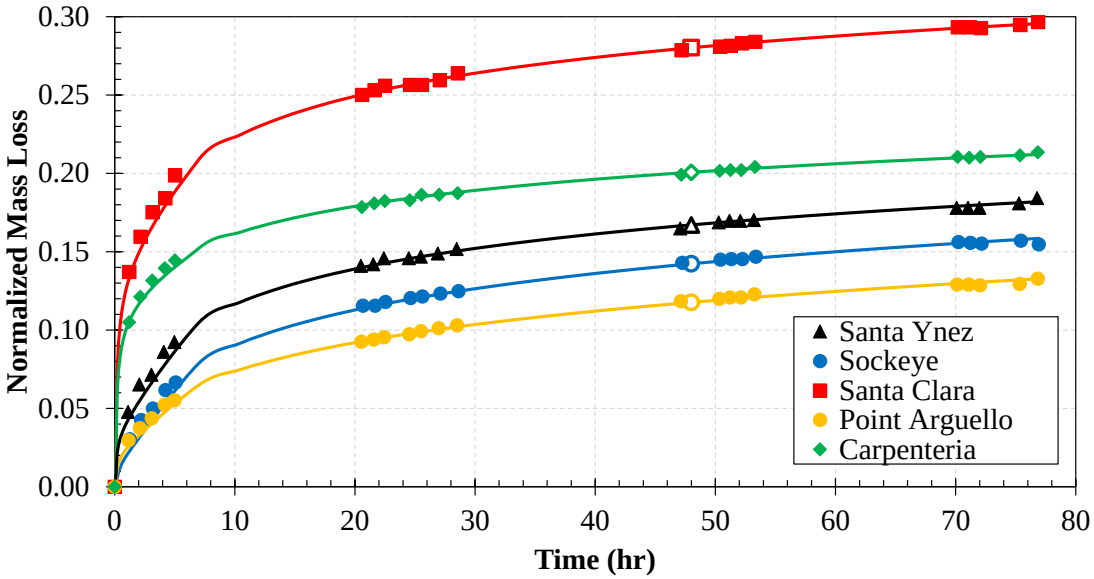

Fig. 1-Weathering data for the five crude oils with polynomial-logarithmic fits. Mass loss corresponding to 48 hours is denoted by a hollow marker.

Table 3-Percent mass loss for each crude oil after 48 hours of weathering.

Santa Ynez	Sockeye	Santa Clara	Point Arguello	Carpinteria
16.7%	14.2%	28.0%	11.8%	20.1%

With the mass loss fractions established, we then artificially weathered tens of liters of crude oil for test samples. The laboratory weathering method described by Jokuty *et al.* [17] calls for a rotary evaporator immersed in a bath of water at 80 °C, with the flask constantly ventilated with air to remove the evaporated oil fractions. In order to replicate the same physical process, a 10-gallon container was placed under a hood and slowly mixed by a drill press while belt heaters raised the oil temperature. Unfortunately, crude oil samples were not retained from the 48 hr time for baseline mass spectrometry comparisons.

Cone Calorimetry

The cone calorimetry experiments used a Fire Testing Technology instrument to measure ignition, flame spread, heat release rate, smoke release rate, products, and oxygen consumption calorimetry [27,28]. Typically, these tests are conducted by placing a coupon of a solid material, such as those that are found in consumer products and buildings, on a load cell under a coiled heater element that radiates the sample at a fixed heat flux until the sample ignites and burns. A test starts when a shutter separating the sample from the heater coil opens and allows the full heat flux to radiate to the sample. To aid ignition, two electrodes suspended over the sample produce a steady arc that ignites flammable vapor and air. Ignition occurs when there is a steady stream of flammable vapor produced by the sample. Once there is steady combustion, the two electrodes are removed. Such instruments are generally not used with liquids since they tend to boil and create an uncontrolled, uncontained burn. In the case of a crude oil slick on water, such a test heats the oil to above the boiling temperature of the water, creating boiling at the water-oil interface that is creates a boilover phenomenon that is equally uncontrollable and uncontained when the underlying water boils [29-32]. The boilover phenomena usually is associated with industrial fires of storage tanks filled with oil, that

have water underlying the oil. In the case of a fire, the oil temperature is heated above the boiling temperature of the underlying water, causing the water to rapidly evaporate and atomize the oil above. The same process can occur in crude oil fire testing if there is underlying water. We have also observed a similar, violent fire behavior for a fuel fire without underlying water when the liquid fuel starts to boil.

To prevent boilover from underlying water and maintain the water temperature at 19.7 °C, a sample burn pan was adapted from the work of van Gelderen *et al.* [33], as shown in Figure 2. Cooling water flows into and out of a jacket surrounding the liquid crude oil sample, through a chiller, and back to the sample pan. The lack of boilover from underlying water is actually more similar to actual ISB where boilover has never actually been observed. In this study, boilover is prevented by separating the water and oil and by imposing a near-constant temperature.

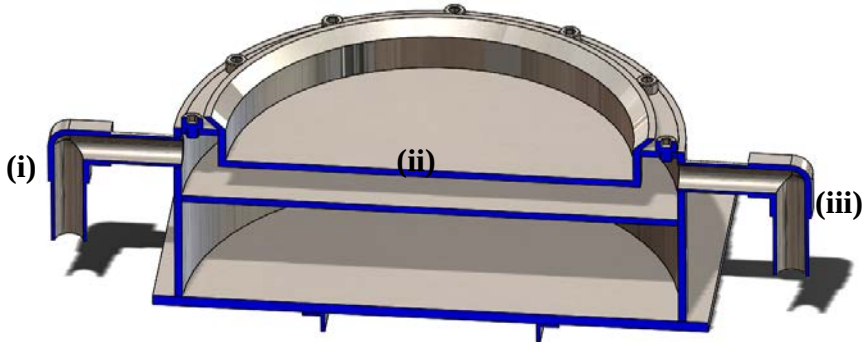

Fig. 2-Cross-section of the cone calorimeter burn pan. Cooling water flows in (i) from the chiller, under the burn sample pan (ii), and returns out (iii) to the chiller.

The test procedure is no different for a liquid sample as it is for a solid sample, with some differences. First, we need to calculate an imposed heat flux that reasonably mimicked that of a gelled fuel accelerant. Furthermore, while solid fuel samples may leave a char, crude oil samples may leave a range of different residues. Heavier crudes may leave a resinous disk with a top layer of char and an under layer of heavy oil. Lighter oils, which more easily transfer heat in the water jacket, leave a thick, resinous, or tar-like residue. Emulsions generally leave a liquid oil reside with an underlying water layer. In both cases with liquid residue, as the sample evaporates and thins, the more heat transfer to the cooled pan quenches the evaporation process and extinguishes the flames.

We calculated the imposed calorimeter heat transfer to approximate the heat transfer from a 4 L pool of accelerant spread over a slick 10 mm thick. Using a 3% transfer fraction, an assumption of 1500 K peak plume temperature, and the relation by Garo *et al.* [19], the radiative heat flux back to the slick is 16.3 kW/m^2. For simplicity and conservatism, we assumed that 15 kW/m^2 was the activating heat flux to the slick from the accelerant and used this value as the imposed cone heat flux.

This experiment mimics, in a controlled environment, some of the aspects of the ignition process but the entire burn process that crude oil may undergo during ISB may actually be quite different. First, as we mentioned previously, an actual burning slick may be much larger, such that the peak heat transfer back to the slick may be many times greater than the sum of the imposed 15 kW/m^2 and that of the small scale flames. As a result, the oil evaporation rates and extinction processes we observed in this experiment are more constrained. Furthermore, a 10 mm slick is a minimum recommend thickness. In practice, a much greater slick thickness is preferred and can be maintained as a boom is pulled through a spill. The work by

Van Gelderen [34] and Van Gelderen *et al.* [33,35] highlights some of the dominating influences of both heat flux and slick thickness during ISB.

In Situ Burn Pan

The pan fire experiments conservatively replicated the environmental and thermodynamic conditions of the crude oil slick on the ocean surface. The experiment was composed of a 1 m^2-square burn pan, 30.5 cm deep (Figure 3). Water was filled up to 24.5 cm, with a heat exchanger coil reaching 1 cm below the water surface. The heat exchanger coil was 12.7 mm-diameter copper tubing and approximately 76 m in length. Coils were separated by aluminum u-channel and compressed by stainless steel hose clamps. A ThermoFlex 10000 air-cooled recirculating chiller cycles water through the heat exchanger to maintain the bulk water temperature at 19.7 °C.

Fig. 3-1 m^2-square burn pan with heat exchanger coils and thermocouples installed.

Temperatures and heat fluxes were measured simultaneously during burn testing. Two thermocouples measured the water temperature 14 cm below the surface. Another four measured temperatures at the water-slick interface. Initially, two Medtherm 64-2SB-20 Schmidt-Boelter heat flux transducers were placed 80 cm from the inside edge of the pan, 20 cm above the oil surface. The original transducers were replaced with two Medtherm 64-10F-20SB/SW-1C-150 Schmidt-Boelter, fast-response (50 ms) heat flux transducers with 1 mm-thick sapphire windows with a viewing angle of 150º to accommodate the higher heat fluxes and allow more rapid cleaning. Each had a limit of 113.5 kW/m^2, were water cooled, and were placed along the centerline of the pan, orthogonal to one another. To protect the wires and cooling water lines from the high heat fluxes, they were covered with aluminum foil. The concrete pad under the burn pan was covered with sheet metal to both reflect the radiant heat and provide a resting place for the oil splattered during testing.

ISB tests were performed by placing the crude oil sample on the water and then igniting it with gelled diesel fuel. We poured 10 L of crude oil on the water and spread it across the water (if the oil was very viscous) with a paddle to form a slick layer of 1 cm. We then poured 1 L of gelled diesel fuel made from ¼ of the gelling agent in an Elastec Safe Start Igniter canister, which was designed to make 4 L of gelled diesel fuel. The smaller accelerant volume was a conservative approach to mimic the slower release of the

accelerant during use as the marine flare melts the canister wall and allows the diesel fuel to leak out and spread across the slick. The gelled diesel fuel was then ignited with a propane torch. The slick will either remain inert or ignite and burn. If ignitable, the oil vapors from the slick burn first. If the slick was an emulsion, water vapor formed bubbles at the slick surface, the bubbles popped and expelled steam, and if there was sufficient crude oil vapor, it burned. As the slick became thinner or hotter, the underlying water boiled and produced steam. When this occurred, the burn process appeared to gain intensity with time as the boil-over process proceeded and then there was a sudden extinction as the heat transfer through the much thinner slick drastically slowed the fuel evaporation process. The residue, liquid or solid, was gathered off the surface and disposed. A sample of the residue was gathered for later analysis.

Chemical Analysis

The chemistry of the crude oil is a critical driver in the ignition, flammability, weathering, and emulsification processes that oils undergo. SARA analysis separated the five crude oils into their constituent saturates, aromatics, resins, and asphaltene so that mass spectrometry could provide the molecular mass distributions of each. These data, discussed below, provided insight into how the crude oils' chemistry influenced the ignition, emulsification, and burn behavior. Mass spectrometry of the neat, weathered, and burn residuals of the crude oils revealed what species, if any, actually burned and the molecular mass distribution of the residual.

SARA Analysis

Prior to testing, we performed saturate, aromatic, resin, and asphaltene (SARA) analysis of the oils to examine their properties in an effort to understand how they would behave. SARA separation is the set of methods used in petroleum chemistry to separate, from a crude oil, saturates, aromatics, resins, and asphaltenes. Though there are variations in the community, we used the method outlined by Muhammad *et al.* [36], which employs a 25-mL gravity column with 70 mL of 60–200 mesh silica. Approximately 3 g of crude was loaded on to the column and each fraction was eluted with 100 mL of solvent. Saturates were eluted with a 1:1 mixture of hexane and cyclohexane. Next, aromatics were eluted with a 7:3 mixture of hexane and toluene. Then the resin fraction was eluted with a 7:3 mixture of carbon tetrachloride and methylene dichloride. Finally, asphaltenes were eluted with a 7:3 mixture of methanol and acetonitrile.

Fig. 4-Eluent from each of the solvent washes during the SARA separation. They are arranged, from left to right, as saturates, aromatics, resins, and asphaltenes.

Figure 4 shows some of the solvent and sample solutions during the washing procedure. The eluent was combined for each fraction and the solvent removed using a rotary evaporator and dried via suction filtration. We dried the fractions to a constant weight to determine the mass percent of each fraction from the total mass. Next, mass spectrometry determined the molecular weight distribution for each fraction.

Mass Spectrometry

Mass spectrometry was used to analyze the fresh crude oil, weathered crude oil, the SARA constituents of each, and the burn test residuals from both the cone calorimetry tests as well as the ISB pan tests. Comparisons of the neat or weathered crudes with the burn residuals indicate what, if any, of the constituents burned and what constituents were added from the diesel fuel accelerant.

Samples were analyzed neat using a Water Xevo TQD triple quadrupole mass spectrometer (MS) (Milford, MA) using a Waters atmospheric solids analysis probe (ASAP). The MS source settings used a corona pin current of 15 µA, a cone voltage of 45 V, an extractor lens voltage of 3 V, a source temperature of 150 ºC, and a cone gas flow of 10 L/h. The probe nitrogen desolvation gas was set to 300 L/h and the temperature was ramped from 300 to 500 °C over 5 min in 10 °C increments. 100 mm double end sealed soda glass capillaries were used fresh for each sample in the probe. The capillary tubes were emerged in the neat samples 2-3 mm then inserted into the probe. The collision gas (Argon) was 1.1 bar with a collision energy of 3, the presence of was collision settings are not to induce fragmentation but improve ion movement through the collision cell and provide a cooling gas for the ions with the overall effect of improving sensitivity. The data was processed using Waters Masslynx software but signal averaging the mass spectra over the desired temperature range 300-340 or 380 ºC unless over wise indicated.

RESULTS

Cone Calorimetry Results

Each test was completed three times to quantify scatter and uncertainty. In particular, we were interested in the heat flux release rate ($\dot{q}''$) over the duration of the test and the burn efficiency (η_B), which was the ratio of the mass burned to the initial mass. The ignition energy, or the heat transferred to the slick, indicated how much heat was necessary to sufficiently break the emulsion and evaporate enough crude oil to create an ignitable concentration of hydrocarbon vapor. This was calculated by the product of the incident heat flux and the time between the start of the test and ignition, divided by the mass of the sample.

The test fixture (Figure 2) was weighed empty, filled with the sample oil, and then again after the test to determine the initial and final mass of the oil. The residual oil was placed in a sample jar for later analysis. Since emulsions typically separated during tests, the residual liquid water was disposed. The volume of the residual water and highly viscous oil was not been measured. Anecdotally, we observed only a small amount of water separated and settles at the bottom of the sample pan. That implies either that the emulsion did not fully separated or that the water boiled off.

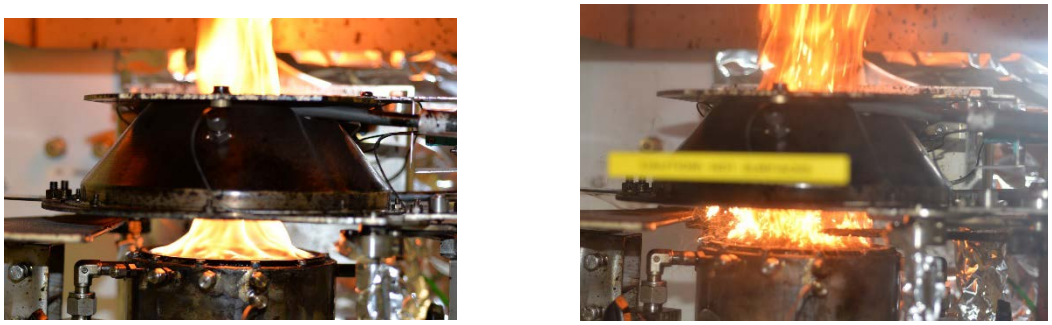

Fig. 5-(L) Neat and (R) 40% emulsified Santa Ynez burning under the cone calorimeter with 15 kW/m^2. Notice the burning splatter from the emulsified slick as the water boiled and scattered oil droplets.

Figure 5 shows photographs of burning Santa Ynez crude oil under the cone calorimeter just after ignition. The neat crude exhibited the expected behavior of a small hydrocarbon pool fire while the emulsified crude splattered to form droplets that burned more rapidly. The emulsified crude oil tests were conducted with a window shield to contain the splatter (as indicated by the yellow strip on the shield, seen in the right photograph of Figure 5).

The ignition and burn behavior between the neat and emulsified crude is distinct. The neat crude oil ignited almost instantaneously once the calorimeter shutters are opened to allow radiative heat from the cone heater coils to reach the oil surface and start evaporation. The weathered oil may take longer, depending on the weight of the crude oil. Heavier, weathered crudes may require more than a minute to heat and produce a steady stream of flammable vapor.

In contrast, the emulsified crude oil required time for the surface temperature to rise. During this warm up period, surface bubbles formed and popped as some of the water boiled and evaporated. The bubble formation both evaporatively cooled the oil and slowed the heat transfer rate by forming an additional layer of to absorb heat between the flames and the oil slick. Intermittently, flames formed, propagated, and then extinguished over the oil surface as the vapor concentration increases. Eventually, the evaporation rate had sufficiently increased to produce a continuously flammable concentration. Once a steady flame formed, the additional radiative heat transfer increased the evaporation rate to rapidly boil the water and create a boilover effect that dramatically increased the heat release rate. What drives the increased heat release rate is clear from the right photograph in Figure 5: the boiling water creates a coarse, flammable aerosol that isolates the crude oil droplets from the heat sink of the sample pan and allows more rapid evaporation and burning in the stream of burning crude oil vapor.

Since boilover has not been observed with ISB in the field, the occurrence of boilover with emulsified crudes can be attributed to either the water separating, sinking, and then boiling or suspended water boiling. We have observed that water separated during the burn for some crude oil emulsions to leave residual water under the residual crude oil, while for other emulsions, there was no residual water after the burn. Without in situ diagnostics of the emulsion during the evaporation and burn process, we can only hypothesize what is occurring during the evaporation and burn process.

Two extinction processes occurred during the cone calorimetry tests and both reduced the availability of flammable vapor. The first extinction process occurred when the oil residue forms a highly viscous or solid residue in the sample pan with a char on the top surface. This occurred generally for the heavier and/or weathered crude oils. In this process, the high viscosity of the residue reduced the transfer of the lighter hydrocarbons and prevented their evaporation and combustion. The second extinction process occurred when the sample remained liquid, but cooling from either the sample pan water jacket and/or from rapid water boiling cooled the sample enough to reduce the continued formation of a flammable, steadily burning vapor concentration.

In this and subsequent plots, the legends indicate the oil by a two letter abbreviation (see Table 1), indicate whether they are fresh or weathered (F or W, respectively), emulsion fraction (E%), and case number if it is from an individual sample. Generally, we show the Santa Ynez results first before we show those of other crudes. It is one of the middle weight crudes of this series and provides a general behavior baseline.

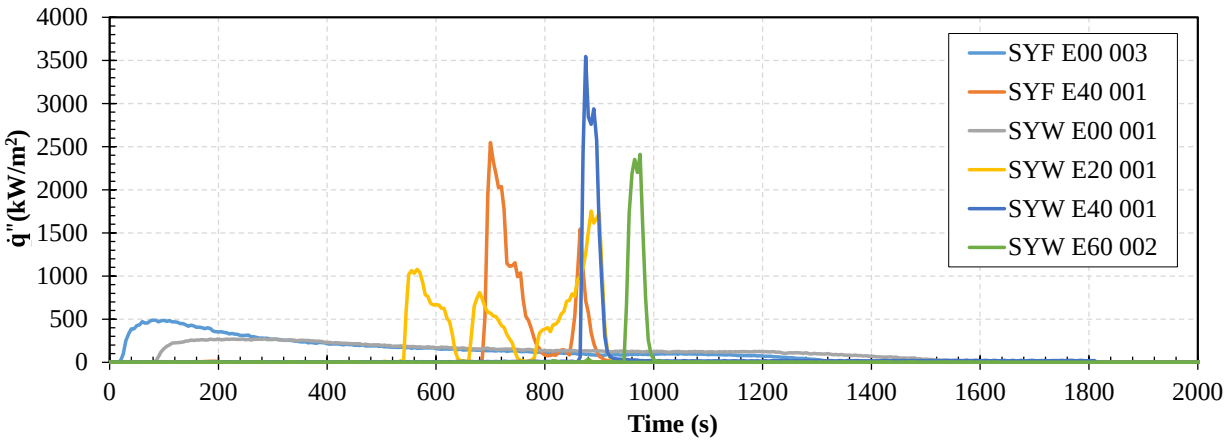

Fig. 6-Cone calorimetry heat release rates measured during tests for Santa Ynez.

Examples of delayed ignition, high heat release rates, and short burn duration periods were measured directly from the heat release rate data for a range of blends of the Santa Ynez crude oil (Figure 6). Comparing the neat and emulsified, there was a significant delay as the emulsion was heated, separated, and water boiled before there was sufficient flammable vapor above the crude oil surface. Once ignited, boilover increased heat flux back to the surface, drove more rapid evaporation and a greater heat release rate. The ignition delay increased and the burn duration decreased with both weathering and emulsion. The delay for emulsified crude oil was a result of the greater heat capacity of the mixture, due to water, which required greater heat transfer to change the temperature of the emulsion. The remaining flammable, volatile constituents in the weathered oil have a lower vapor pressure than the fresh oil, so the mixture needed to be heated to a higher temperature to produce sufficient flammable vapor. The decrease in the duration of heat release was due to a decrease in the concentration of flammable constituents with both weathering and emulsification. Therefore, less time passes before the heat sink cooling quenched the evaporation and combustion processes.

The heat release traces in Figure 6 for fresh, emulsified 40% (SY E40) and weathered, emulsified 20% (SYW E20) both show multiple ignition or burn peaks. These same mixtures exhibited ignition, extinction, and re-ignition behavior in both cone calorimetry and pan fire testing. There appeared to be a time lag during the burn process as the oil was heated while the emulsion separated and the water sank or evaporated. We hypothesize that one or both processes slow or reduce, respectively, the fuel vapor concentration and extinguish combustion until there is sufficient hydrocarbon vapor for ignition or re-ignition. As a result, the sample periodically ignited, extinguished, and re-ignited until the heat sink cooling limited evaporation.

Similar behavior was observed for the other crude oils, with some variation. Those plots (Figures 7 through 10) are shown below, where example plots are shown for all of the test conditions, except those that would not burn.

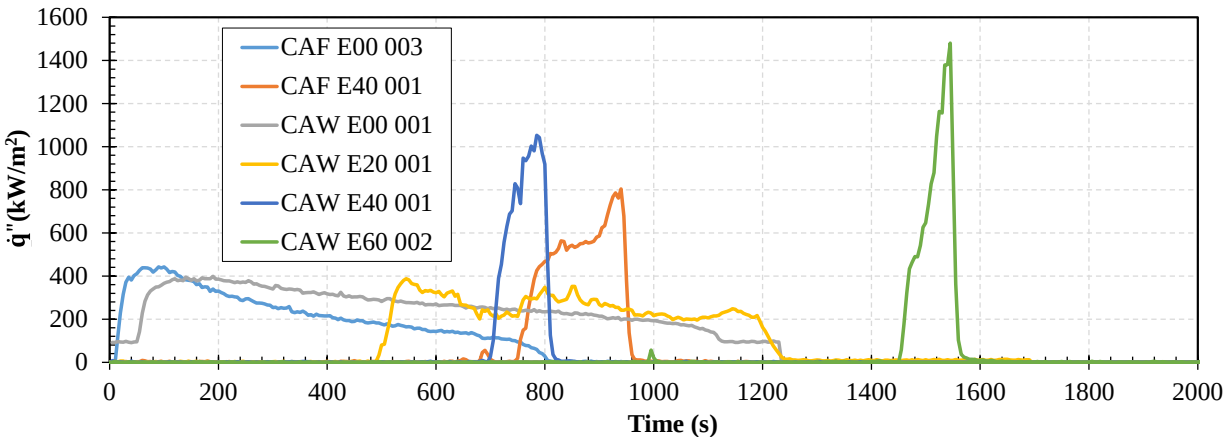

Fig. 7- Cone calorimetry heat release rates measured during tests for Carpinteria.

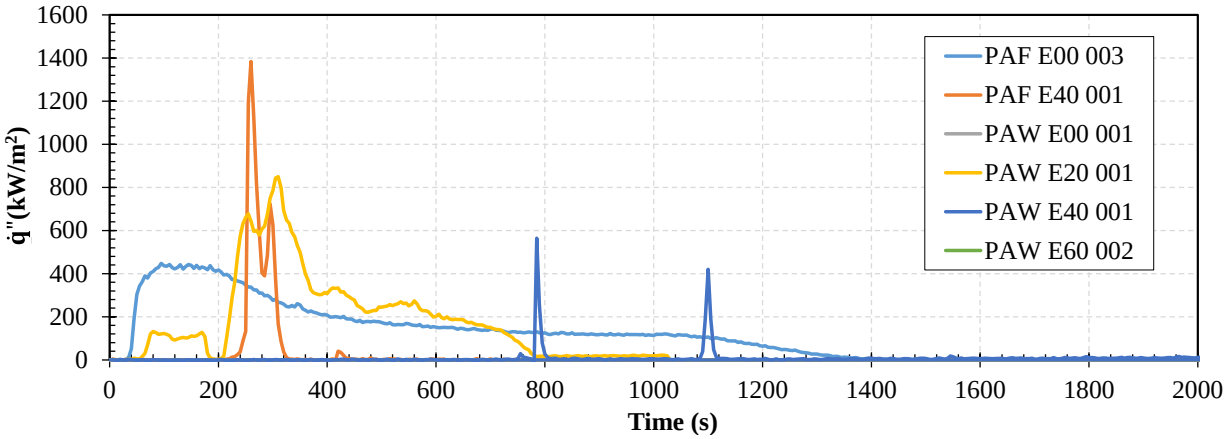

Fig. 8- Cone calorimetry heat release rates measured during tests for Point Arguello.

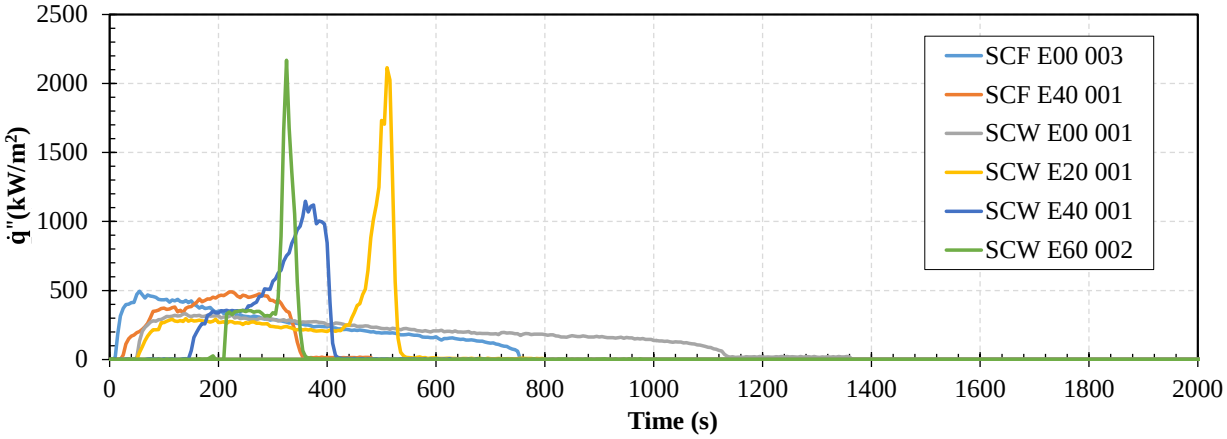

Fig. 9- Cone calorimetry heat release rates measured during tests for Santa Clara.

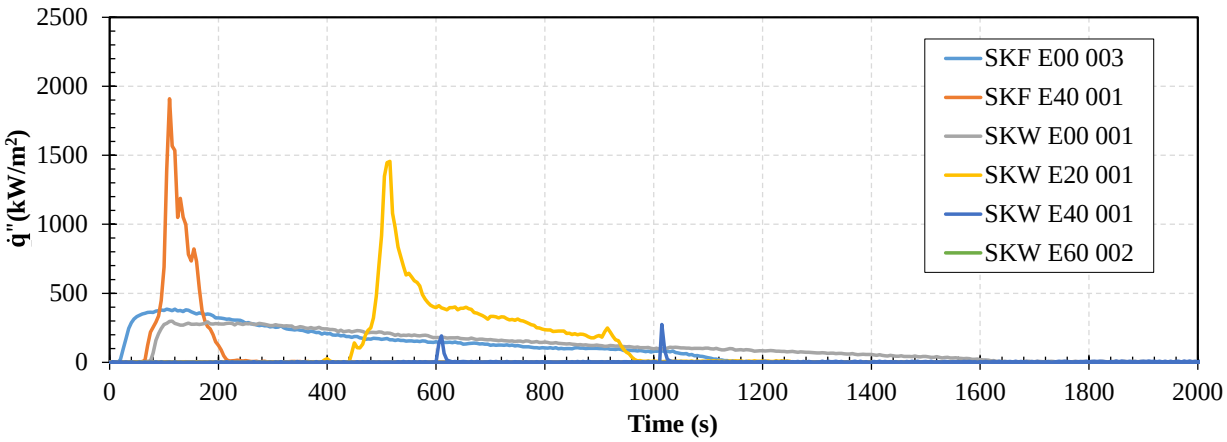

Fig. 10- Cone calorimetry heat release rates measured during tests for Sockeye.

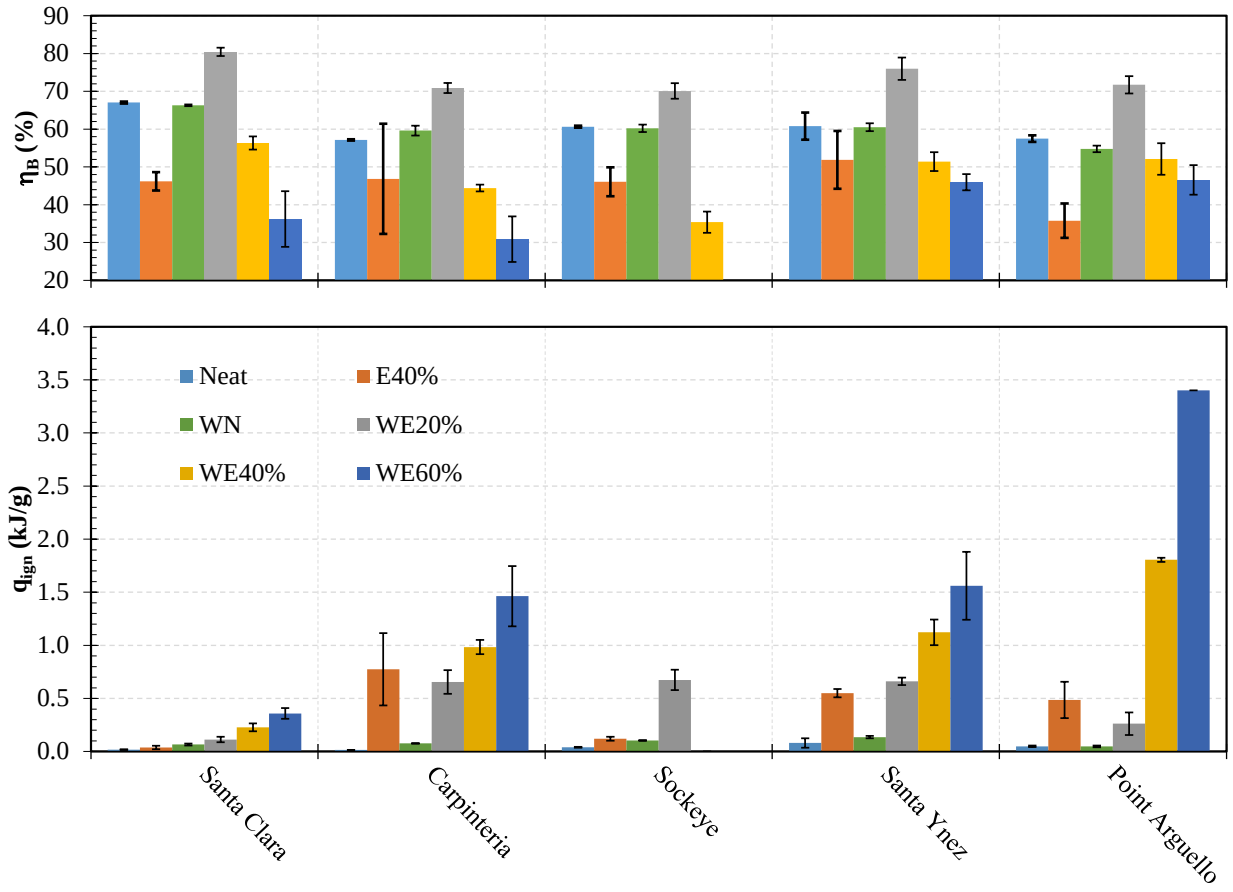

Fig. 11-Burn efficiency (top), η_B, and ignition energy (bottom) comparison.

The burn efficiency (η_B) plot (top, Figure 11) shows a clear dependence on emulsion, but there was no clear dependence on the oil density, weathering, or the oil constituents. For these tests, the initial and

final masses of the oil were measured to calculate the burn efficiency, η_B. This is calculated by the expression:

$$\eta_B = \frac{m_i - m_f}{m_i} \quad (2)$$

where m_i and m_f are the initial and final masses of the oil or emulsion sample. As we would expect, there was a decrease in η_B with emulsification from neat to 40%, but there was a burn efficiency peak for 20% emulsions for all of the weathered mixtures tested.

In order to understand what drives the peak burn efficiency, we should consider what drives or limits burn efficiencies. In this experiment, the longer the burn duration, the greater the amount of the sample was evaporated (oil or water) and burned. Any process that amplifies or limits oil evaporation will, in turn, increase or decrease efficiency. Clearly, the surface boiling and atomization that emulsions undergo when the constituent water boils assists in reducing the mass of the slick or sample. We also need to consider that the water in emulsions limited the burn efficiency by acting as a heat sink during evaporation and as a fire suppressant when vapor by displacing oxygen, fuel, and absorbing heat from combustion. These two latter effects increase as the water concentration increases, such that at concentrations of 40% and greater, the burn efficiency was reduced.

The efficiency peak at 20% indicates that there is an optimum emulsion fraction that will improve the efficiency. A more detailed study in the future should determine both the optimum emulsion for a range of typical crudes and the driving chemistry and thermodynamics. There appears to be sufficient water to aerosolize the crude oil, but not enough to increase the heat capacity or displace oxygen and fuel vapor to extinction.

The ignition energy plot (q_{ign}, bottom, Figure 11) shows a clear dependence on the emulsion fraction. The ignition energy is calculated by multiplying the cone heat flux ($\dot{q}"_{Cone}$) by the area of the calorimeter pan ($A_{C,P}$), the delay time (t_{ign}), and dividing by the initial mass of the sample (m_{sample}):

$$q_{ign} = \frac{\dot{q}"_{cone} A_{C,P} t_{ign}}{m_{sample}} \quad (3)$$

The bottom plot of Figure 11 shows that the ignition energy generally increased as emulsion and weathering increased. Though not unexpected, we should note some particular behaviors. For the emulsified mixtures, emulsion not only added water to the mixture, which cooled the crude oil as it evaporated, but also increased the heat capacity and thus greater energy needed to be transferred to raise the sample temperature. Additional energy and time was also required to break the emulsion and allow the water to sink or evaporate. The same plot also shows a general increase in ignition energy as the crude was weathered. This can be understood from the loss of the lighter, higher-vapor pressure constituents. The remaining heavier, lower-vapor pressure constituents needed to be heated to higher temperature to produce a flammable vapor concentration.

The presence of emulsion breakers complicate the emulsion and evaporation processes. For the Santa Clara blends, the ignition energy for the fresh 40% emulsified blend was noticeably lower in comparison to that of the other crude oils. It is possible that the addition of the Flow 12021 emulsion breaker decreased the energy required to break the emulsion and allow ignition. The same was not observed for the Carpinteria, which also contains an emulsion breaker but the fresh-40% emulsion still required substantial heating to break.

The peak heat release rates of the cone calorimetry tests are plotted in Figure 12. These represent distinct behavior from that of the burn efficiency, as we can see. As we should expect, the emulsified crudes produced much higher heat release rates as the boiling water provided a mechanism to atomize and entrain crude oil droplets into the vapor plume above the sample. This suggests that a possible method to increase crude oil burn rates and efficiencies would be to increase the amount of heat transfer to the slick to more rapidly boil the water in the emulsion or the water underlying the slick.

There are some additional trends that should be noted. First, the maximum burn efficiency corresponded to the weathered-20% emulsified mixtures shown in Figure 11 while the maximum heat release rates corresponded to weathered oil with either 40% or 60% emulsification. Furthermore, the weathered-emulsified crudes at 40% and 60% produced greater heat release rates than those of fresh-40% emulsions, suggesting that the heavier weight constituents which remain drive high peak release rates. We do not think that this was an effect of chemistry. Instead, we suspect it has to do with the higher viscosity and density that prevented the water from sinking and allowed it to stay suspended longer in the sample until the water vaporized and atomized the crude. A more detailed examination of the evaporation, separation, and atomization mechanisms associated with emulsified crude would reveal these details.

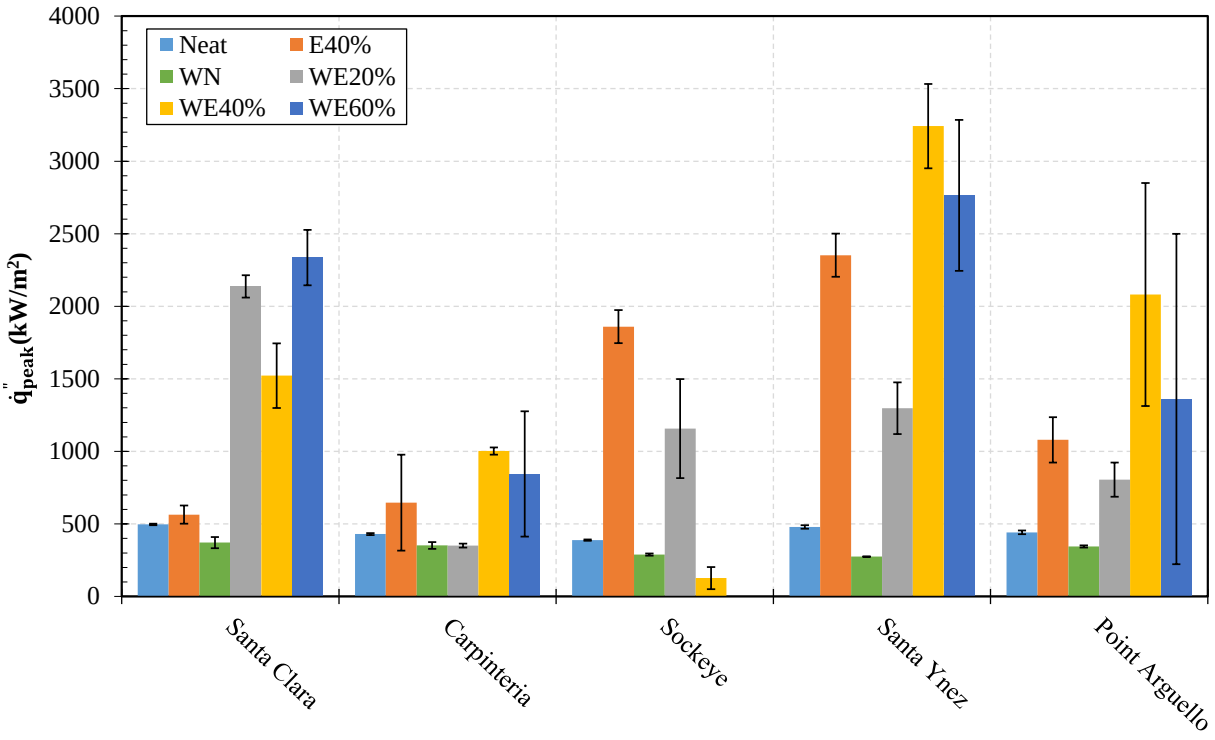

Fig. 12-Peak heat release rates for the various crude oils and blends tested. Notice that all of the emulsified crudes produce higher peak heat release rates when compared to the neat crude oil, whether fresh or weathered.

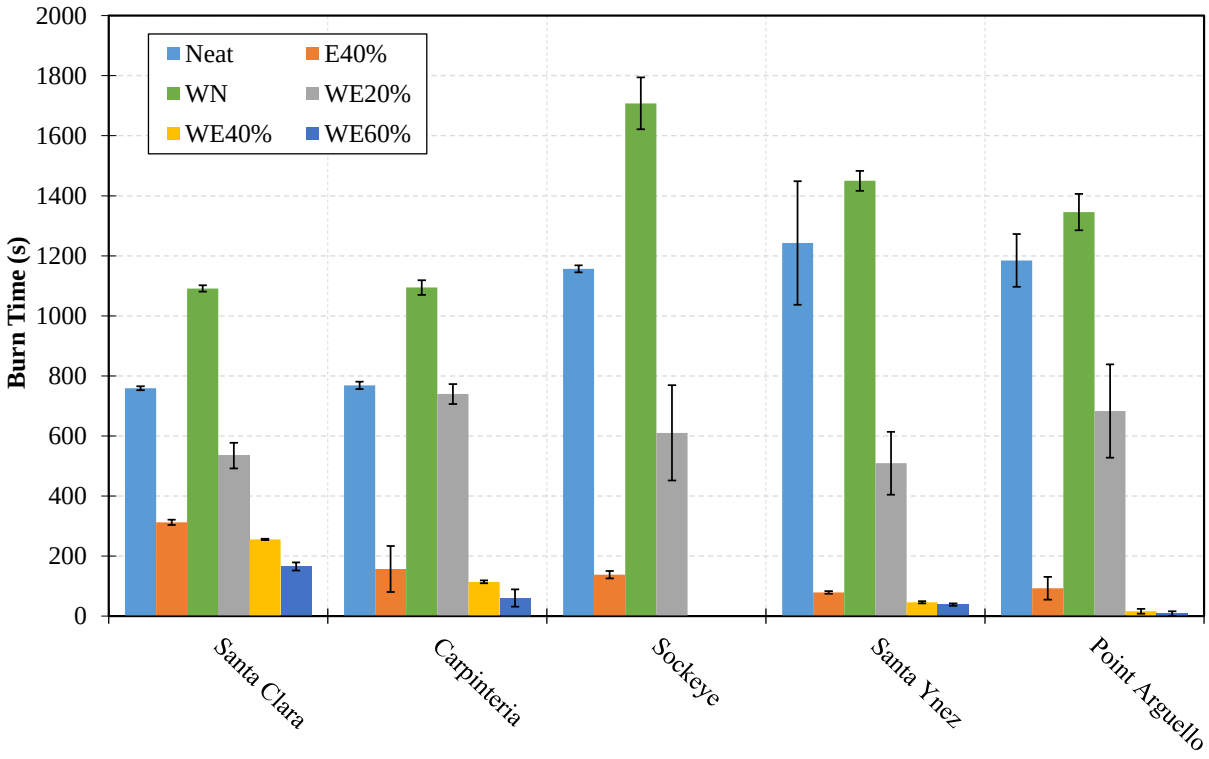

Fig. 13-Mean burn times for the various crude oils and blends tested. There is a clear dependency on both weathering and emulsification. Weathering increased the burn time while emulsification decreased the burn time.

In Situ Burn Pan Results

In these tests, we measured the temperature of the pool and of the water-oil interface, as well as the heat flux, but the most valuable information was observing how different oils ignite and burn. Over the course of testing, there were some inconsistencies of where the thermocouples at the pool surface were placed. Therefore, those data will not be fully described but reported for some example cases.

Figure 14 shows a typical ISB in the 1 m^2 test pan for fresh, neat Santa Ynez crude oil. The behavior demonstrated in this image was typical of the fresh oil burns. Once ignited, the flames spread to the edges of the pan and the flames produced a thick, sooty black smoke. Because the outdoor test site was near the Chesapeake Bay, there were periodic changes in both wind speed and direction. This introduced some repeatability challenges for these tests, but were realistic of the wind behavior on any large body of water. Because of the size of the flames and the intensity of the fire, it was difficult to reliably observe when the fire transitioned from the diesel to the crude oil, had completely enveloped the slick, or when boil-over phenomena occurred. During early testing, we attempted to track these behaviors, but we discovered there was a great deal of subjectivity and ambiguity in defining when these events occurred. Therefore, we qualitatively observed how the fire propagated, stabilized, extinguished, and, for many of the emulsified crudes, reignited.

We should note some significant differences between the cone calorimetry and the ISB tests. First, the presence of the underlying water provided a significant heat sink, but due to the fairly stationary water, there was much less convective cooling than with the actively cooled cone calorimeter sample pan. As a result, boiling at the water-oil interface eventually occurred for neat oils, but rarely for the emulsified samples. The exception being the 20% emulsions. In contrast, because of the persistent heat flux to the

sample from the cone calorimeter heater and the formation of water pockets separated from emulsions during testing, the underlying water almost always boiled eventually. Another significant difference is that the cone calorimeter heater provided a constant heat flux to the sample that never ceased until there was ignition. In contrast, the gelled diesel fuel accelerant would only burn for two minutes and then extinguish if the sample did not ignite. Finally, it should be noted that the burn extinction process was very different for the two test platforms. For the cone calorimeter, the constant heat transfer from the heater coil allowed the sample to burn longer and more completely, even with the water jacket cooling the sample. For the ISB pan, heat to the sample relied on the combustion alone while the heat sink to the underlying water may not have been as great. Once the fuel evaporation rates started to reduce because of heat transfer, water transpiration cooling, or emulsion breaking delays, the burn rate, thus heat release and transfer rate, decreased and the fuel evaporation rate further decreased.

Fig. 14-Typical ISB pan fire of Santa Ynez crude oil. There was steam around the edges of the pan as the flames heated the water through the oil.

Temperature traces for Santa Ynez burn tests using fresh-neat are shown in Figure 15. These traces gave us some insight into what thermodynamic changes the oil mixture experienced at the slick during the burn process and how it changed with emulsification and weathering. The first significant detail to notice was that the peak temperatures were well over boiling as the test proceeded. The temperatures revealed the radiative and convective loading the oil was experiencing over the burn and that they continued to increase until a sudden drop at extinction. The increase in temperature followed from the raising temperatures of the oil and underlying water and the higher temperatures needed to evaporate the heavier crude oil constituents. Simultaneously, the water temperature stayed fairly uniform throughout the test.

There was a first-order time response in the measured temperature as the water surrounding the thermocouples influenced their measurement. If we consider these plots, there was an almost 1 minute lag as the thermocouple temperature increased to what we assume was the plume temperature. This was a result of the thermocouples being immersed in the pan and the conductive cooling they experience from the water. These data were interesting, but do not accurately reflect the dynamics of the burn process.

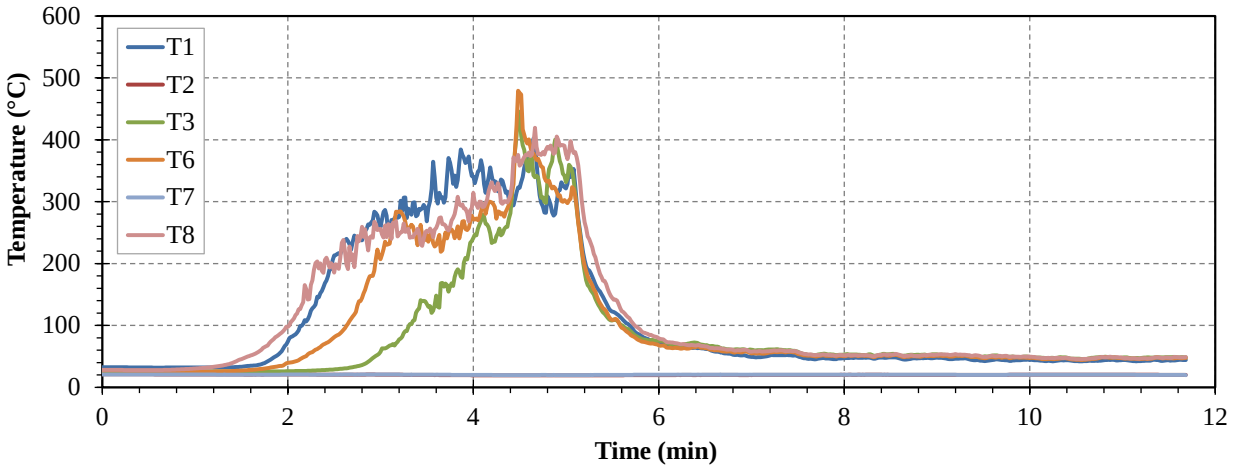

Fig. 15-A temperature trace for fresh-neat Santa Ynez crude oil. T1, T3, T6, and T8 were located near the interface of the water and the slick. T2 and T7 were submerged 14 cm below the surface. T4 and T5 were damaged early in testing so they were excluded.

The heat flux traces revealed the timing of the burn behavior more reliably than the thermocouples since they responded more rapidly than the pool. The 64-2SB-20 heat flux gages (data shown in Figure 16) had a time constant of 250 ms while that of the 64-10F-20SB was 50 ms. The shorter response time allowed a more precise determination of when processes started or stopped. Because of the influence of the wind, frequently flames enveloped one gage, increasing both convective and radiative heat flux, while leaving the other to detect solely the radiative heat flux.

The heat flux and burn event traces shown in Figure 16 clearly show when ignition occurred and when the flames extinguished, but the other events were not clear from the heat flux traces. There were some general behaviors that can be correlated from observations and the heat flux which we will describe.

Comparing the heat flux traces of the fresh-neat, fresh-40% emulsified, and weathered-20% emulsified oils shown in Figure 16, there were some distinctions we can explain. First, we observed that the heat flux for the fresh-neat oil was high and nearly steady for the entire test. Winds shift the burning plume, but combustion remained steady until extinction. For the fresh-40% mixture, flames did not completely envelope the slick other than very early in the burn. Instead, the flames extinguished and then spread back intermittently over sections of the slick. This created large peaks in the heat flux measurements, shown in the middle plot of Figure 16. This corresponds with the intermittent heat release peaks observed for the same mixture during cone calorimetry measurements. Finally, the weathered-20% emulsified mixture burned very vigorously and continuously, with no intermittent flameouts.

We should also note that for the emulsified oils, the water level of the entire pan generally increased after each burn. Though this was not immediately discernible after a test, repeated tests of emulsified crudes required that some of the water be drained. This reveals that for many of the emulsified crudes, the emulsion started to break down with ignition and then likely continued during the burn. Given the high viscosity of these oils, we suspect that the emulsion separated at the surface and then some time passed before the water on top of the oil could either boil off, which would have cooled the oil, or sink through the remaining oil. This lag between emulsion breaking and the water either evaporating or sinking may be what produced intermittent burning across the emulsion slicks.

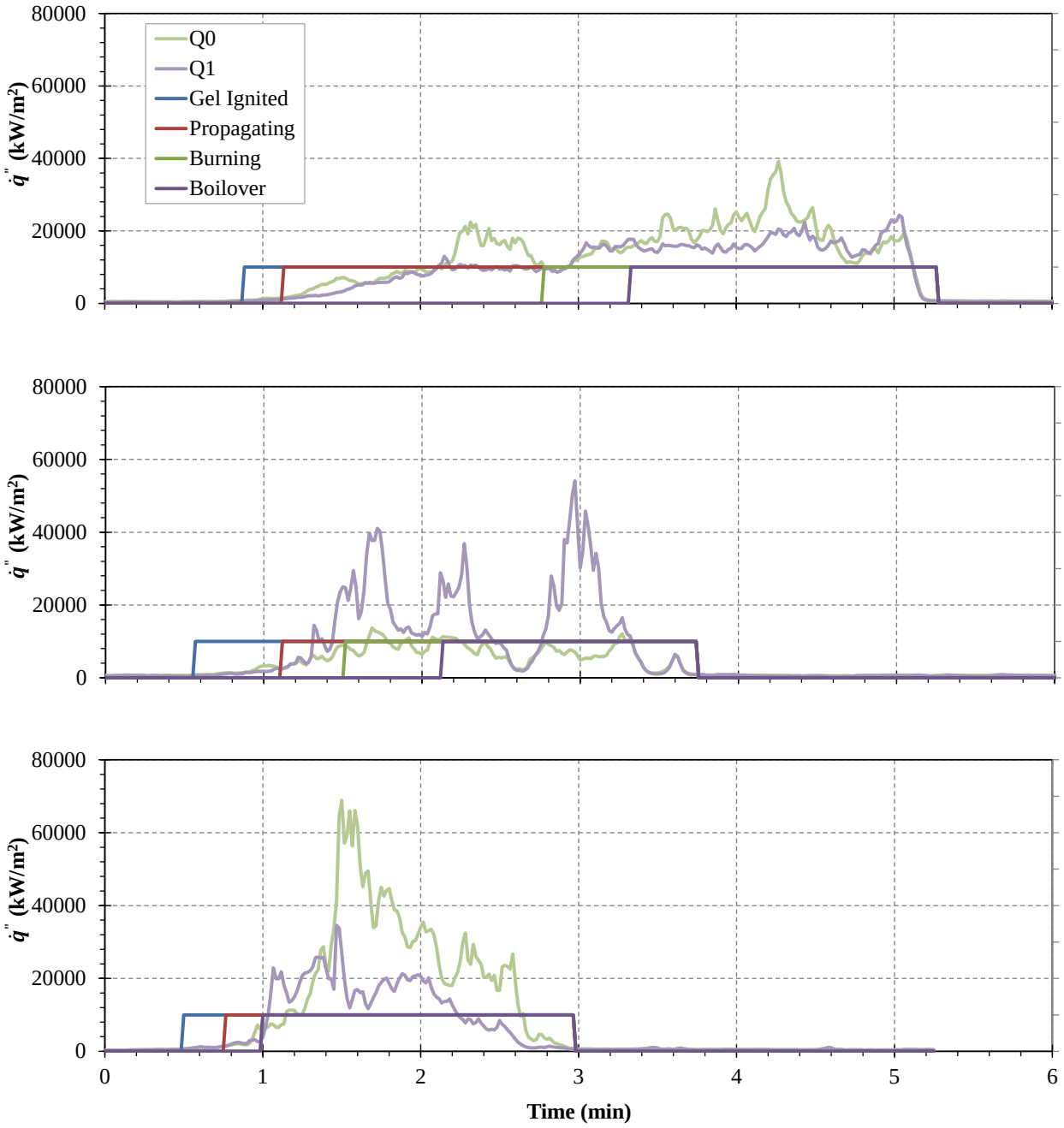

Fig. 16-Heat flux and burn event traces for fresh-neat (top), fresh-40% emulsified (middle), and weathered-20% emulsified (bottom) Santa Ynez crude oil.

Graphs of the average burn durations and peak heat fluxes for the pan fire tests were plotted in Figure 17. Even with the windy test conditions, both quantities were fairly consistent. It should be noted that the fresh-40% emulsion of Carpinteria would not ignite. There was difficulty in forming a stable emulsion until the Span® 85 concentration was increased to an unrealistic value of 6%, after which the mixture emulsified into a cream-like mixture that would neither burn nor separate with heat.

As we would expect from emulsified crudes, the burn durations decreased from the influence of the water. The chemically inert, high-heat-capacity water slowed the heating of the oil slick. Once the water boiled, it formed insulating bubbles at the slick surface and evaporatively cooled the crude oil while it also displaced hydrocarbon vapor and oxygen in the vapor plume above the slick. This same effect was seen in the decrease in peak heat flux values for the fresh-40% emulsions, but not for the weathered-20% emulsions. The lower water concentration appeared to be able to provide enough moisture to aerosolize the crude but not significantly impede the heating process. This implies there was a water concentration that would create optimum, high heat fluxes. The work by Van Gelderen *et al.* [35] demonstrated that burn efficiency of even highly emulsified oils can be increased by increasing the heat flux. If there was an optimum emulsion range that will help amplify the heat flux back to the slick during ISB, the corresponding slick age should be considered when deploying ISB during a spill. We should note that for burn durations on the order of 120 s, only the diesel fuel appeared to burn.

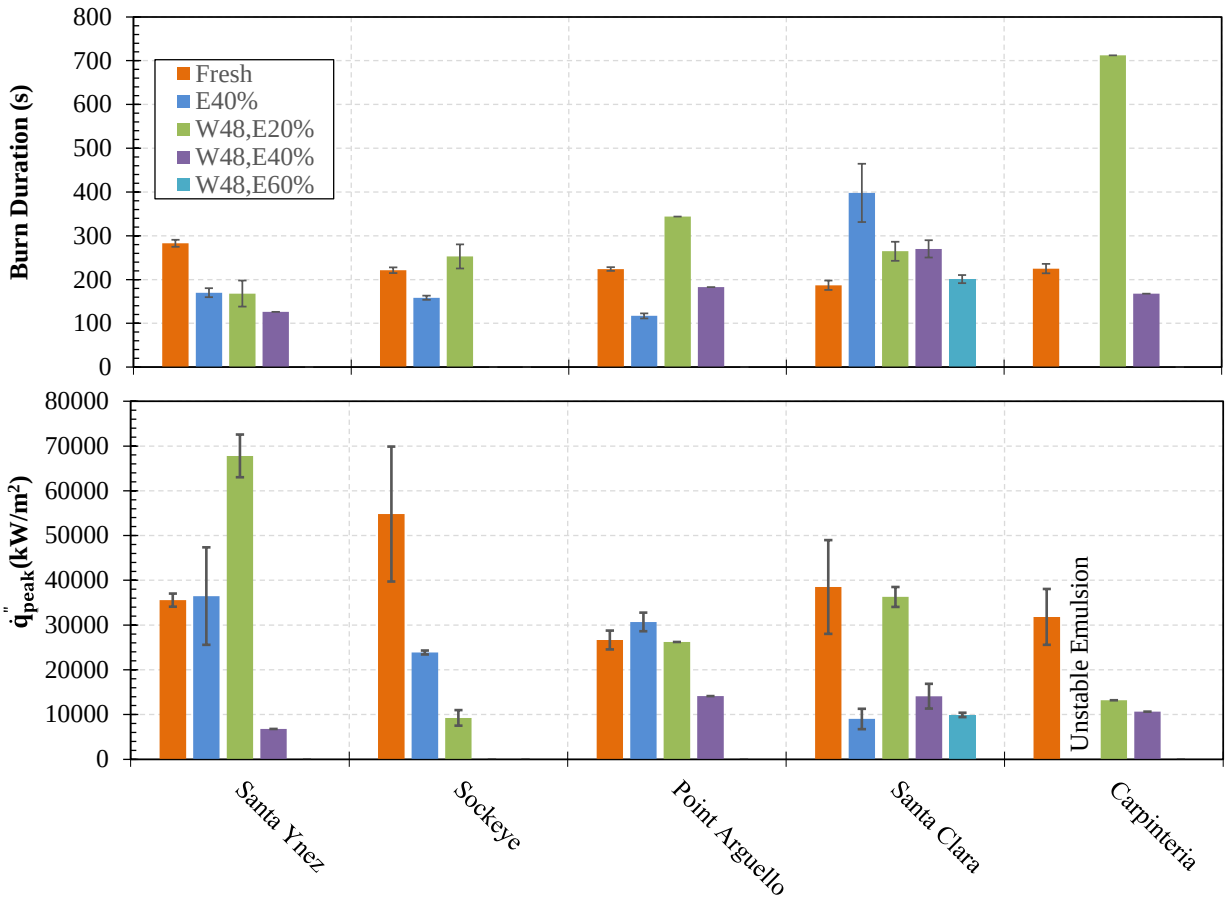

Fig. 17-Burn duration and peak heat flux for ISB pan fire tests. Blank spaces, unless otherwise noted, denote that only the gelled diesel fuel burned or, because a lesser emulsion fraction did not burn, no test was executed.

In comparing the residual crude from these tests, we can qualitatively observe how efficient the burns were. The fresh-neat burn test left a thin layer of 1-2 mm over the slick that quickly hardened into a toffee-like texture for the heavier crudes like Santa Ynez, Sockeye, and Point Arguello. The lighter crudes left a heavy, viscous slick that resembled heavy crude and did not harden. In contrast, the fresh-40% emulsified oil burn left a slick over 3 mm. Finally, the weathered-20% emulsified burn test left a slick that covered

about 50% of the water and was around 1 mm thick. We should note that it was difficult to accurately measure the slick thickness because of the high viscosity and opacity of the residual oil, so it was not advisable to use these values to calculate a burn efficiency. A careful method of measuring the slick thickness or volume needs to be developed that will accommodate the high viscosity and opacity of the residual slick.

Analytical Chemistry Results

The analytical chemistry results revealed the nature of the constituents of the crude oils as well as the different effects of both weathering and combustion on the oil. All of the analysis, as of the writing of this report, was limited to mass spectrometry. This analytical method reveals the mass distribution of the constituents, as separated into discrete mass bins. Shifts in these distributions between crude oils and with weathering or combustion reveal both why different oils respond or the effects of different processes on the constituent distributions. There is significant variation in how weathering, emulsification, and the two burn tests change the chemistry of each oil, all of which is driven by how the chemistry, thermodynamics, and transport interact during the burn test. The discussion below will provide some insight into the effect of these interactions, but there is still much to be learned and each oil behaves distinctly.

This section will describe the SARA analysis results as well as the mass spectrometry results for the cone calorimetry and the ISB residuals. Plots with comparisons from the same test conditions from both cone calorimetry and ISB experiments are shown without discussion in Appendix A.

Table 4-Figure key for comparison of different crude oil baselines and residues. F denotes fresh oil, W denotes weathered, and E##% denotes ##% emulsification fraction. Numbers are linked to the mass spectrometry figures.

Comparison		Santa Ynez	Carp-interia	Point Arguello	Sock-eye	Santa Clara
SARA		18	22	20	19	21
Baseline Fresh & Weathered		23	24	25	26	27
Cone	Fresh, E00% & E40%	28	29	30	31	32
	Weathered, E00-E60%	33	34	35	36	37
Pan	Fresh, E00% & E40%	38	39	40	41	43
	Weathered, E20-E60%	44	45	46	47	48
Pan & Cone	F, E00%	49	50	51	52	53
	F, E40%	54		55	56	57
	W, E20%	58	59	60	61	62
	W, E40%	63	64	65		66
	W, E60%					67

Table 4 provides a map of the various mass spectra and difference plots from burn residuals for the various burn tests, in comparison to the baseline oil, fresh or weathered. For reference, the first five plots compare the mass spectra from the SARA analysis. These are followed by comparisons of the weathered baseline oils with the corresponding fresh oil. Cone calorimetry residual mass spectra comparisons are

provided first, followed by those for the ISB burn pan tests. The final set of plots compare the residual mass spectra from both burn pan and cone calorimetry residual samples.

In general, we will begin each set of MS plots with a discussion of those for the Santa Ynez oil, which has the median, measured API of the oils used in this study (Table 1). We observed that many of the behaviors exhibited by this oil were generally exhibited by the others, with some variation. In particular, we observed that the two exceptions were Santa Clara, a much lighter crude, and Point Arguellow, a much heavier crude.

SARA Analysis

The SARA analysis results are shown in Table 5. There is some difference between the SARA mass fractions that were reported in Jokuty *et al.* [17], but it is not unexpected that the reservoirs should change over the eighteen years since that data was compiled.

Table 5-SARA Mass fraction splits for each crude oil.

Crude Sample	Saturates	Aromatics	Resins	Asphaltenes	R + As
Santa Ynez	39.7%	33.0%	14.5%	12.7%	27.2%
Sockeye	40.3%	24.6%	23.2%	11.8%	35.1%
Point Arguello	32.4%	29.8%	25.8%	12.1%	37.8%
Santa Clara	65.8%	22.3%	4.29%	7.68%	12.0%
Carpenteria	52.2%	28.9%	8.60%	10.4%	19.0%

If we consider the cone calorimetry results with the SARA fraction splits, there are some intriguing implications. First, burn efficiencies are higher and ignition energies are lower for the higher saturate fractions oils from the Santa Clara and Carpinteria reservoirs. This is to be expected since both saturates and aromatics evaporate before burning, while resins and asphaltenes need to endothermically decompose to produce combustible vapor [37-39].

For the emulsified crude oils, we can observe a subtle relationship between the ignition energy and mass fractions. Examining the mass fraction splits with the burn efficiency, peak heat release, or ignition energy, there are no apparent qualitative or quantitative correlations. If we add the asphaltene and resin fractions together and compare them with the ignition energies for the unweathered 40% emulsified mixture, we see that there is a possible relationship: in the unweathered 40% emulsion cases, ignition energies are higher for the crude oils with higher combined resin and asphaltene fractions. This is driven by the influence these molecular classifications have, acting in concert, in the formation and stability of emulsions, which has been established in the literature for some time [11,40,41]. The exception is the Sockeye crude oil, which has a high resin content and asphaltene content, but a low ignition energy for both neat and emulsified cone calorimetry tests.

For each SARA fraction, the mass spectrometry (MS) data were normalized as a histogram, effectively turning each MS plot into a probability distribution, which we then multiplied by the respective SARA fraction. The distributions were then plotted on top of one another, in order of greatest to least SARA fraction. This same approach was used for Figures 18 through 22. The horizontal axis is reflective of the molecular weight distribution while the vertical is the normalized and mass-fraction-weighted probability of the respective molecular weight. The minimum m/z value of 50 corresponds to a molecular weight of 50 amu (a carbon number of around 3) while the maximum corresponds to 900 amu (a carbon number of 64). These numbers were based on that assumption that each hydrocarbon link corresponds to a carbon and two hydrogens, or 14 amu.

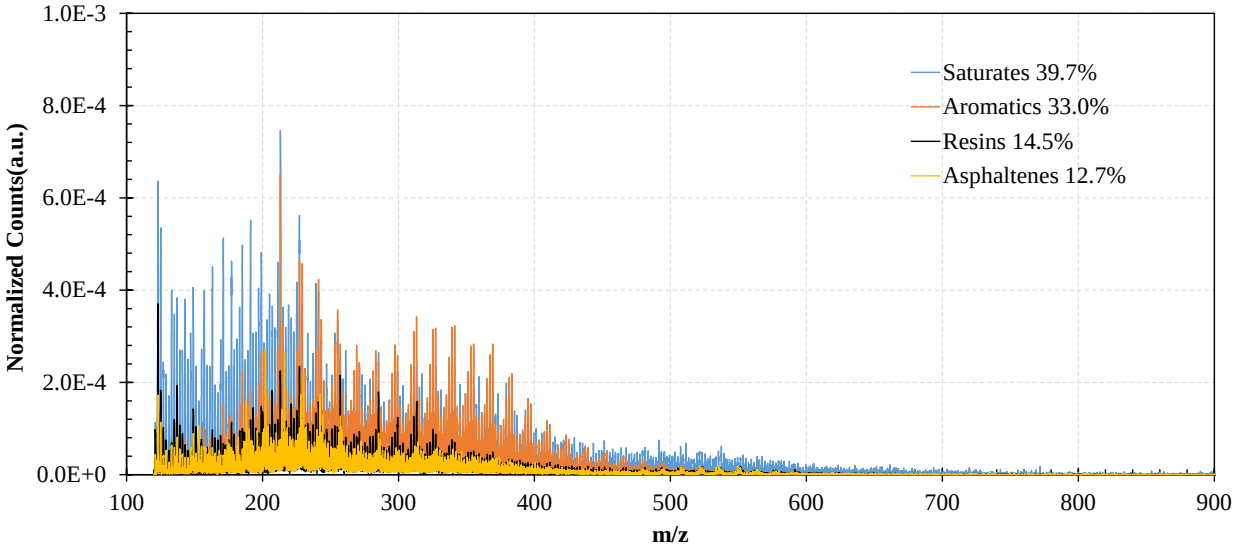

Fig. 18-Santa Ynez mass spectrometry distributions, normalized and weighted by SARA fraction.

Examining Figure 18 and considering the high viscosity and density of Santa Ynez, we can understand how the fractions and their respective distributions drive the oil properties. Though the saturate fraction contains lightweight components, the aromatic fraction was fairly heavy. Furthermore, the more polar resin and asphaltene fractions were relatively high when compared to lighter, less viscid Santa Clara and Carpinteria (Figures 21 and 22). The higher viscosity, due to the large fraction and mass distribution of the aromatics and asphaltenes, and influence of polar asphaltenes and aromatics, make emulsions more stable and slow ISB ignition; the emulsions require more heat to break the emulsion and more time, and thus energy, for the released water to either boil or sink.

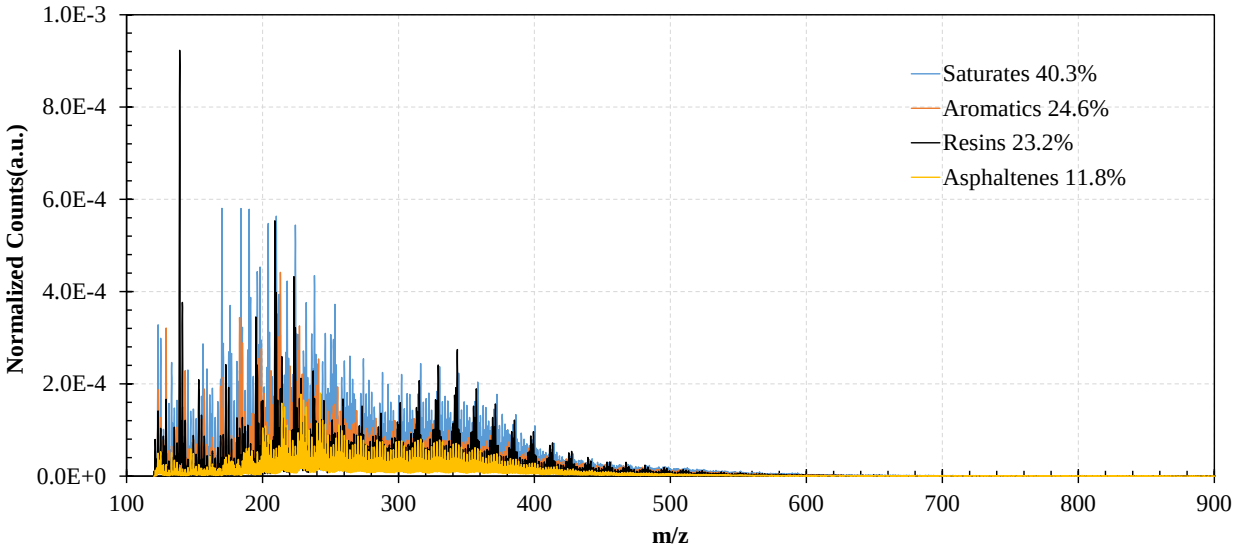

Fig. 19-Sockeye mass spectrometry distributions, normalized and weighted by SARA fraction.

The normalized and weighted mass spectrometry data in Figure 19 for Sockeye crude oil again show a very high saturate fraction and large masses in the distributions of the saturates and asphaltenes. Similar to the Santa Ynez, this oil is highly viscous, but the viscosity appears to be driven by the large fractions of heavy saturates and resins. The resin content, though appreciably high, is largely composed of both lightweight and heavy molecules, of which the lightweight constituents will endothermically decompose faster than the heavier resins. This may explain why the fresh 40% emulsion has a much lower ignition energy than all but the Santa Clara crude oil. The behavior of the fresh-emulsion of Sockeye suggests that the molecular mass distribution, not just the respective SARA fractions drive how stable crude oil emulsion may be at both water temperatures and at the elevated temperatures found in burning slicks. This suggests a possible examination of these emulsions and the development of stability metrics for both water temperatures and ISB temperatures. Furthermore, pyrolysis-mass-spectrometry of these oils would reveal how combustion drives the formation of gas-phase species [42].

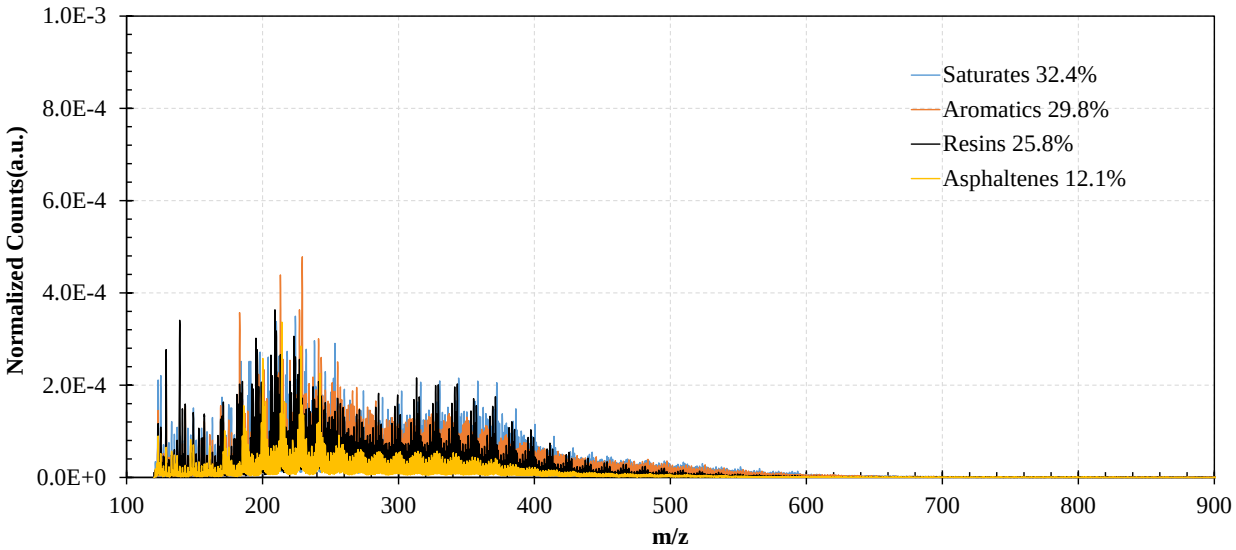

Fig. 20-Point Arguello mass spectrometry distributions, normalized and weighted by SARA fraction.

Point Arguello (Figure 20) is the highest viscosity oils in this study and we can observe large molecular weights for the resins and aromatics. The resins, in particular, are some of the most viscous components in the crude oil. In the asphaltene fraction, there was a higher proportion of lightweight hydrocarbons than in the Sockeye and Santa Ynez, concentrated in narrow bands between 150 and 250 m/z. Though it might be assumed that the lighter asphaltenes would reduce the viscosity and tendency to emulsify, we should recall that asphaltenes are not liquids in the crude oil solution but suspended solids, and even light asphaltenes' polarity can strengthen an emulsion. As a result, we can see how the higher concentrations of both asphaltenes and resins stabilize the emulsions. The ignition studies of the weathered Point Arguello oil revealed that reducing the aromatics and saturates increased the emulsion stability and ignition energy.

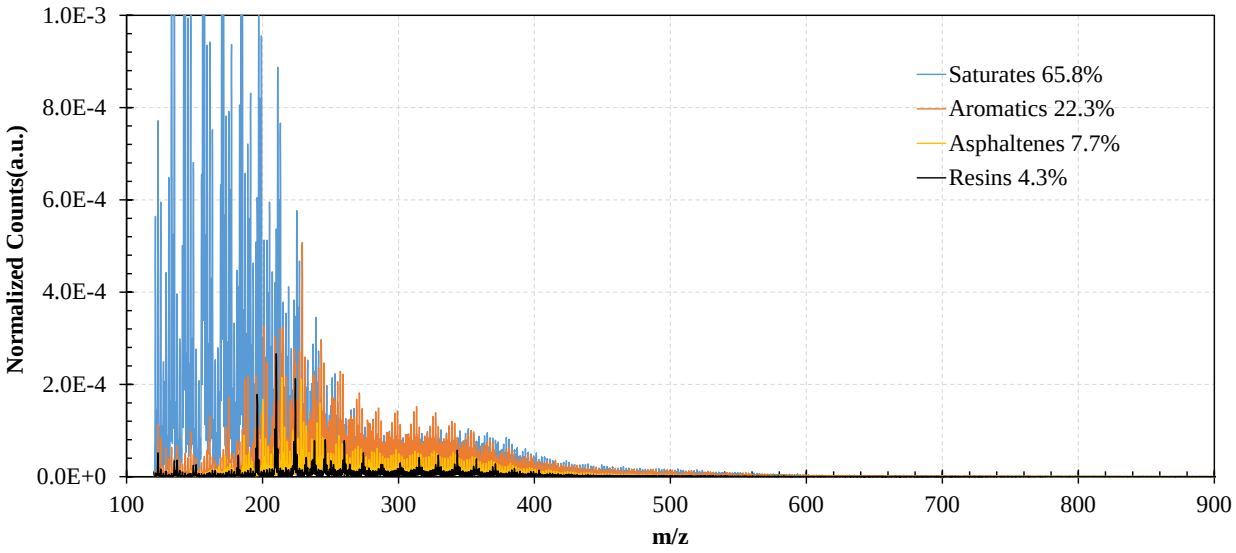

Fig. 21-Santa Clara mass spectrometry distributions, normalized and weighted by SARA fraction.

The mass spectrometry distributions of the Santa Clara (Figure 21) are significantly different than those previously described. First, all of the fractions are significantly lighter than those of the more viscous, heavier crudes. Furthermore, the saturate fraction is much greater. This results in a less viscid crude that is more difficult to emulsify and with a much larger weathering loss fraction. The concentration of the Nalco Flow 12021 in this crude was unknown, but it likely influenced the low viscosity directly or by the influence it had on crude oil in the reservoir by freeing up lighter fractions. The MSDS of Nalco Flow 12021 specifies that it contains mainly methanol (60-100%), heavy aromatic naphtha (1-5%), and naphthalene (0.1-1%), a double-ringed aromatic hydrocarbon. Depending on the amount injected, it may have formed a significant portion of this oil. The Santa Clara asphaltene fraction, according to Jokuty *et al.* [17] is 13%, while this study showed an asphaltene fraction of 7.68%. This suggests that both time and the injection of Flow 12021 has changed the SARA fraction distribution. Our study has demonstrated that the addition of Flow 12021 has severely limited the emulsion formation and has allowed the ready use of ISB as an oil spill response method.

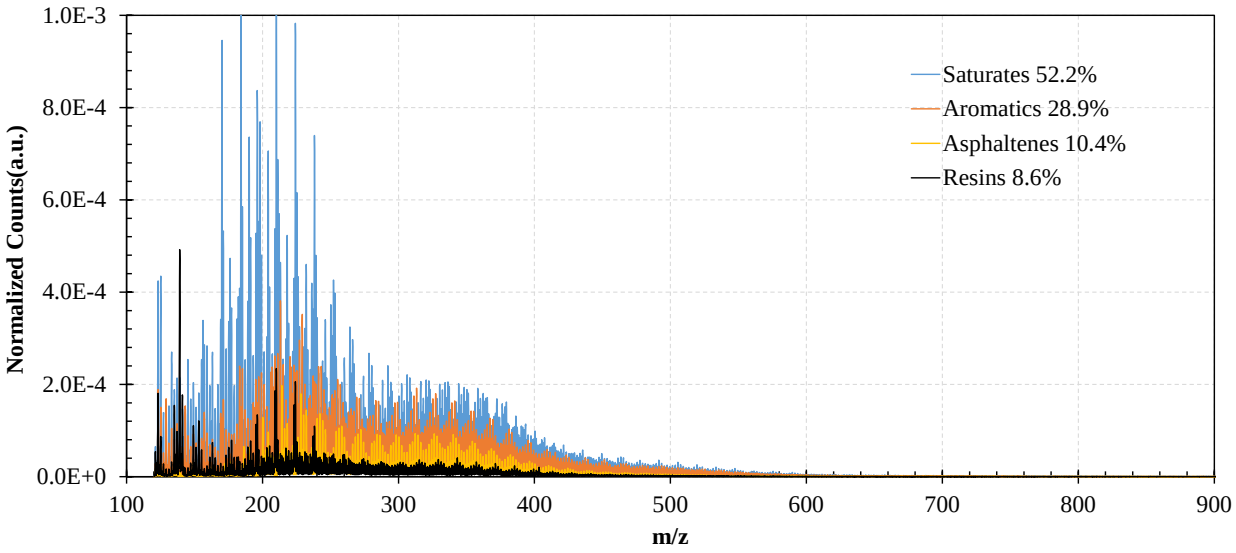

Fig. 22-Carpenteria mass spectrometry distributions, normalized and weighted by SARA fraction.

Carpentaria (Figure 22) also has an additive or well injectant. In this case, it was TerraChem's EB596, an emulsion breaker. Like Flow 12021, it also contains naphtha (50-65%), naphthalene (5-10%), with proprietary ingredients forming the balance of the mixture. In this case, the asphaltene fraction has increased from the time Jokuty *et al.* [17] gathered their data, so we cannot estimate how much of the crude can be attributed to EB596. As we stated for the Santa Clara crude, the addition of EB596 limits emulsion formation, which allows ISB to be a more viable oil spill response method to protect the Santa Barbara Channel coastlines.

Fresh and Weathered Crude Oil Mass Spectrometry Comparisons

It is useful to compare the mass spectrometry of the neat and weathered crudes to understand the effects of the laboratory weathering process. In general, there was a redistribution of the crude constituent distributions, as indicated by the mass spectra. There was indication that weathering at temperatures around 100 ºC for up to three weeks allowed cracking kinetics to the break apart heavier hydrocarbons. We learned that this is one of the risks of laboratory weathering large volumes oil to produce sufficient amounts for the ISB testing that was more apparent for some crude oils than for others.

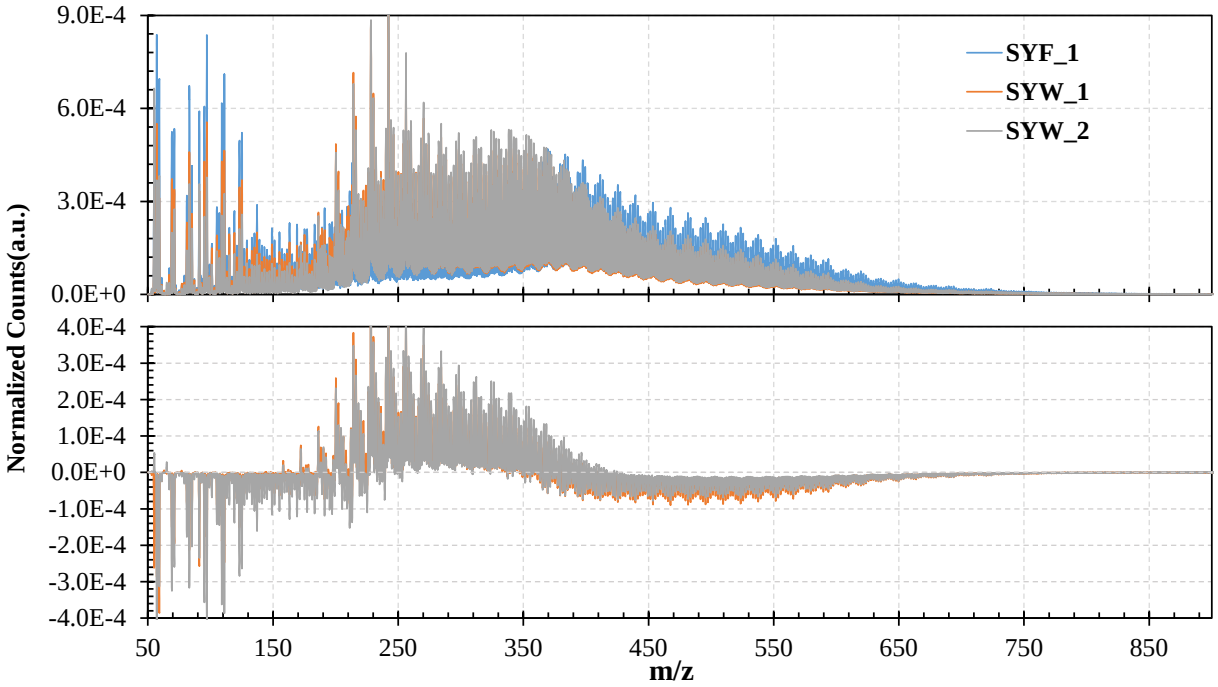

Fig. 23-Comparative MS of fresh and weathered Santa Ynez. The bottom plot shows how much the original distribution lost or gained in each weathering batch. A negative value denotes loss while a positive value denotes a gain.

Figure 23 shows the mass spectra for the fresh Santa Ynez (SYF) and two batches of weathered Santa Ynez (SYW) crude oils. The top plot shows the mass spectra while the bottom shows the changes in the spectral distribution. Negative values indicate a loss while positive values indicate a gain. The fresh, neat oil is denoted by the F while the weathered is denoted by W. As with the SARA spectra, each was normalized so that the redistribution between constituents could be shown. Figures 24 through 26 show the same plots for the other crude oils.

The two weathered batches are distinct, but they have similar trends that we can extract from the comparative plots. For the first weathering batch, the heated evaporation appears to have evaporated the lighter constituents (<170 m/z) and cracked some of the heavier constituents (>370 m/z) to increase the fractions in the intermediate range between. Similar behavior occurred with the second batch and with the other crude oils, but the bottom limit of the cracking appears to be at smaller m/z values. This implies that the weathering process allowed significant variation in chemical processes for the same overall mass loss.

If we compare this result to those of previous studies, we find some significant differences. In the GC/MS and GC/FID measurements reported by Wang and Fingas [43], they show that weathering evaporated unbranched alkane constituents up to C17 (~250 amu or m/z), beyond which the heavier constituents did not evaporate. Sørheim observed the same process in a separate study [44] where oil was heated to higher temperatures, such that it is generally assumed that the lighter hydrocarbons evaporate to leave the heavier hydrocarbons [45]. Evaporation modeling conventionally treats the oil as a single component substance [46], while qualitatively considering that the heavier constituents are what remain behind [2]. For weathering on the ocean, temperatures are much lower than even 80 ºC, so we can assume minimal cracking, but UV-driven photochemistry and the formation of biologically-formed compounds will influence the behavior of spilled oil.

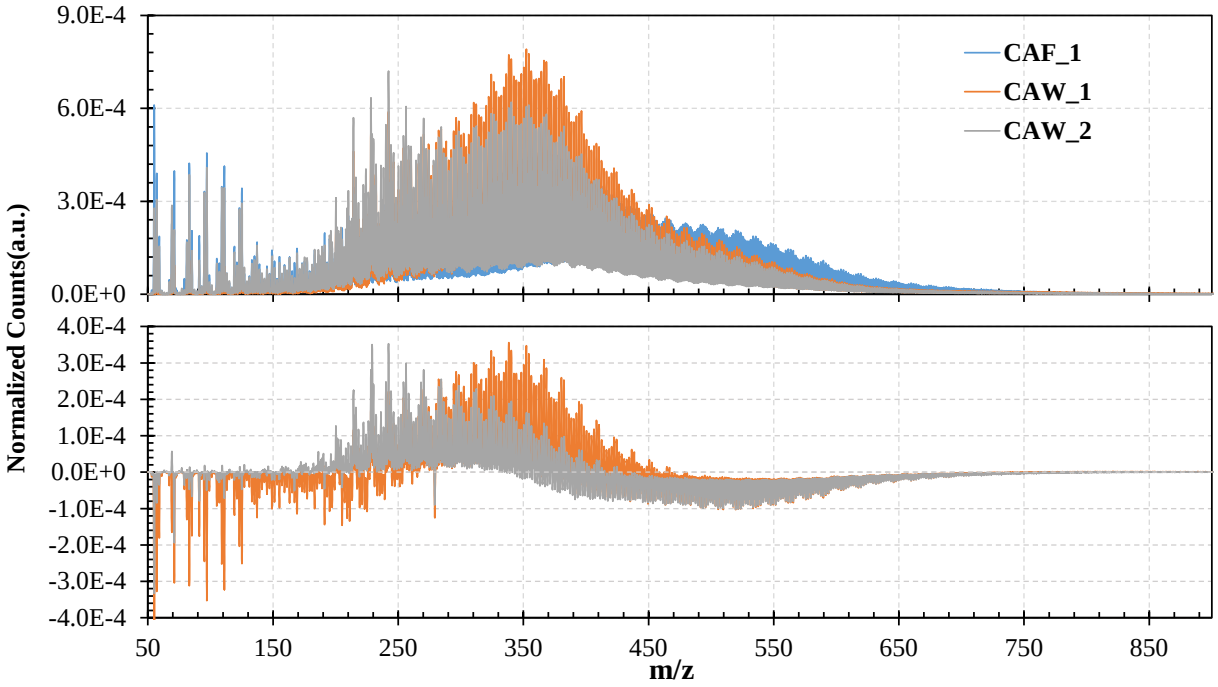

Fig. 24-Comparative MS of fresh and weathered Carpinteria.

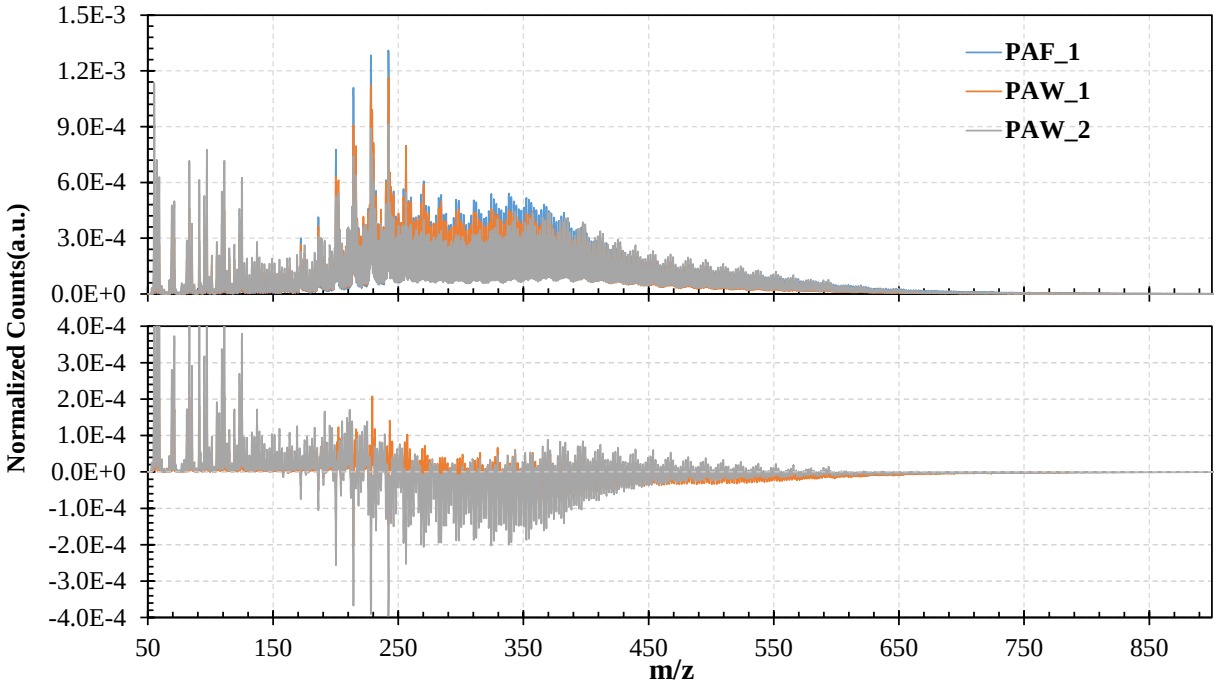

Fig. 25-Comparative MS of fresh and weathered Point Arguello. In order to emphasize losses and gain, the upper and lower limits were adjusted to truncate the lines of some of the more prominent peaks.

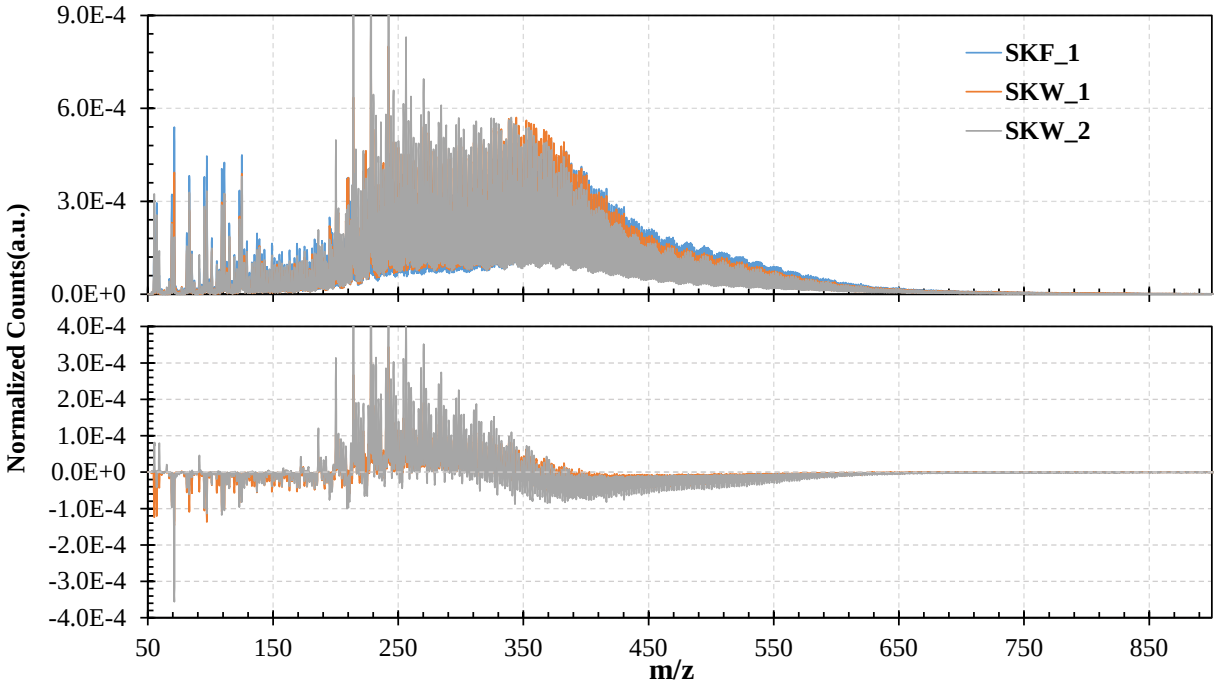

Fig. 26-Comparative MS plots of fresh and weathered Sockeye.

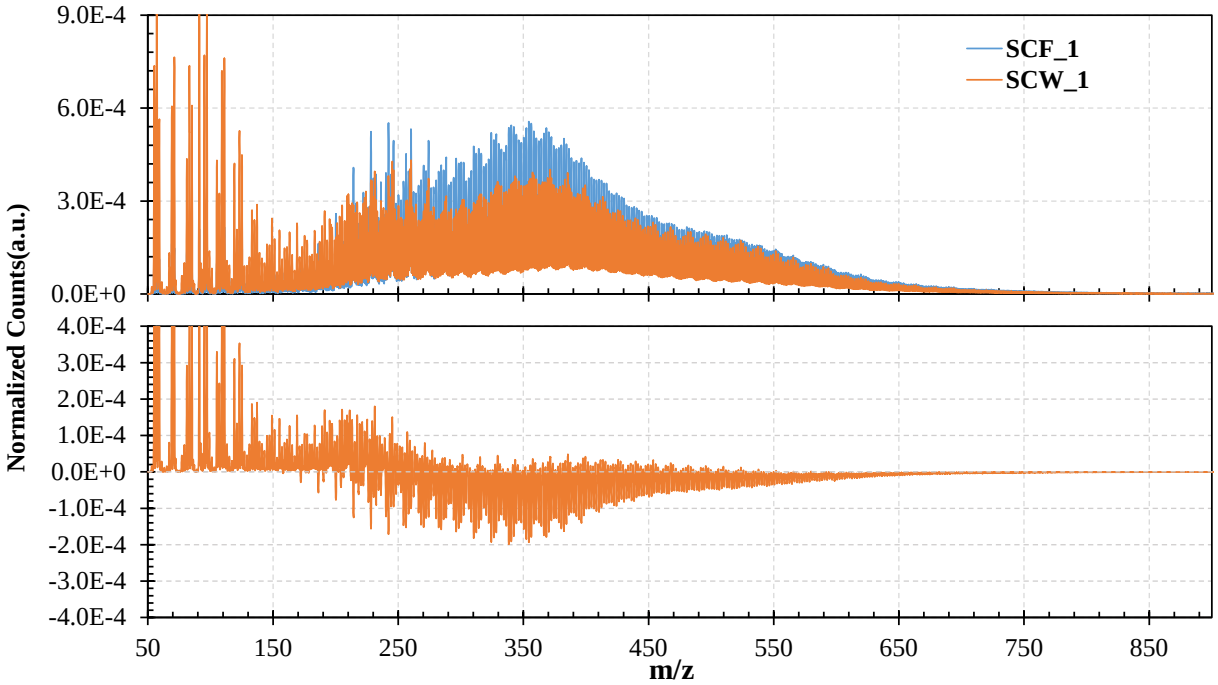

Fig. 27-Comparative MS plots of fresh and weathered Santa Clara.

Though weathering Carpinteria (Figure 24) and Sockeye (Figure 26) produced similar MS trends to Santa Ynez (Figure 23), with variation of where different shifts occurred, while Point Arguello (25) and Santa Clara (27) behaved noticeably different. If we examine the changes in mass for the Point Arguello crude in Figure 25, we see that the constituent mass decreases occurred largely in the middle weight constituents, with some increases in the heavier and lighter weight distributions. The heavy weight constituent increase could have occurred from the effect of mass loss increasing their fraction of the mixture with losses from evaporation. The middle weight constituent losses is most likely from cracking. The increase in lightweight constituents is difficult to understand since it is these constituents that would have needed to evaporate to reduce the mass of the oil. It is possible that the increase is due to the cracking of the middle weight constituents, but it is difficult to know for sure why this oil behaved so differently than the other crudes. Santa Clara, in Figure 27, exhibited similar trends as Point Arguello. There is also the possibility of mass increases from gum deposition reactions with metals in the crude oil [47].

Given the difference in viscosity, density, and asphaltene fractions reported by Jokuty *et al.* [17] and in this report (see Tables 1 and 5), this similar behavior would not have been expected. If we compare the MS plots of the SARA analysis for these two oils (Figures 20 and 21), we can observe little in common. From these results, we can only suggest that the common element between these two crudes must be the chemistry of the constituent hydrocarbons, which is difficult to discern from what data we have.

Cone Calorimetry Residual Mass Spectrometry

All or most of the residual of each cone calorimetry test was gathered for chemical analysis. Of particular interest was which constituent mass ranges increased or decreased from the combined influence of heating, pyrolysis, and evaporation. In the following plots, we will also observe how the presence of water influenced the evaporation and loss of different mass ranges of the hydrocarbon distributions. The cone calorimetry tests were performed in triplicate, so the spectra were averaged before they were normalized.

Fresh Crude

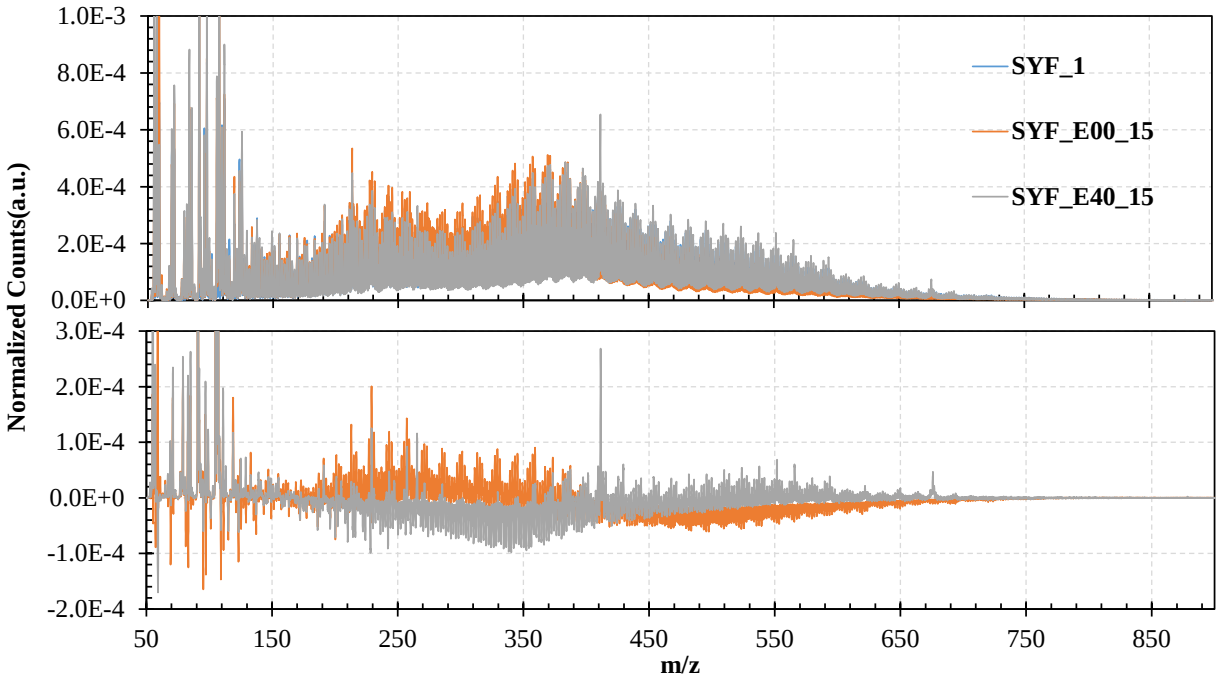

Fig. 28-Comparative MS from fresh and cone calorimetry residues from fresh and 40% emulsions of Santa Ynez. In order to emphasize losses and gain, the upper and lower limits were adjusted to truncate the lines of some of the more prominent peaks.

Figure 28 shows the mass spectra of fresh, unburned Santa Ynez with the averaged mass spectra of the residuals of the neat Santa Ynez crude and a fresh, 40% emulsions in the top plot; the bottom shows the differences between these residuals and the unburned oil. In the legend, F or W define the oil as fresh or weathered, while E## denotes that the sample was emulsified with ##% seawater and the 15 denotes that the cone calorimeter heat loading was 15 kW/m^2. Negative values in the bottom plot denote a loss of that mass component while positive values denote a gain. What is immediately noticeable is that the MS of the fresh oil is completely obscured by the residuals in the top plot; their counts span higher and lower than the baseline oil. For this reason, the bottom difference plot is essential to visualizing the changes in the oil. In the bottom difference plot, we can see that there is both gain and loss across wide regions.

There are some general trends that we can observe in Figure 28. First, the neat oil underwent more loss of the heavier hydrocarbons above ~410 m/z than the emulsified. This can be understood in terms of the higher flame temperatures and oil temperatures of the neat oil: the fuel vapors were undiluted by water vapor, the liquid oil was not cooled by water evaporation, and the longer burn times allowed evaporation or cracking of the heavier hydrocarbons (see Figure 6). In contrast, the emulsion produced a positive shift in the heavier hydrocarbons, which we can attribute to minimal cracking and the general evaporative mass loss increasing their fraction – which we can term evaporative concentration. Another possible mechanism that could have increased the heavier fractions is thermal oxidation that can form larger, heavier hydrocarbon molecules. These reactions have been studied in fuels since they form solids and surface deposits [47-49]. Metal ions, more prevalent in crude oils than in distillates, initiate these reactions by forming alkyl free radicals, which form peroxides, which then form solid deposits [47,48]. Oxygen from

the surrounding air or from heated water assists in the process, as well as dissolved oxygen that has diffused into the oil prior to and during combustion [49].

Between 170 and 410 m /z, there is also opposite behavior between the two samples: for the neat crude's residual, the middle weight constituents increased while they decreased for those of the 40% emulsion. The increase of the middle weight constituents of the fresh crude's residual suggests that the heavier weight constituents cracked instead of evaporated. If the heavier constituents had evaporated, it is reasonable that the middle weight constituents would have also evaporated and undergone a net decrease too. The loss of the middle weight constituents of the emulsified crude suggest evaporation and/or cracking. The lightweight constituents (<170 m/z) underwent both gains and losses as evaporation and combustion removed some constituents and heavy-hydrocarbon cracking added others. Given that the final, burned crude residue was very viscous, sometimes nearly solid, and frequently exhibited indications of coking, the increase in the lightweight fractions suggest that they were formed and then may have been trapped within the residual by the very slow mass transport.

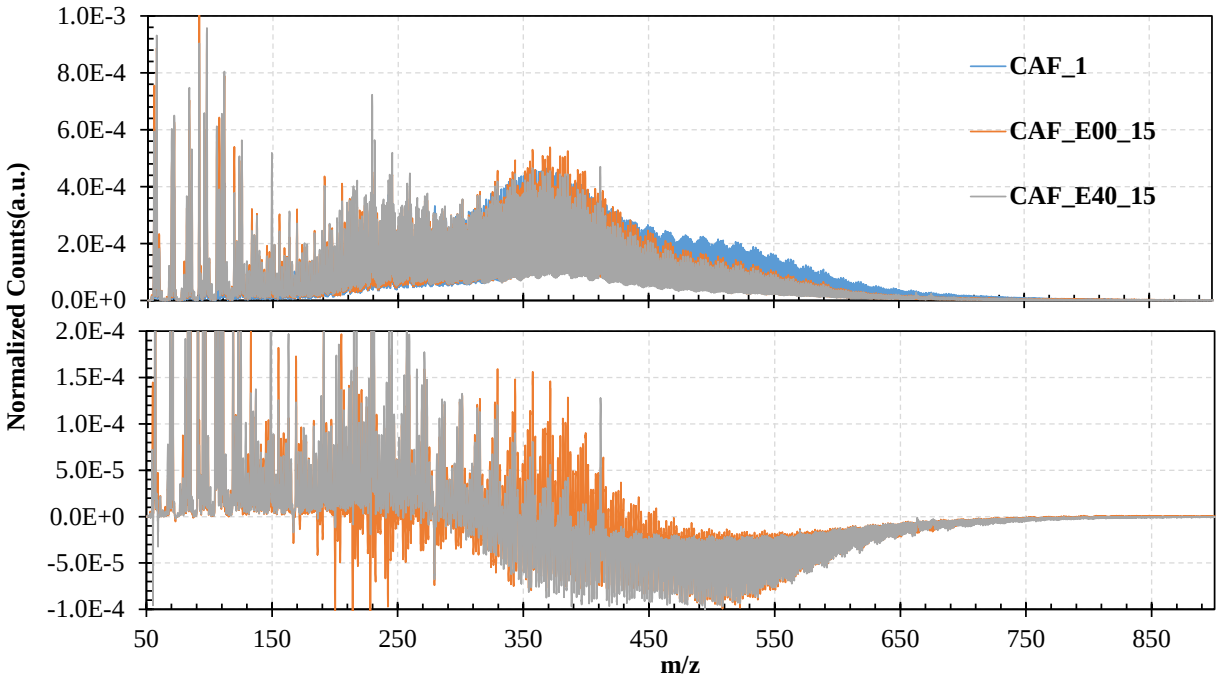

Fig. 29-Comparative MS from fresh and cone calorimetry residues from fresh and 40% emulsions of Carpinteria.

Though the MS plots for fresh and 40% emulsified Carpinteria in Figure 29 are similar to those for the Santa Ynez in Figure 30, we can observe some significant differences that we can attribute to the lighter weight of the Carpinteria and different chemistry. First, we see that hydrocarbons with masses greater than 290 m/z underwent cracking losses for the emulsion, there were regions or bands in the same span that underwent net gains as cracking rearranged hydrocarbon constituent mass distribution. Shifts to both sides of zero extend down to 170 m/z for the neat crude. As we find the other crudes, there is rarely any region for any oil that does not undergo some change by evaporation or cracking. What is curious to note is that there was a net gain for the lightweight hydrocarbons under 170 m/z, suggesting that even with evaporation in that range, the cracking from the heavier hydrocarbons played a significant role in the change in chemistry.

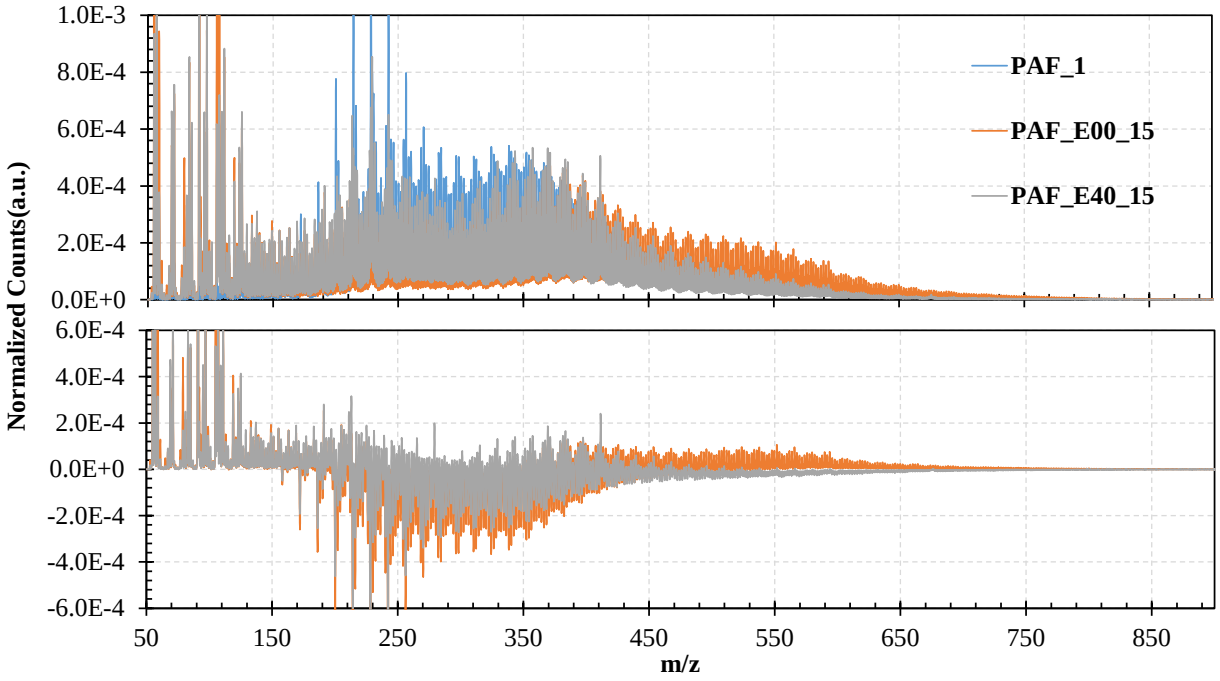

Fig. 30-Comparative MS from fresh and cone calorimetry residues from fresh and 40% emulsions of Point Arguello.

The Point Arguello residuals in Figure 30 show significant differences that either the Santa Ynez or the Carpinteria oils discussed. First, there was significant gain in the heavier hydrocarbon ranges for the neat crude and only a moderate loss for the emulsified, while both exhibited loss in the midrange and gains in the lightweight fractions. The heavier fraction gains for the neat Point Arguello could be attributed to evaporation losses across the middle weight fractions, but there is also the possibility that reactions could also form heavier hydrocarbons to increase the heavier fractions, which corresponds to the coking at the sample surface, as discussed earlier. If such reactions occurred, the lower temperatures of the emulsion, cooled by water evaporation, may have been what prevented similar coking reactions. We should also consider that the Point Arguello is much more viscid than the other oils, even at high temperatures, which would have prevented the transport of the lightweight hydrocarbons to the sample surface to burn and allowed significant coking of the oil at the surface. This suggests that the chemistry of the residual is not only influenced by that of the original oil, but by the transport and thermodynamic cooling behaviors of the oil and emulsion.

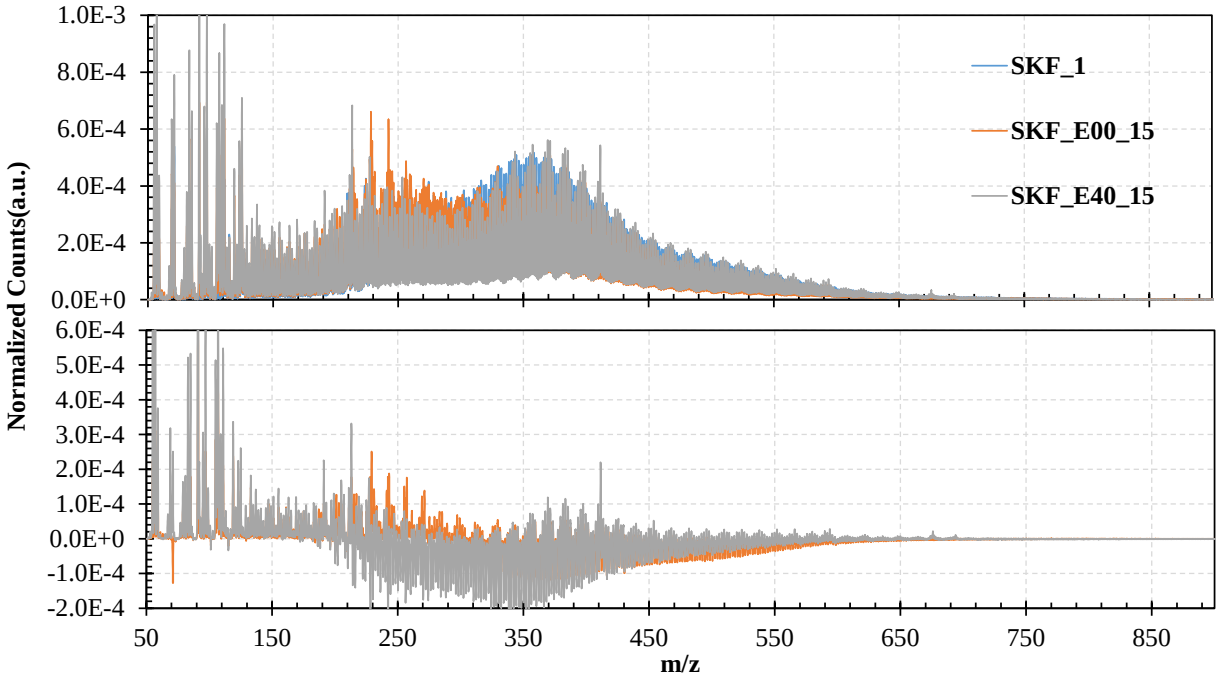

Fig. 31-Comparative MS from fresh and cone calorimetry residues from fresh and 40% emulsions of Sockeye.

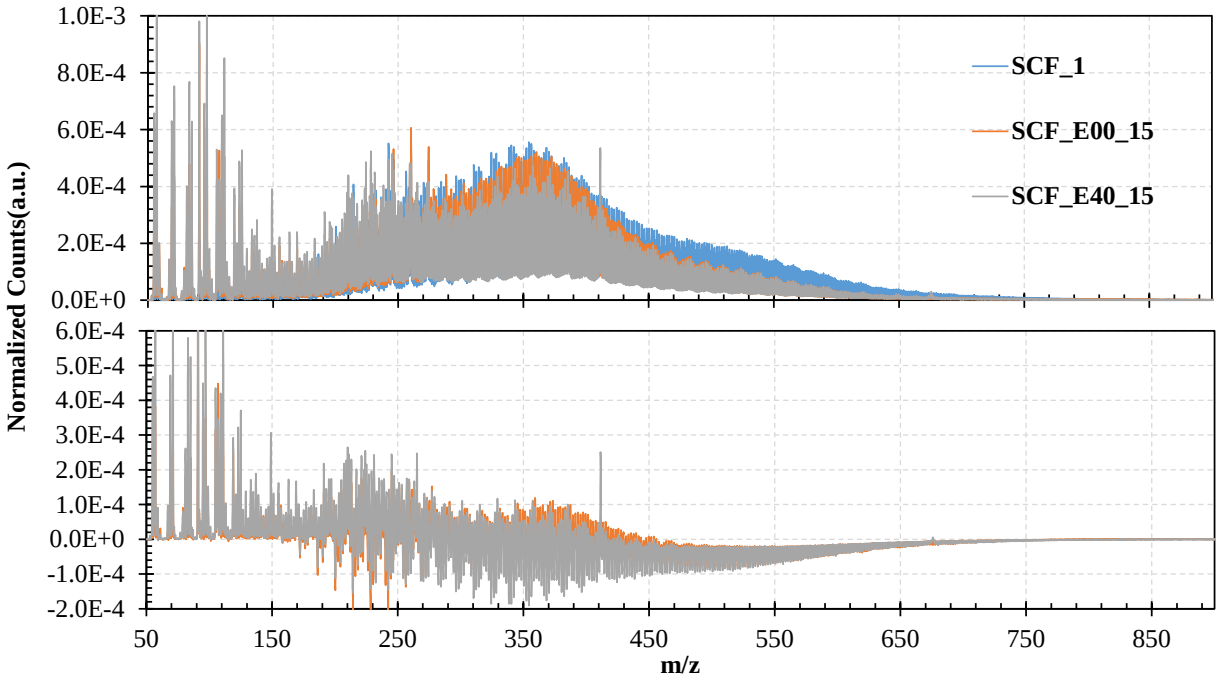

Fig. 32-Comparative MS from fresh and cone calorimetry residues from fresh and 40% emulsions of Santa Clara.

The MS plots in Figures 32 and 31 for Santa Clara and Sockeye, respectively, show similar trends those found in Figures 28 and 29 for Santa Ynez and Carpinteria, respectively. There is a general loss in

mass for the heavy and middle weight fractions that show dependency on emulsification, and thus sample temperature, while there are gains for middle and lightweight fractions and some ranges of the heavy fractions.

Weathered Crude

Figure 33 shows the mass spectra of weathered Santa Ynez crude oil with the corresponding residuals from the neat weathered and a range of emulsion fractions. If we recall from the Cone Calorimetry Results and the heat release trace in Figure 6, emulsified crude oils burned for shorter periods of time with short durations of high heat release rates, with decreased burn durations as the emulsion fraction increased. We can also assume that the presence of water vapor in the plume would act as a diluent to lower the flame temperatures. The effects of these influences are seen in the mass spectra and the associated trends in Figures 33 through 36. We also observed similar trends in the emulsified crude results from the ISB testing shown in Figures 38 through 47.

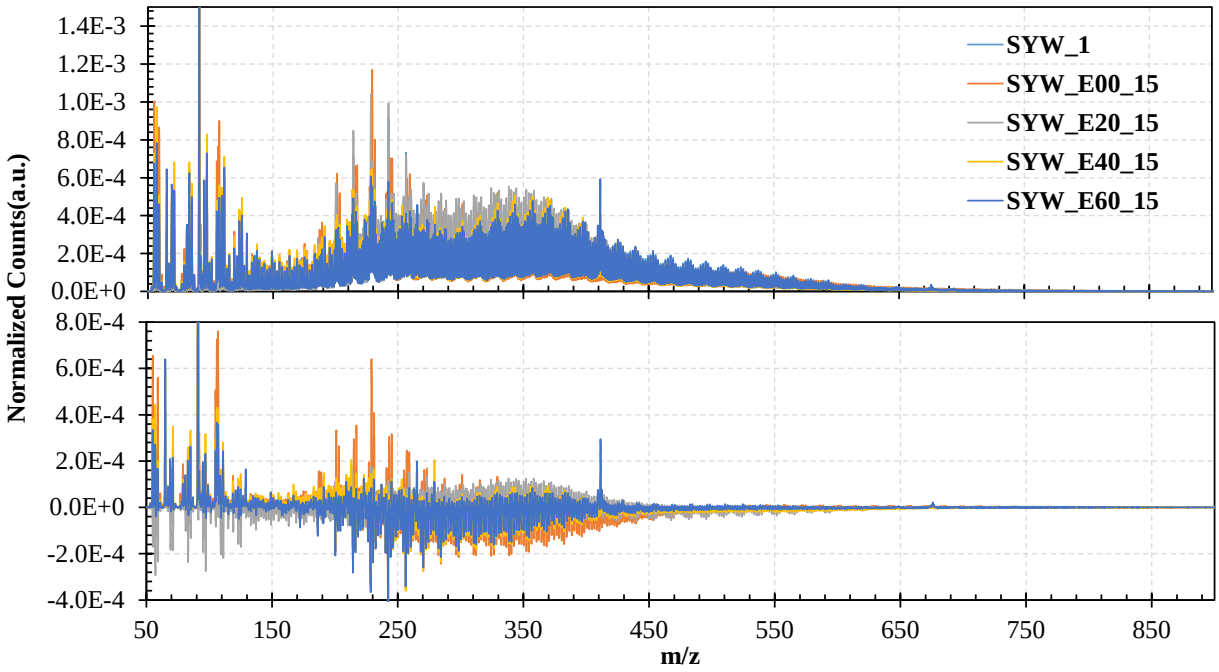

Fig. 33-Comparative MS from weathered and cone calorimetry residues from weathered and emulsified (0-60%) Santa Ynez.

From Figure 33 plots, we observe some general trends with this oil that we observe with other crudes. First, there is a decrease in the loss of the heavier hydrocarbons as the emulsion fraction increased. Higher temperatures are necessary to decompose heavier crudes [37-39], and as the water fraction increased, the combustion temperature decreased. Cracking could not then occur at higher molecular weights with the added cooling of the water. We can see a general shift left of the cracked mass distribution in the bottom plot of Figure 33 as the mass emulsion fraction increased. Second, the middle weight constituents may either generally increase, generally decrease, or adjacent bands will undergo both, depending on the crude. If there is significant cracking of the heavier constituents, some bands will increase, while others might decrease from cracking or evaporation. Third, lighter weight constituent fractions may increase, even though it is these compounds that evaporate and burn, from the cracking of both the heavier and middle weight constituents. At low enough emulsion fractions, namely 20%, the generation and movement of steam

may increase low-weight hydrocarbon evaporation (as seen in Figure 33 under 170 m/z). Beyond that water fraction, the cooling effect likely dominates and the newly cracked compounds do not readily evaporate.

In subsequent MS plots, the spectra reveal that changes in the constituent mass distribution with cone calorimetry were unpredictable and varied between oils, weathering, and emulsification. Though we can find some similarities in behavior for a given oil, the behavior can change noticeably after weathering, such that their behavior from fresh to weathered cannot reliably be extrapolated or predicted a priori.

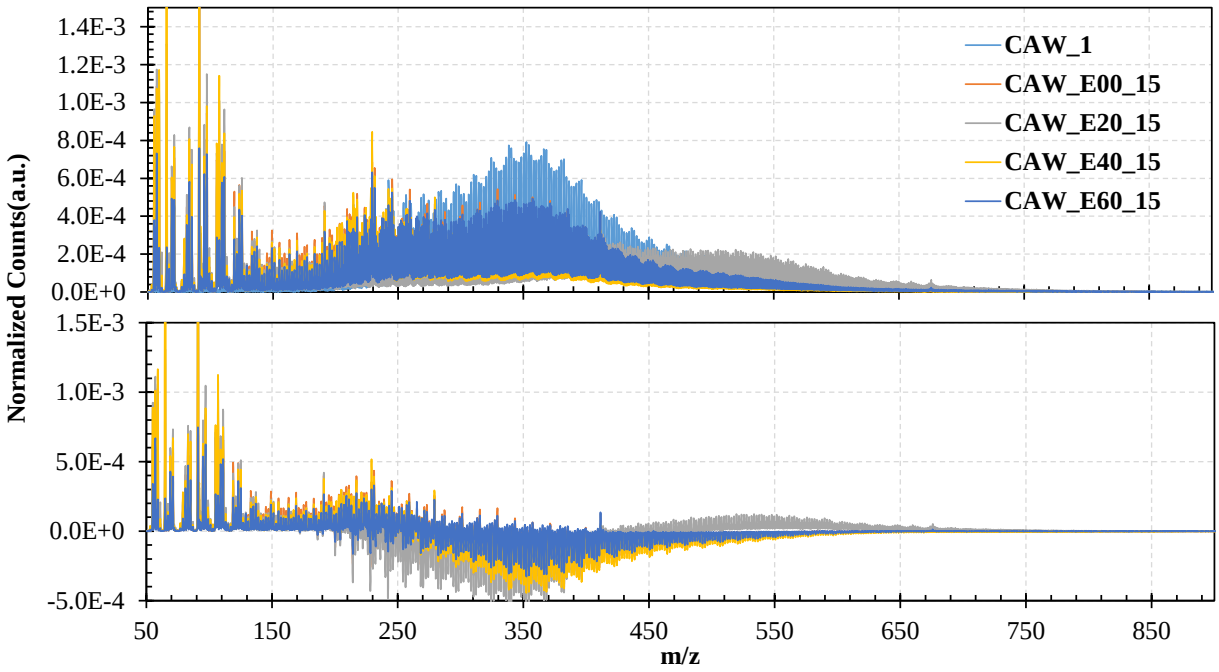

Fig. 34-Comparative MS from weathered and cone calorimetry residues from weathered and emulsified (0-60%) Carpinteria.

The peculiarities of the weathered Carpinteria residual mass spectra differences (Figure 34) show are worth discussion. First, we observe that there is significant increase in the light bands of the mass spectra for all of the emulsions. This suggest that the middle weight constituents underwent significant cracking and shifted mass over to the lighter weight bands. The curious outlier in this study was the 20% emulsion, which showed significant increased mass distribution for the heavier weight constituents, which is likely from the cracking and evaporation of the other constituents increased the contribution or fraction of these heavier constituents, as well as the possibility of reactions forming heavier hydrocarbons.

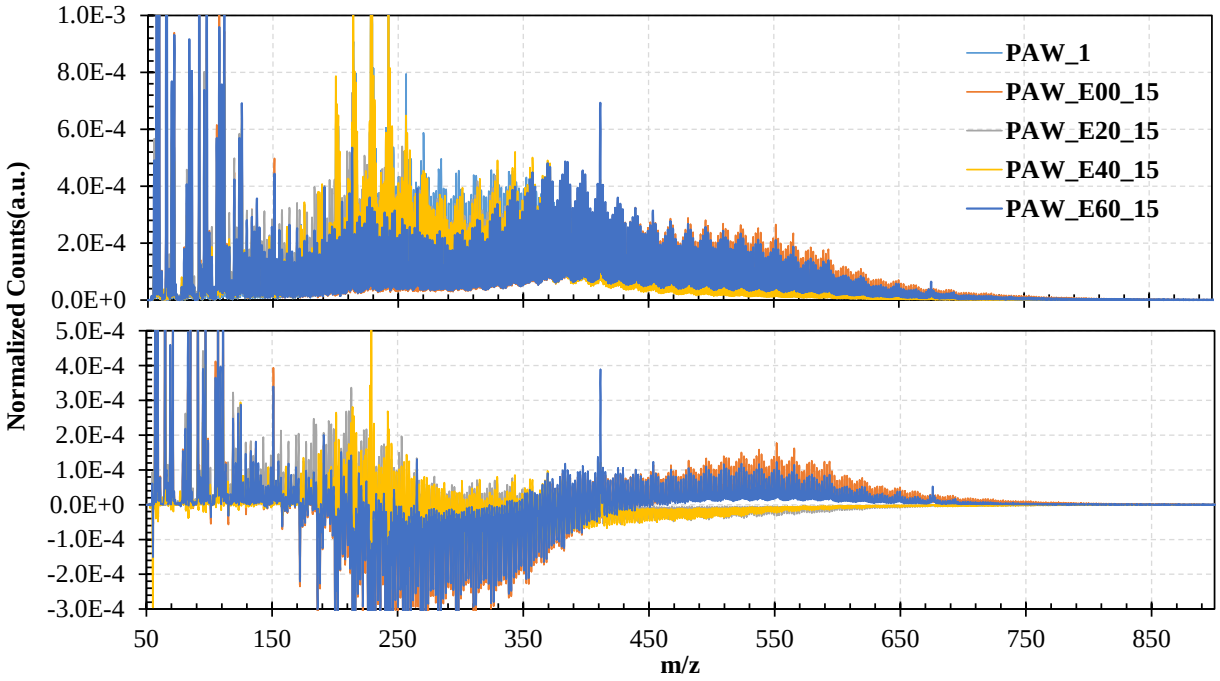

Fig. 35-Comparative MS from weathered and cone calorimetry residues from weathered and emulsified (0-60%) Point Arguello.

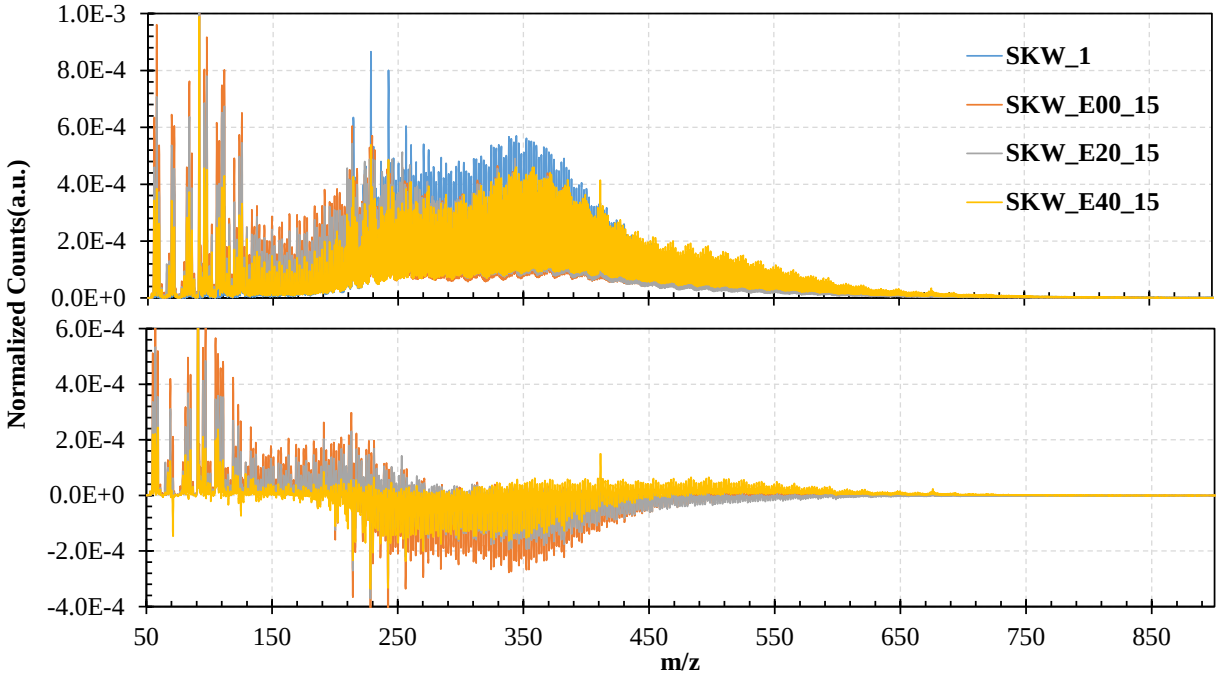

Fig. 36-Comparative MS from weathered and cone calorimetry residues from weathered and emulsified (0-60%) Sockeye.

The MS plots shown in Figure 35 for the weathered, either neat or emulsified, Point Arguello burn residual MS shows some significant similarities and differences from those shown in Figure 30 for the fresh, neat or emulsified, burn residuals. First, the residual MS from the neat, weathered Point Arguello shows increases for the heavier constituents, losses for the midweight constituents and gains for the lightweight constituents that is similar to the residual from the fresh neat Point Arguello. Simultaneously, the weathered, emulsified residual MS plots almost all look similar to that from the fresh, emulsified MS plots; small losses for the heavy constituents, moderate losses and gains for the middle weight, and gains for the light weight fractions. This suggests that the low weathering fraction changed little of the chemistry, which allowed consistent behavior between the fresh and weathered residual chemistry. This same behavior was observed for the weathered Sockeye residuals in Figure 36, which produced similar trends as with the unweathered Sockeye residuals in Figure 31.

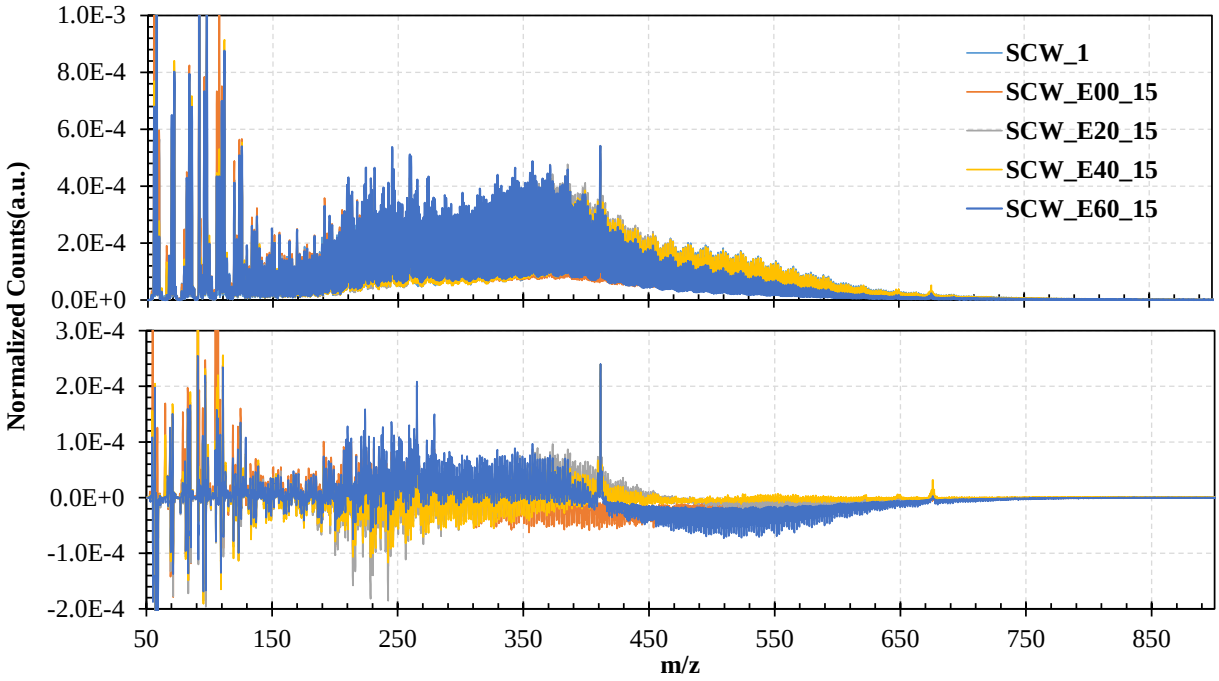

Fig. 37-Comparative MS from weathered and cone calorimetry residues from weathered and emulsified (0-60%) Santa Clara.

Unsurprisingly, the shifts in mass distribution for a lighter crude like Santa Clara was significantly different than others, as shown in Figure 37. For all but the neat and 60% emulsion, there was little significant loss or gain of heavier hydrocarbons and considerable drop in the middle weight constituents, which might be explained by the lower emulsion flame temperatures, which would have left the heavier hydrocarbons less affected. The losses of the neat, weathered oil extended from the heavy constituents into the middle weight constituents. For the weathered 60%, there was significant losses for the heavier constituents and gains for the midweight constituents. If we consider the cone calorimetry peak heat fluxes shown in Figure 12 for the weathered, 20-60% emulsified, there was significant heat transfer back to the sample. For the weathered, 60% emulsified Santa Clara oil, the additional water must have enabled higher peak temperatures and cracked the heavier hydrocarbons. Though, the reasons or mechanisms are not clear at this time.

In Situ Burn Pan Residuals Mass Spectrometry

In general, we observed similar behavior in the MS for the ISB residuals as we observed for the cone calorimetry, but some experimental differences between the two platforms should, as expected, drive some different results. The first significant difference is that the water separated from an emulsion in the ISB experiment either evaporated at the slick surface or sunk below the oil to the large reservoir beneath the sample slick. As a result, there was much less boiling at the oil-water interface for emulsions, other than at 20%, and when there was it was delayed. The reduction in boiling and the freedom for the separated water to sink to the reservoir below influenced the MS of the emulsified samples. Similar to the cone calorimetry, some ISB oil conditions were performed in triplicate, while others were performed singly as a witness burn to determine whether or not that oil condition ignited. Therefore, some conditions were tested multiple three times, providing three residual samples, while others were not.

Fresh

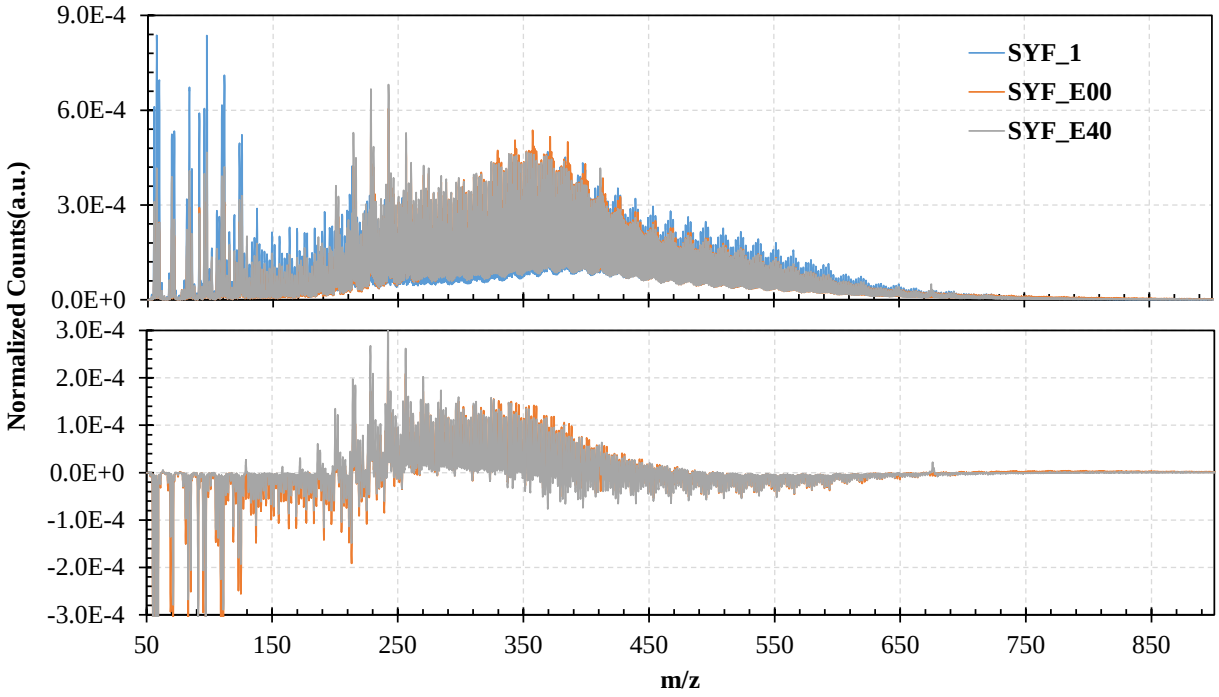

Fig. 38-Comparative MS plots of neat and ISB residues from neat and 40% emulsion of Santa Ynez.

Figure 38 compares the MS of the fresh crude with those of the ISB residues from the neat and 40% emulsified Santa Ynez. It is curious to note that the burn residues of all three samples appear very similar, while the differences from the residues reveal that in general, the heavier fractions reduced from cracking, there was an increase in the middle weight fractions, and there was a significant decrease in the lighter weight fractions. If we recall from the ISB behavior discussed in In Situ Burn Pan Results and Figure 17, the burn stability was not as widespread over the slick and the burn duration for the emulsified was significantly shorter than for the neat crude. Even with this difference in burn behavior, the MS plots suggest that emulsification had very little influence on the evaporation and cracking of the oil. This suggests that the preheating from the accelerant broke the emulsion before or early in the ignition process, such that the burn behavior of both samples produced similar chemical changes. More careful measurement and analysis of the burn process is necessary to elucidate the details of the ISB emulsion breaking process.

Figures 39 through 41 show and compare the MS of the neat oil with those of the residuals from fresh and 40% emulsions. For the most of the oils, there are similar trends: the heavier fractions cracked and reduced that drove an increase in the middle weight fractions, and there was a significant decrease in the lighter weight fractions.

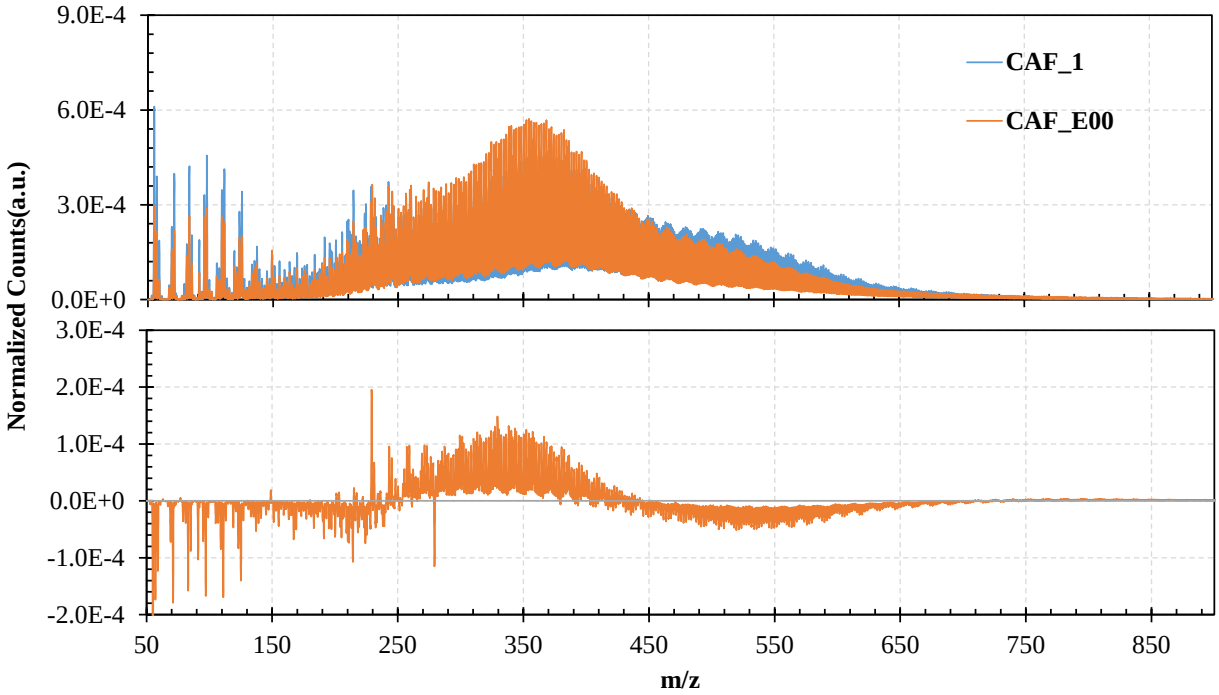

Fig. 39-Comparative MS plots of neat and ISB residues from neat Carpinteria. The 40% emulsion did not ignite.

The MS plot for the fresh Carpinteria ISB residual in Figure 39 is remarkable similar to that of the fresh cone calorimetry residual shown in Figure 29 in shape, except for one aspect. There were net losses instead of net gains for the light fractions as observed for the cone calorimetry tests. We could suspect that a possible reason for this is that boilover occurred during the ISB tests for the fresh, neat oil but did not occur for the corresponding cone calorimetry tests. When the water at the oil-water interface boils, it drives convective mixing and aeration that allows the lighter constituents to freely evaporate and diffuse. Similar boiling and the resulting mixing and aeration is impeded by the water jacket surrounding the cone calorimetry sample pan. In contrast, we see that for the Sockeye (Figures 31 and 41) and Santa Clara (Figures 32 and 43) crude oils, the lightweight fractions increased as they did for the cone calorimetry tests, revealing that these remained in the oil while they evaporated for the Carpinteria. Yet, all of the fresh, un-emulsified crude oils underwent boilover during ISB pan testing, so we cannot assume that boilover is primary driver. Why the lightweight constituents underwent a net loss for one crude oil and not the other is difficult to surmise, since it depends so much on the aspects of the crude and processes that we did not measure in detail during either of the burn experiments.

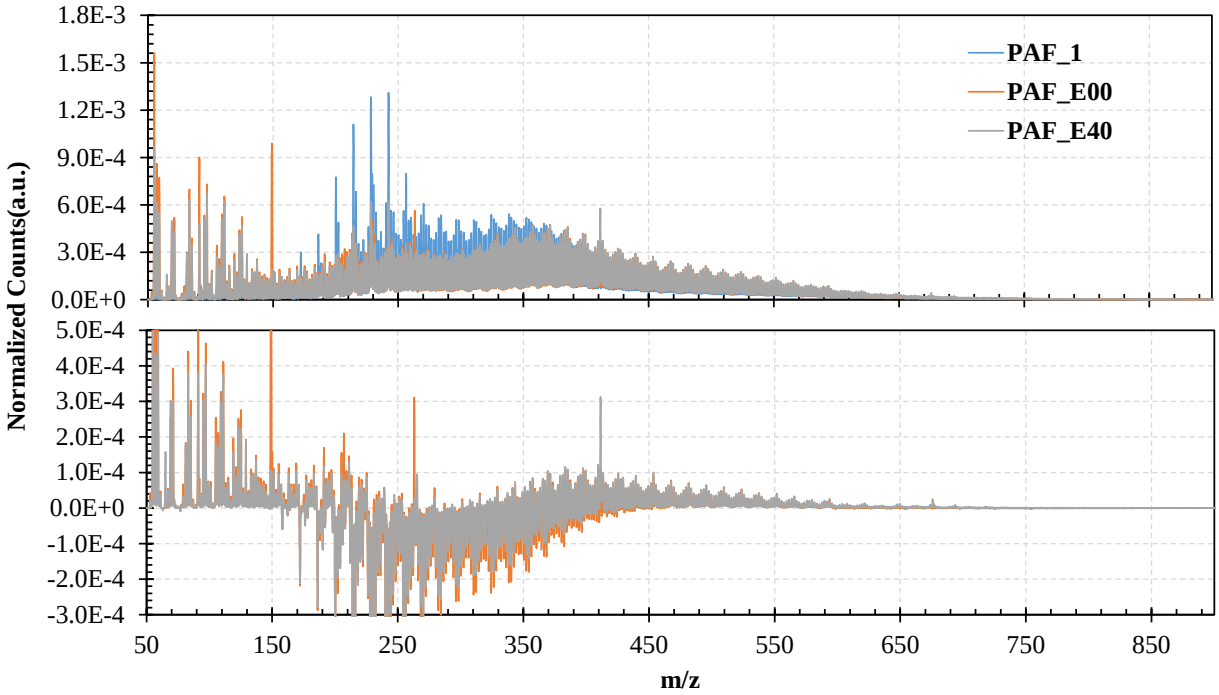

Fig. 40-Comparative MS plots of neat and ISB residues from neat and 40% emulsion of Point Arguello.

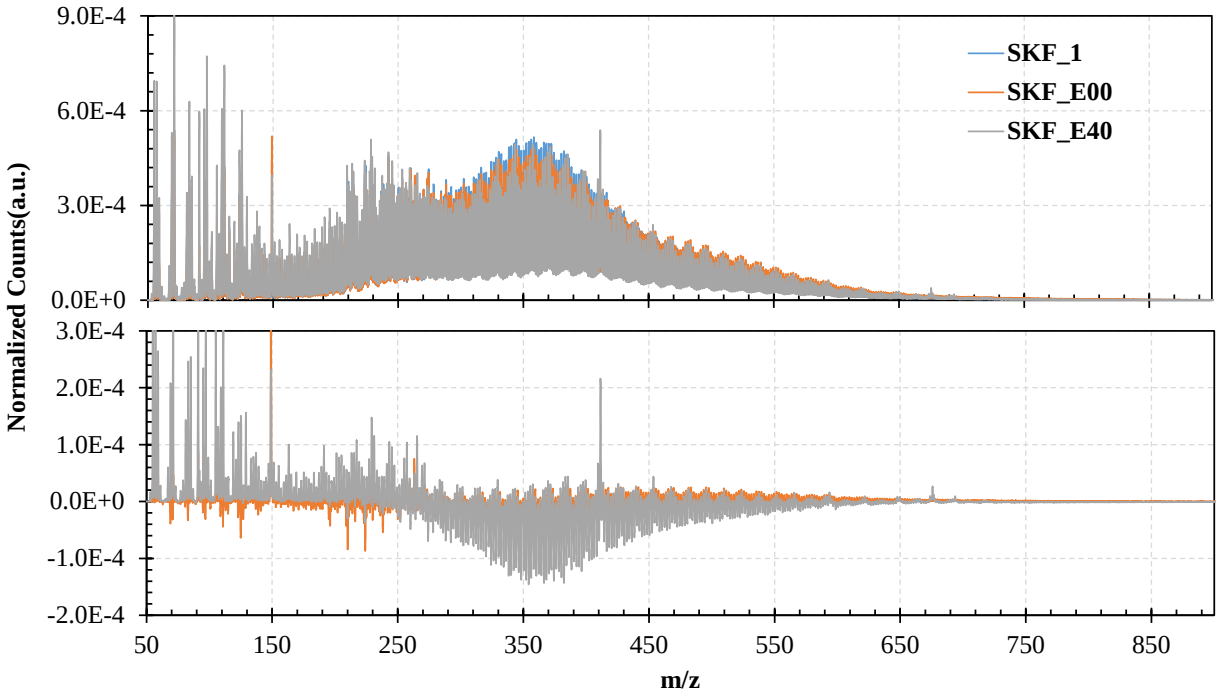

Fig. 41-Comparative MS plots of neat and ISB residues from neat and 40% emulsions of Sockeye.

The MS plots in Figure 40 show that Point Arguello, one of the most viscous and heavy crudes, with the highest combined resin and asphaltene fraction, behaved differently than the others. The heavier fractions increased, presumably from evaporation and chemical reactions discussed previously. These trends are quite similar to the residual MS plots from the neat fresh and weathered Point Arguello cone calorimetry tests shown in Figures 30 and 35. In this case, as with the Santa Ynez, the ISB testing processes appears to have broken the emulsion before the burn process proceeded enough to allow the emulsion to significantly influence the chemistry of the residual.

The residual MS from the fresh Sockeye exhibited both similar and distinct behavior from what was observed with other oils, regardless of the experimental platform. The most unique aspect of this averaged mass spectra is that there appears to be very little mass loss or gain for the neat-fresh oil. Yet, we observed this oil underwent normal ignition, flame spread, stable combustion, and then oil-water boiling leading to extinction, with significant mass and volume loss from the original oil.

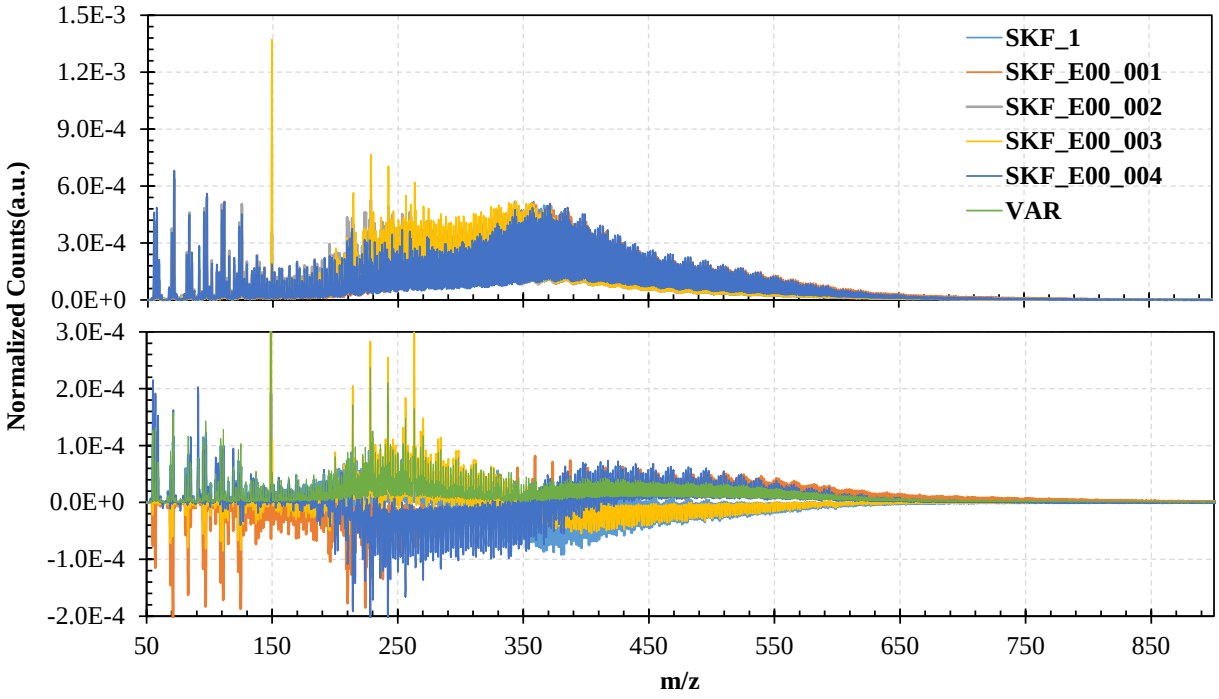

Fig. 42- Comparative, individual MS plots of neat and ISB residues from neat Sockeye. The variance of the ISB tests is plotted by the green line.

In order to understand why the mean spectra appears to imply insignificant loss, it is prudent to examine the residual MS from individual tests, as shown in Figure 42. Unlike tests with other oils, each burn process proceeded so differently that the chemistry of the burn residuals were significantly different. This variability is implied by the large uncertainty of the peak heat flux for the neat, fresh Sockeye in Figure 17. The averaged, normalized spectra implied that there was very little change in the constituent fractions. There are two significant implications from this result. First, test conditions, such as wind conditions, need to be kept as constant as possible. Second, the uncertainty of the MS, needs to be quantified and displayed in some manner. The variance of these tests is shown in the difference plots of Figure 42. Plotting the variance on top of the spectra makes an already noisy plot even more difficult to interpret.

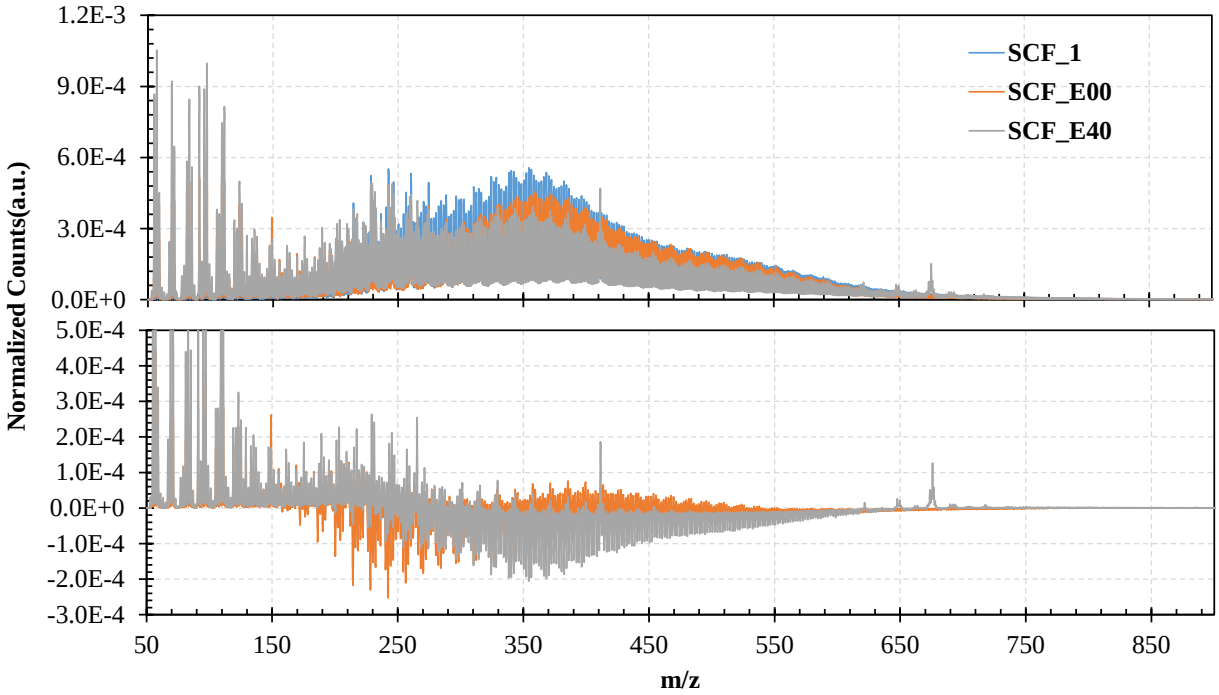

Fig. 43-Comparative MS plots of neat and ISB residues from neat and 40% emulsion of Santa Clara.

Figure 43 plots the mass spectra from the fresh-neat and fresh-40%-emulsified burn residuals for Santa Clara. The most remarkable aspects of these spectra is how similar they are to the corresponding cone calorimetry residual spectra shown in Figure 32. In this case, the two test platforms provided similar chemical processes to yield similar residual chemistries. Why this occurred with the Santa Clara and Point Arguello while it did not occur with Santa Ynez, Carpinteria, and Sockeye is not clear. The inconsistencies point to the individual chemistry of each oil and the influence each experimental platform has on how combustion changes that chemistry.

Weathered

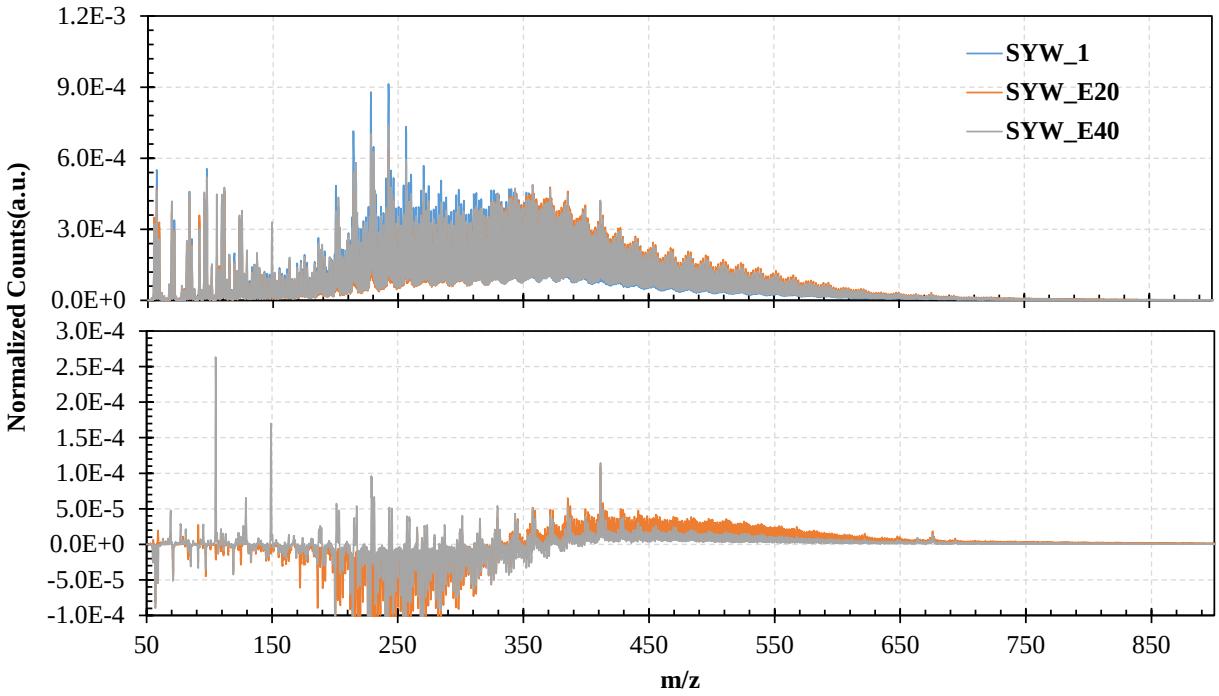

Fig. 44-Comparative MS plots of weathered and ISB residues from emulsions of Santa Ynez.

Figure 44 shows the residual MS from the ISB burn pan experiments for the weathered and emulsified Santa Ynez crude oils. It is immediately clear from the MS spectra and their difference plots that there was significant difference between the 20% and 40% emulsions of the weathered Santa Ynez. First, the 20% emulsion burned more vigorously and produced greater flame heat fluxes than the 40% emulsion, which appeared to only burn off the diesel fuel and then extinguish (Figure 17). The vigorous combustion of the 20% emulsion was accompanied by rapid evaporation of the emulsified water, but there was not significant cracking of the heavy constituents; rather this exhibits evaporative concentration. The MS plots reveal that for the most part, the bulk of the 40% did not undergo significant chemical changes, supporting the hypothesis that most of the observed combustion was due to the diesel fuel, while the 40% emulsion remained largely intact. There was some increase in heavy constituents from evaporative concentration and some significant decrease in middle weight constituents from evaporation and possible cracking. Otherwise, there was little noticeable changes. From this comparison, we can see that the MS data can provide an objective indication of whether the crude oil burned by comparing the MS between the initial and final oils.

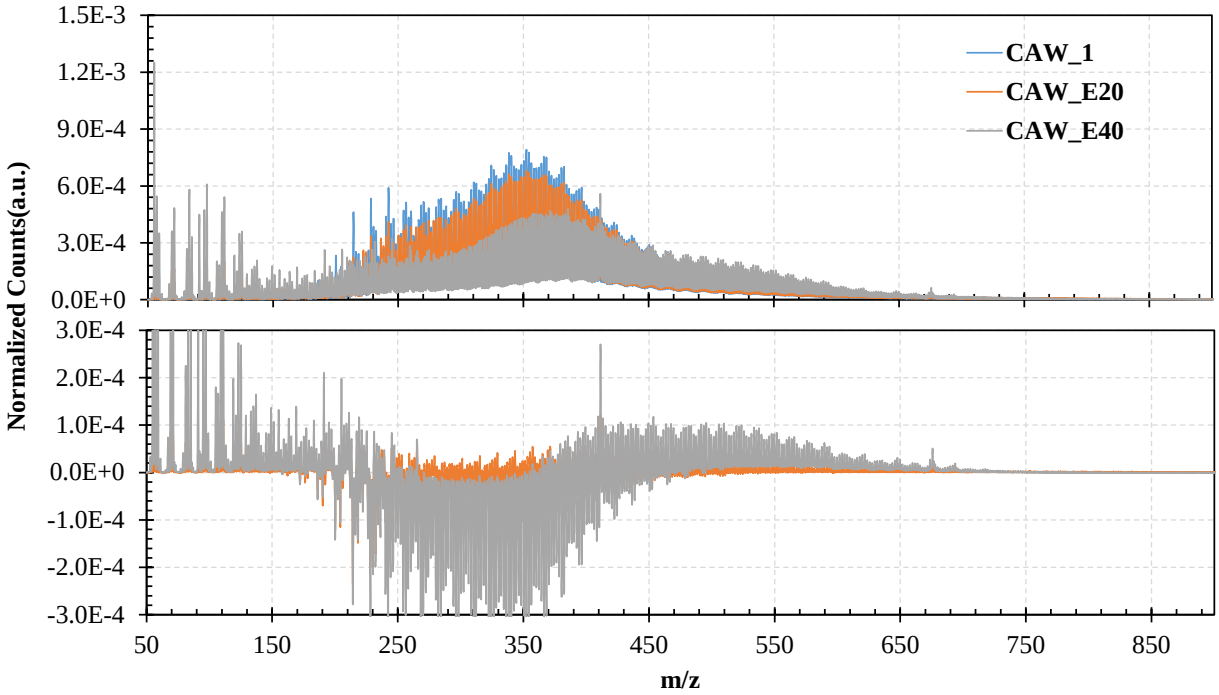

Fig. 45-Comparative MS plots of weathered and ISB residues from emulsions of Carpinteria.

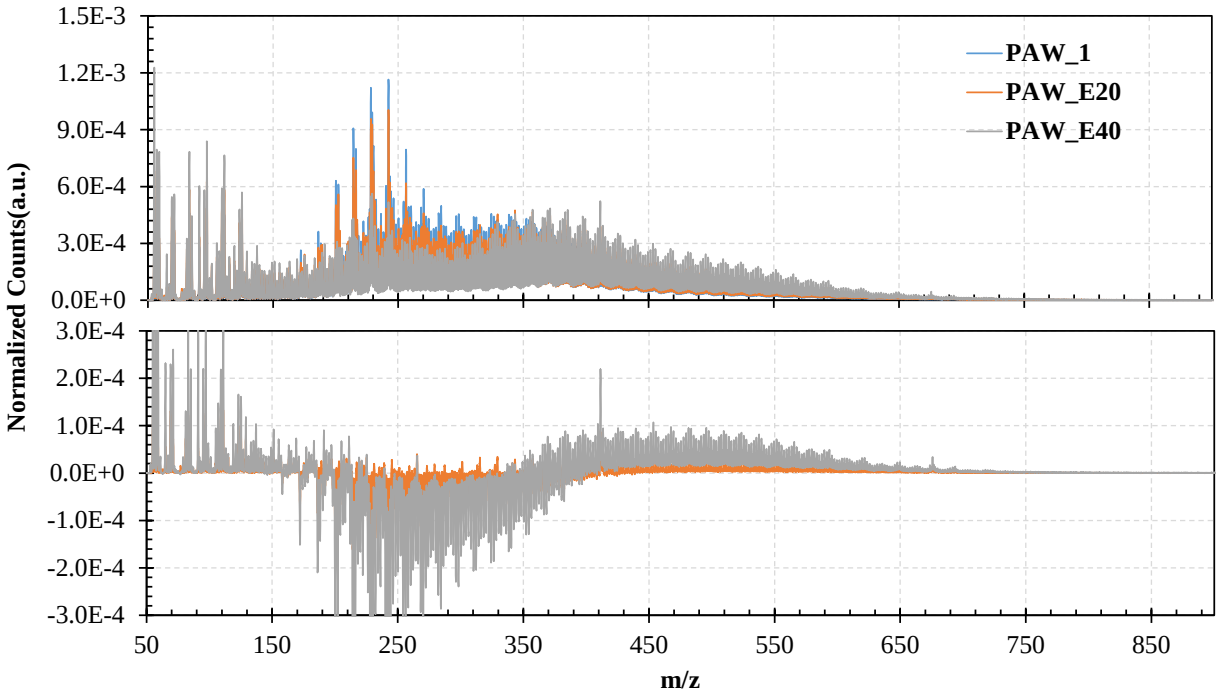

Fig. 46-Comparative MS plots of weathered and ISB residues from emulsions of Point Arguello.

Both the Carpinteria and the Point Arguello residuals exhibited similar behavior for the weathered crude oil ISB tests, as seen in Figures 45 and 46. For the weathered-20%-emulsion tests, the heavier fractions increased, presumably from evaporative concentration, while the middle weight fractions underwent both losses and gains from selective evaporation or cracking that created net losses and gains. The consistent increase in lighter fractions suggest cracking from middle and heavy weight fractions that may not be able to evaporate as easily. The 40% emulsions from Carpinteria and Point Arguello also exhibited similar gains and losses. This is curious in that the chemistry of the two oils is not similar to one another, but the resulting trends of similar test conditions and processes are similar.

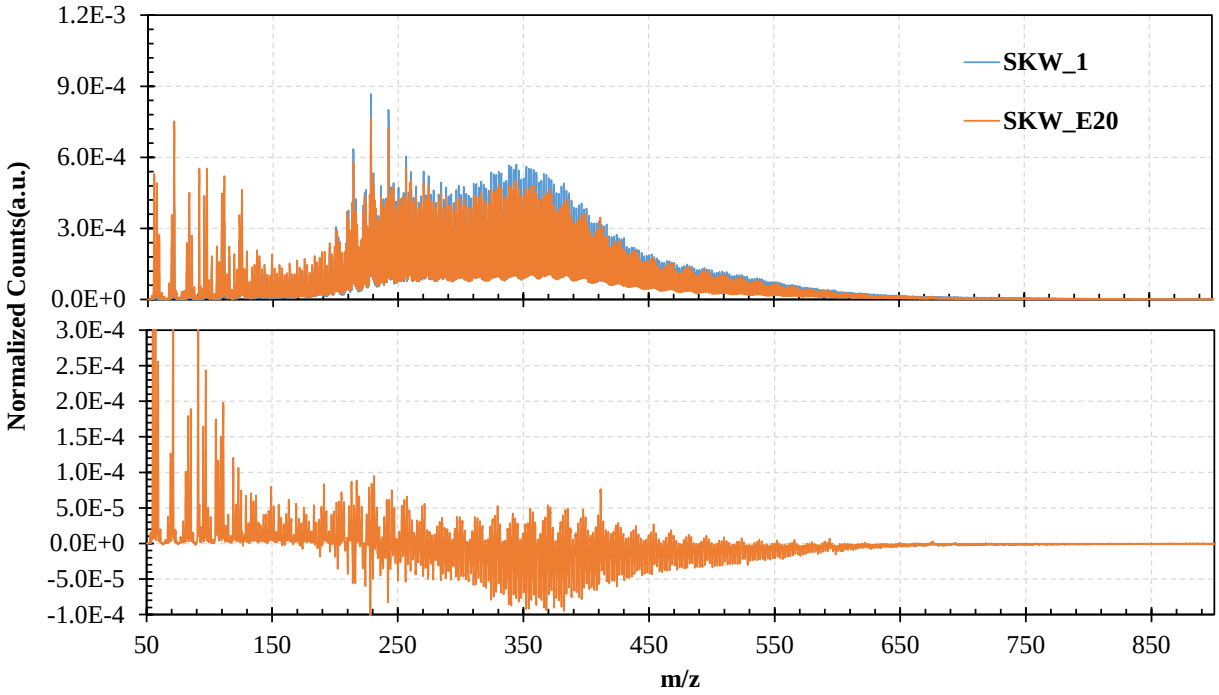

Fig. 47-Comparative MS plots of weathered and ISB residues from emulsions of Sockeye.

As Figure 47 implies, only the 20% emulsion of the weathered Sockeye ignited. The trends appear similar to the fresh-40%-emulsified spectra shown in Fig. 41: the heavier and middleweight constituents underwent net losses while the lightweight constituents increased. Clearly, the same oil underwent similar processes when emulsified, whether weathered or not.

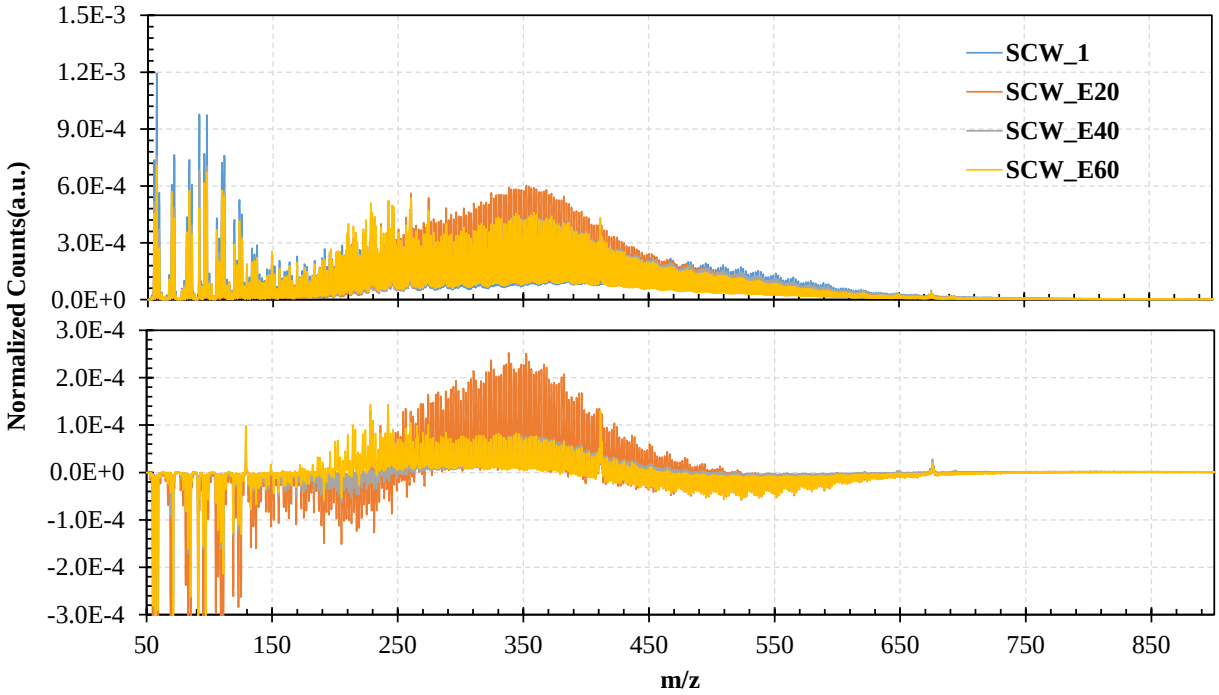

Fig. 48-Comparative MS plots of weathered and ISB residues from emulsions of Santa Clara.

Figure 48 shows the residual mass spectra from ISB of weathered Santa Clara at 20, 40, and 60% emulsions. In general, the trends in the difference plots appear similar to one another. The 20% emulsion, which produces the most efficient burn, showed significant middle weight increases, presumably from evaporation, heavy constituent cracking, and lighter weight chemical reactions. The 40% and 60% emulsion mimicked this behavior, but with less intensity. The most curious detail is that the 40% and 60% emulsion residuals appear to be nearly the same, suggesting that the emulsion breaking and burning processing were very similar between the two.

SUMMARY AND CONCLUSIONS

Pan fire and cone calorimetry experiments have been formulated to replicate in situ ignition and burn conditions found in practical oil spill remediation conditions. Parallel analytical chemistry measurements of the oil before and after testing provide comparative overviews of how initial fractions and constituent mass distributions of the saturates, aromatics, resins, and asphaltenes influence ignition and burn behavior. The pan fire test was been designed to capture, with some conservatism, the ignition behavior of an in situ burn. Actively-cooled water underlying the slick provides a realistic initial condition for the ignition process. Heat flux gages and thermocouples provide time-resolved measurements to qualitatively assess burn rate, vapor plume behavior, and how the oil fire may or may not spread across a larger slick. The cone calorimetry experiment was also designed to capture the ignition behavior and burn behavior, but was able to measure many more burn characteristics because of the size and instrumentation of the experiment.

There were a number of ramifications that this research demonstrates for practical ISB applications. The first implication was that realistically-scaled ignition and burn tests need to be used to determine the ignitability of a particular oil. This burn testing effort has revealed that crude oils previously observed to

be non-flammable can be ignited and burned as long as certain practical ignition practices and scales are used. Of primary importance was that an initial accelerant volume of at least 1 L needs to be spread on a slick of at least 1 m^2 to insure adequate heat transfer rates and sufficient accelerant burn duration to both ignite and sustain initial combustion of emulsified crude oils. Greater accelerant volumes (e.g., 4 L) and slick areas are common in practice and would provide longer duration ignition burns, higher heat fluxes to the slick, and may ignite oils deemed non-flammable by this study. Such considerations are essential when formulating oil spill response plans for government agencies.

Additionally, the passage of time over a reservoir's production lifetime and the use of emulsion breakers or flow improvers alter the chemistry and properties of an oil along with the weathering and emulsion process, which needs to be accounted for in the ISB ignition tests and when formulating and updating oil spill response protocol. Oil properties in Table 1 reveal that crude properties change as different reservoir management and extraction methods change over the time, such as the injection of a flow improver or emulsion breaker. Early in a spill, the emulsion breaker or flow improver will undoubtedly influence emulsification and weathering. In this study, these additives contained light aromatics, saturates, and/or alcohols, which would evaporate more rapidly. As a result, a crude oil may emulsify more as it weathers not only because the original, lighter crude oil constituents evaporate but also because of the emulsion breaker or flow improver constituents evaporates.

Chemical analysis revealed a number insights into how the constituents and their properties influenced the physical and chemical properties of the crude and thus the ignition and burn behavior. Higher fractions of saturates and aromatics assisted ignition, while higher combined fractions of asphaltenes and resins slowed ignition. Saturates and aromatics have higher vapor pressures, resist emulsion formation because of their near-zero polarity, and assist in the early stages of ignition by providing a ready supply of ignitable vapors. Asphaltenes and resins, in contrast, are polar and viscous, which assists in the formation and stability of emulsions. Both resins and asphaltenes require significant heat to endothermically decompose and produce ignitable vapors. Emulsion also require additional heat to break and time for the separated water to evaporate, sink below the slick, or both. The emulsion breaking and water separation (and/or evaporation) processes introduce a crucial delay while the accelerant is burning and suggests that emulsified crudes, especially those with high resin and asphaltene fractions, may need greater accelerant volumes for effective ignition.

Emulsion ignition behavior cannot be predicted by the SARA fraction alone; the distribution of these fractions should also be considered. Greater fractions of lighter weight constituents in resins or asphaltenes may assist in emulsion formation and stability, but these require relatively higher temperatures to endothermically decompose and produce flammable vapors at lower temperatures than heavier resins; two equally stable emulsions at room temperature may separate differently once heated. The converse is also true: greater fractions of heavier weight constituents in the saturates, aromatics, resins, or asphaltenes will slow the ignition process because of their higher boiling and cracking temperatures.

The MS data also show that the presumed higher burning temperatures of fresh, un-emulsified oils appeared to crack heavier constituents during cone calorimetry tests, which sometimes increased the fractions of middle and, in some cases, lighter weight constituents. The lower burning temperatures of fresh oil emulsions did not exhibit this behavior, but instead tended to concentrate evaporatively, or chemically bond to form, heavier constituents. The exception was the weathered, 20% emulsion, which exhibits unusually rapid, vigorous burning. We suggest that the higher heat flux to the slick and the boiling-driven motion allow the heavier constituent fractions to increase through evaporation.

Though ISB and cone calorimetry are good analogs to examine crude oil ignition, we should acknowledge that crude oil undergoes different thermal processes between ISB and cone calorimetry burning, thus we need to expect that the chemistry of the residues will likely be distinct. For example, the

ignition heat flux is unsteady during ISB and constant during cone calorimetry. Once the oil ignited, the heat flux to the oil was from combustion alone during ISB, while the imposed heat flux in the cone calorimetry was both from combustion and the cone heater, insofar as the added radiative heat flux was transmittable through the soot and flames. Furthermore, when the emulsion broke during ISB, the water sank to the large reservoir beneath, while it remained between the pan and the oil during cone calorimetry testing and at times boiled. We also observed that variation in the ISB process from unsteady wind conditions or other variability can influence the resulting mass distribution of the residue. These differences should be kept in mind when seeking to explore the residue chemistry.

We observed that individual MS data can confirm whether an oil actually ignited or was artificially weathered by an accelerant burning. In the case of the Santa Ynez oil, we observed that the MS data indicated some changes in the chemistry for a case that did not ignite, but they appeared to be less significant than weathering. This may indicate a need for different accelerant protocol.

FUTURE WORK AND RECOMMENDATIONS

Future research in this area can address a number of persistent questions about crude oil properties, constituents, and how emulsion characteristics are measured and relate to one another. Current emulsion measurement conventions appear to determine how well a crude oil will emulsify, remain stable, and disperse into the water column [11]. In contrast, ISB ignition is related more to the emulsified water's behavior in the oil during ignition. In particular, what temperatures or energies are required to break the emulsion and whether the water sinks (low viscosity oil) or remains suspended in a crude oil matrix (high viscosity oil). We suggest that the oil's surface tension, viscosity, and the emulsion's initial micelle size distribution drives some of these behaviors and can be related to the thermal stability and the general ignitability of the emulsion. Careful measurement of the emulsion micelle distribution by sampling and microscopy prior to ignition and then during the emulsion breaking process that leads up to ignition would characterise the dependence of ignition with a quantifiable metric of emulsion quality.

These studies required that large volumes of crude oil be weathered, in comparison to laboratory research studies described by Jokuty *et al.* [17] and Fingas [2]. This required weeks of careful monitoring and measuring to insure both safe heating and evaporation, but also that the evaporated fraction was correct. Given the long period of time devoted to evaporative weathering, imposing photochemical reactions by UV exposure may be done, but the amount of photochemical reaction needs to be validated against actual exposures and measurement of those changes.

One of the difficulties with cone calorimetry post-test handling of samples was dealing with hardened residuals. In future tests, we will attempt to separate and measure the residual volumes, but the residual oil is very viscous. Therefore, we will add a solvent, such as heptane, to reduce the oil viscosity and aid in the separation and measurement of the emulsion.

There are a number of experimental changes that would improve both the experiment and the applicability to real in situ burn processes. In future studies, one of the first observed differences between these type of studies and actual in situ burns is that the water underlying the crude has not been observed to boil. The authors have discussed this difference with a number of other investigators and with those that have actually used ISB in the spill remediation efforts. We can point out two principle differences between research studies and practical ISB. The first is that practical ISB does not exhibit oil-water boiling is the much larger convective cooling from the ocean water. The simplest methods to replicate the same cooling behavior may be to impinge the bottom of the slick with low velocity water jets or to create a similar flow past the underside of the test slick.

Another possible reason that research studies usually use relatively thin slicks, on the order of 10-20 mm, to conserve the test article and to provide enough oil or emulsion to ignite. The thinner slick allows much greater oil-water interface temperatures for the same heat transfer rates, if we assume Fourier's conductive heat transfer law [50]:

$$\dot{q}" = -k\,\frac{\Delta T}{\Delta x} \tag{4}$$

where q̇" is the heat flux to and through the oil surface from the flame, k is the thermal conductivity of the oil, ΔT is the temperature difference between the slick surface and the oil-water interface, and Δx is the slick thickness. Of course, evaporation in the slick would further increase the temperature difference and reduce the heat flux to the water. Anecdotally, a practical oil slick can be an order of magnitude thicker, which produces an order of magnitude increase in temperature difference and, if we assume constant proportionality, a much lower temperature at the oil-water interface – presumably below the boiling temperature of water. This can be replicated in ISB experiments by using much larger slick thicknesses.

We should note that we assumed that the edge of the ISB pan has little effect on the ignition behavior, in practice it probably has some influence on the overall burn behavior. If this experimental platform is modified, it would be prudent to place a 1 m^2 (1.13 m diameter) ring in the middle of much larger pan, with a 1 cm edge above the water surface. This would minimize edge effects on the stability and anchoring of the pool fire flames.

We also need to develop a method to gather and accurately measure the volume or mass of remaining oil for accurate ISB efficiency measurements. Cone calorimeters use load cells to measure mass loss, but since the mass of the burn pan, water, heat exchanger, and instruments were so much greater than that of the oil and accelerant, the mass of the residue will not be much greater than the uncertainty of the load cells used to measure the total mass. This is especially troublesome given the temperature sensitivity of most load cells. A volumetric measurement was complicated by the residue: it could be so viscid that it clung to the heat exchanger, tools, and vessels used to remove it from the surface, making accurate measurement impossible. A structural change to the burn pan that would allow the water level to be raised and the slick to be shunted in one direction to be emptied into a container could be a possible solution for the less viscid residues. The more viscid resides may need to be thinned with heptane to allow accurate volumetric and gravimetric measurements.

There were also problems with the temperature measurements. The thermocouples, though useful, can only reliably and accurately measure the water temperature 14 cm below the surface. The other thermocouples, because they were immersed in the liquid and oriented perpendicularly to the oil surface, could not provide an accurate measurement of the vapor plume temperature or of temperatures at the water-slick interface. A thermocouple rake suspended above the slick, in the burning vapor plume, would provide accurate plume measurements, as long as the plume remained stationary. At the water-slick interface, the thermocouple leads need to be oriented parallel with the water surface for some distance to ensure that there was no thermal leakage along the length of the thermocouple into the water.

Finally, the ISB experiments would be more repeatable if performed inside of an enclosure to prevent wind from blowing the plume from side to side. In the next year, there will be a building available to conduct these tests that will correct for this inconsistency.

In conclusion, this study has brought forward a number of fundamental questions about how crude oil and crude oil emulsion burn and how that behavior changes with crude oil chemistry. In particular, how emulsions behave during accelerant ignition, burning, and extinction would shed light on how we can

manipulate these processes to expand ignition envelopes, increase burning rates, and delay extinction. This requires a study of the fundamental thermochemistry of crude oil emulsions during combustion processes.

ACKNOWLEDGEMENT

This study was funded by the U.S. Department of the Interior, Bureau of Safety and Environmental Enforcement through Interagency Agreement E16PG00038 with the Naval Research Laboratory.

PERSONNEL

The Navy Technology Center for Safety and Survivability of the Naval Research Laboratory has an established history of successfully supporting the combustion and fire testing of the Navy's facilities and operations.

Dr. Steven Tuttle is a Mechanical Engineer and Section Head in the Combustion and Reacting Transport Section of the Navy Technology Center for Safety and Survivability (NTCSS) at the U.S. Naval Research Laboratory (NRL). Dr. Tuttle worked in the gas turbine industry for seven years while managing and conducting his doctoral research at the University of Connecticut. As an engineer, he developed and validated heat transfer, thermoacoustic, and spray combustion stability models for main burners, afterburners, and nozzles in the engine technology development and demonstration organizations. At the same time, he directed and managed funding to the University of Connecticut that supported his research and that of others. As a student, he designed and built an afterburner combustion experiment and the associated electronic fuel control and safety systems. Dr. Tuttle mentored undergraduates and led the team of MS and PhD students as they conducted experiments and measured the fuel distribution, flowfield, and combustion behavior. For his postdoctoral studies, he was the principle investigator for velocity measurements of a reacting scramjet cavity and shear layer at the U.S. Air Force Research Laboratory. He joined the staff at NRL in 2011, where he is the principle investigator of a Department of Interior-sponsored program examining combustion behavior of emulsified crude oil slicks and sprays. He also collaborates with other NRL investigators in projects ranging from novel fuels to fire characterization and instrumentation.

Mr. Christopher J. Pfützner is a Mechanical Engineer in the Combustion and Reacting Transport Section in the Navy Technology Center for Safety and Survivability (NTCSS) at the U.S. Naval Research Laboratory. Mr. Pfützner has worked in a technical capacity with an oil and gas blending company in Houston, Texas, in addition to working in the refrigeration and automotive industries since 2009. At Colorado School of Mines, he studied Mechanical Engineering, contributed to research involving heat transfer and oxidation in concentrated solar cells, and managed the school's battery-electric vehicle efforts throughout its lifecycle. He joined NRL in 2017 and serves in various design and test engineering roles in support of internal and external programs.

Dr. Thomas N. Loegel is a research chemist within the Chemical Sensing and Fuel Technology Section of the Chemistry Division at the Naval Research Laboratory. He is a recipient of the Jerome and Isabella Karle Fellowship and tasked to developed response factors among different gas chromatography and mass spectroscopy detectors to enhance modeling of fuel properties and to develop new multidimensional separation strategies for the analysis of complex mixtures. His areas of research include characterization petroleum and alternative fuels using a combination of gas chromatography and mass spectrometry. He has extensive experience with a wide variety of chromatography techniques and has worked with a variety of sample types ranging from heavy crude products to pharmaceuticals. Through the use of gas chromatography–mass spectrometry (GC-MS), liquid chromatography–mass spectrometry (LC-MS), and the powerful two dimensional GC time of flight (GCxGC TOF), Dr. Loegel has been able to improve and develop methods that probe the complicated make up of petroleum fuels. Dr. Loegel's Ph.D. dissertation

research focused on separations of glycoaminoglycans (heparin) by capillary electrophoresis (CE) and asphaltenes, a heavy fraction of crude oil, by high performance liquid chromatography (HPLC). While at Miami University, he initiated an asphaltene-based, Ph.D.-level research project and forged collaboration with the H. Kenttämaa group at Purdue University using high resolution MS.

Dr. Brian Fisher's research interests include engines, rocket propulsion, combustion, alternative fuels, and the application of laser-based and optical diagnostics in thermal sciences. After completing his Ph.D. at the University of Florida in 2004, he held a National Research Council post-doctoral appointment at the Naval Research Laboratory, followed by a post-doctoral appointment in the Combustion Research Facility at Sandia National Laboratory. Dr. Fisher was an associate professor in the Department of Mechanical Engineering at The University of Alabama for three years (2011-2014) before joining the Combustion & Reacting Transport Section (Code 6185) at the Naval Research Laboratory as a full-time scientist/engineer in 2015. His research focuses on characterization of multiphase reacting flows, namely spray and solid-fuel combustion, with particular emphasis on understanding fundamental chemical and physical behaviors relevant to practical combustion systems. Dr. Fisher's current efforts include basic research programs on metal particle and composite solid fuel combustion mechanisms, and an applied research program on petroleum wellhead fires.

Ms. Iwona Anna Leska graduated in 1995 Summa Cum Laude with a Master of Science degree in Chemistry from the Warsaw University, Warsaw, Poland, followed by work as a Senior Staff Scientist in Department of Basic and Applied Pharmacy at National Institute of Public Health in Warsaw where she was developing analytical methods of drug testing for regulatory approval. In 2009 she joined Nova Research Inc., currently holding position as a Staff Scientist II and a member of the Fuel Team at the Naval Research Laboratory in Washington, DC. Her expertise includes analytical method development for fuel composition determination as well as detection and characterization of strategically important trace constituents of fuels. She is also involved in research of compositional changes associated with thermal degradation of aviation and diesel fuels during long-term storage. Previously she worked at the Center for Bio/Molecular Science and Engineering, also at NRL where she was involved in developing of self-decontaminating materials, including synthesis, characterization, and validation of multifunctional porous porphyrin-based organosilica compounds.

Ms. Katherine M. Hinnant has been actively involved in research at NRL since 2014. She received her Bachelor's degree in Chemical Engineering from the University of Virginia and is pursuing her Ph.D. in Physical Chemistry at George Washington University. Ms. Hinnant provides liquid characterization measurements for crude oils by measuring viscosity, surface tension, and refractive index. She is the experimental lead for military firefighting foam testing where she conducts liquid property measurements and is able to use the same techniques for analyzing crude oils. She has a background in developing a range of experimental platforms that include fuel sulphur characterization, lithium battery fire testing, and crude oil weathering methods that use a wide range of chemical and optical measurement methods.

REFERENCES

[1] Buist, I. A., McCourt, J., Potter, S., Ross, S., and Trudel, K., "In Situ Burning," *Pure and Applied Chemistry* Vol. 71, No. 1, 1999, pp. 43–65. doi: 10.1351/pac199971010043

[2] Fingas, M. F., Fingas, M. F. (ed.) *Oil Spill Science and Technology*, Evaporation Modeling, Elsevier Science, Burlington, Massachusetts, 2010, pp. 202-242.

[3] Fingas, M. F., Fingas, M. F. (ed.) *Oil Spill Science and Technology*, Photo-oxidation, Elsevier Science, Burlington, MA, 2010, p. 192.

[4] Garrett, R. M., Pickering, I. J., Haith, C. E., and Prince, R. C., "Photooxidation of Crude Oils," *Environmental Science & Technology* Vol. 32, No. 23, 1998, pp. 3719-3723. doi: 10.1021/es980201r

[5] Yakimov, M. M., Timmis, K. N., and Golyshin, P. N., "Obligate oil-degrading marine bacteria," *Current Opinion in Biotechnology* Vol. 18, No. 3, 2007, pp. 257-266. doi: https://doi.org/10.1016/j.copbio.2007.04.006

[6] Hassanshahian, M., Emtiazi, G., and Cappello, S., "Isolation and characterization of crude-oil-degrading bacteria from the Persian Gulf and the Caspian Sea," *Marine Pollution Bulletin* Vol. 64, No. 1, 2012, pp. 7-12. doi: https://doi.org/10.1016/j.marpolbul.2011.11.006

[7] McFarlin, K. M., Prince, R. C., Perkins, R., and Leigh, M. B., "Biodegradation of Dispersed Oil in Arctic Seawater at -1°C," *PLOS ONE* Vol. 9, No. 1, 2014, p. e84297. doi: 10.1371/journal.pone.0084297

[8] Atlas, R. M., "Petroleum biodegradation and oil spill bioremediation," *Marine Pollution Bulletin* Vol. 31, No. 4, 1995, pp. 178-182. doi: https://doi.org/10.1016/0025-326X(95)00113-2

[9] Atlas, R. M. and Hazen, T. C., "Oil Biodegradation and Bioremediation: A Tale of the Two Worst Spills in U.S. History," *Environmental Science & Technology* Vol. 45, No. 16, 2011, pp. 6709-6715. doi: 10.1021/es2013227

[10] Head, I. M., Jones, D. M., and Röling, W. F. M., "Marine microorganisms make a meal of oil," *Nature Reviews Microbiology* Vol. 4, 2006, p. 173. doi: 10.1038/nrmicro1348

[11] Fingas, M. F., Fingas, M. F. (ed.) *Oil Spill Science and Technology*, Models for Water-in-Oil Emulsion Formation, Elsevier Science, Burlington, Massachusetts, 2010, pp. 243-273.

[12] McCourt, J. and Buist, I., "Laboratory Testing to Determine Operational Parameters for In Situ Burning of Six U.S. Outer Continental Shelf Crude Oils," United States Department of the Interior. Herndon, Virginia, March 1998.

[13] McCourt, J., Buist, I., and Buffington, S., "Results of Laboratory Test on the Potential for using In Situ Burning on Seventeen Crude Oils," *23rd Arctic and Marine Oilspill Program (AMOP) Technical Seminar*, Environment Canada, 1999.

[14] McCourt, J., Buist, I., and Mullin, J. V., "Operational Parameters for In Situ Burning of Six U.S. Outer Continental Shelf Crude Oils," *International Oil Spill Conference Proceedings*, 1999.

[15] McCourt, J., Buist, I., and Buffington, S., "Results of Laboratory Tests on the Potential for Using In Situ Burning on 17 Crude Oils," *International Oil Spill Conference Proceedings*, 2001.

[16] Zagorski, W. and Mackay, D., "Water in Oil Emulsions: a Stability Hypothesis," *5th Arctic and Marine Oil Spill Program Technical Seminar*, Environment Canada, 1982.

[17] Jokuty, P. L., Whiticar, S., Wang, Z., Fieldhouse, B., and Fingas, M. F., "A Catalogue of Crude Oil and Oil Product Properties for the Pacific Region," Environment Canada. Ottawa, ON, 1999.

[18] Buist, I. A., Potter, S. G., Trudel, B. K., Shelnutt, S. R., Walker, A. H., Scholz, D. K., Brandvik, P. J., Fritt-Rasmussen, J., Allen, A. A., and Smith, P., "In Situ Burning in Ice-Affected Waters: State of Knowledge Report," Arctic Response Technology, Final Report 7.1.1.

[19] Garo, J. P., Vantelon, J. P., Gandhi, S., and Torero, J. L., "Determination of the Thermal Efficiency of Pre-boilover Burning of a Slick of Oil on Water," *Spill Science & Technology Bulletin* Vol. 5, No. 2, 1999, pp. 141-151.
doi: 10.1016/S1353-2561(98)00049-8

[20] Tuttle, S. G., Fisher, B. T., Pfützner, C. J., Loegel, T. N., and Hinnant, K. M., "In Situ Burn Ignition Testing Methods and Results for California Crude Oils,"*Spring Technical Meeting of the Eastern States Section of the Combustion Institute*, 2B04, 6-8 March 2018.

[21] ASTM D1141-13, "Standard Practice for the Preparation of Substitute Ocean Water", ASTM International, West Conshohocken, PA, 2013.

[22] NOAA. "National Data Buoy Center." 2017.
http://www.ndbc.noaa.gov/

[23] Tuttle, S. G., Loegel, T. N., Hinnant, K. M., Tuesta, A. D., and Fisher, B. T., "Fundamental Measurements of Crude Oil Spray Behavior," *40th Arctic and Marine Oil Spill Program (AMOP) Technical Seminar*, Environmental Canada, 2017.

[24] Tuttle, S. G., Hinnant, K. M., Loegel, T. N., Fisher, B. T., Tuesta, A. D., and Weismiller, M. R., "Development of a Low-Emission Spray Combustor for Emulsified Crude Oil," Naval Research Laboratory, NRL/MR/6185-17-9720. Washington, DC, March 2017.

[25] Hollebone, B., Fingas, M. F. (ed.) *Oil Spill Science and Technology*, Measurementof Oil Physical Properties, Elsevier Science, Burlington, Massachusetts, 2010, pp. 63-86.

[26] NOAA. "Overview of Automated Data Inquiry for Oil Spills (ADIOS)." NOAA, 2016.
http://response.restoration.noaa.gov/oil-and-chemical-spills/oil-spills/response-tools/adios.html

[27] ASTM E1321-13, "Test Method for Determining Material Ignition and Flame Spread Properties", ASTM International, West Conshohocken, PA, 2013.

[28] ASTM E1354-17, "Test Method for Heat and Visible Smoke Release Rates for Materials and Products Using an Oxygen Consumption Calorimeter", ASTM International, West Conshohocken, PA, 2017.

[29] Arai, M., Saito, K., and Altenkirch, R. A., "A Study of Boilover in Liquid Pool Fires Supported on Water Part I: Effects of a Water Sublayer on Pool Fires," *Combustion Science and Technology* Vol. 71, No. 1-3, 1990, pp. 25-40.
doi: 10.1080/00102209008951622

[30] Koseki, H., Kokkala, M. A., and Mulholland, G. W., "Experimental Study Of Boilover In Crude Oil Fires," *Fire Safety Science* Vol. 3, No. 1, 1991, pp. 865-874.
doi: doi:10.3801/IAFSS.FSS.3-865

[31] Ping, P., Zhang, J., Kong, D., Xu, Z., and Yang, H., "Experimental study of the flame geometrical characteristics of the crude oil boilover fire under cross air flow," *Journal of Loss Prevention in the Process Industries*, 2017.
doi: https://doi.org/10.1016/j.jlp.2017.12.005

[32] Garo, J. P., Vantelon, J. P., and Fernandez-Pello, A. C., "Boilover burning of oil spilled on water," *Symposium (International) on Combustion* Vol. 25, No. 1, 1994, pp. 1481-1488.
doi: https://doi.org/10.1016/S0082-0784(06)80792-7

[33] Van Gelderen, L., Brogaard, N. L., Sørensen, M. X., Fritt-Rasmussen, J., Rangwala, A. S., and Jomaas, G., "Importance of the Slick Thickness for Effective In-Situ Burning of Crude Oil," *Fire Safety Journal* Vol. 78, 2015, pp. 1-9.
doi: http://dx.doi.org/10.1016/j.firesaf.2015.07.005

[34] Van Gelderen, L. *In-situ* burning of crude oil on water: A study on the fire dynamics and fire chemistry in an Arctic context [Ph.D. Thesis]. Department of Civil Engineering, Technical University of Denmark, Kgs. Lyngby, 2017.
[35] Van Gelderen, L., Malmquist, L. M. V., and Jomaas, G., "Vaporization order and burning efficiency of crude oils during in-situ burning on water," *Fuel* Vol. 191, 2017, pp. 528-537. doi: http://dx.doi.org/10.1016/j.fuel.2016.11.109
[36] Muhammad, I., Tijjani, N., Dioha, I. J., Musa, A., Sale, H., and Lawal, A. M., "SARA Separation and Determination of Concentration Levels of Some Heavy Metals in Organic Fractions of Nigerian Crude Oil," *Chemistry and Materials Research* Vol. 3, No. 4, 2013, pp. 7-14.
[37] Kök, M. V., Karacan, Ö., and Pamir, R., "Kinetic Analysis of Oxidation Behavior of Crude Oil SARA Constituents," *Energy & Fuels* Vol. 12, No. 3, 1998, pp. 580-588. doi: 10.1021/ef970173i
[38] Ambalae, A., Mahinpey, N., and Freitag, N., "Thermogravimetric Studies on Pyrolysis and Combustion Behavior of a Heavy Oil and Its Asphaltenes," *Energy & Fuels* Vol. 20, No. 2, 2006, pp. 560-565. doi: 10.1021/ef0502812
[39] Mahinpey, N., Murugan, P., and Mani, T., "Comparative Kinetics and Thermal Behavior: The Study of Crude Oils Derived from Fosterton and Neilburg Fields of Saskatchewan," *Energy & Fuels* Vol. 24, No. 3, 2010, pp. 1640-1645. doi: 10.1021/ef901470j
[40] Sjöblom, J., Hemmingsen, P. V., and Kallevik, H., Mullins, O. C., Sheu, E. Y., Hammami, A., and Marshall, A. G. (eds.), *Asphaltenes, Heavy Oils, and Petroleomics*, The Role of Asphaltenes in Stabilizing Water-in-Crude Oil Emulsions, Springer New York, New York, NY, 2007, pp. 549-587.
[41] Berridge, S. A., Dean, R. A., Fallows, R. G., and Fish, A., "The Properties of Persistent Oils at Sea," *Journal of the Institute of Petroleum* Vol. 54, 1968, pp. 300-309.
[42] Speight, J. G. and Pancirov, R. J., "STRUCTURAL TYPES IN PETROLEUM ASPHALTENES AS DEDUCED FROM PYROLYSIS/GAS CHROMATOGRAPHY/MASS SPECTROMETRY," *Liquid Fuels Technology* Vol. 2, No. 3, 1984, pp. 287-305. doi: 10.1080/07377268408915354
[43] Wang, Z. and Fingas, M., "Study of the effects of weathering on the chemical composition of a light crude oil using GC/MS GC/FID," *Journal of Microcolumn Separations* Vol. 7, No. 6, 1995, pp. 617-639. doi: doi:10.1002/mcs.1220070609
[44] Sørheim, K. R., "Physical and Chemical Analyses of Crude and Refined Oils: Laboratory and Mesoscale Oil Weathering." SINTEF, Anchorage, AK, 2016.
[45] USEPA. "Understanding Oil Spills And Oil Spill Response," U.S. Environmental Protection Agency, EPA 540-K-99-007.
[46] Mishra, A. K. and Kumar, G. S., "Weathering of Oil Spill: Modeling and Analysis," *Aquatic Procedia* Vol. 4, 2015, pp. 435-442. doi: https://doi.org/10.1016/j.aqpro.2015.02.058

[47] Mayo, F. R. and Lan, B. Y., "Gum and deposit formation from jet turbine and diesel fuels at 100.degree.C," *Industrial & Engineering Chemistry Research* Vol. 26, No. 2, 1987, pp. 215-220.
doi: 10.1021/ie00062a008

[48] Hazlett, R. N., *Thermal Oxidation Stability of Aviation Turbine Fuels*, Chemical Aspects of Thermal Stability, ASTM, Philadelphia, 1991, pp. 72-94.

[49] Balster, W. J. and Jones, E. G., "Effects of Temperature on Formation of Insolubles in Aviation Fuels," *Journal of Engineering for Gas Turbines and Power* Vol. 120, No. 2, 1998, pp. 289-293.
doi: 10.1115/1.2818119

[50] Incropera, F. P. and DeWitt, D. P., *Fundamentals of heat and mass transfer*, 4th ed., One-Dimensional, Steady-State Conduction, Wiley, New York, 1996, pp. 73-160.

Appendix A

Comparison between Cone Calorimetry and ISB Pan Residuals

The following plots are provided for reference and will not be described or discussed. These plots show the residual mass spectra from similar oils and test conditions from both cone calorimetry and ISB burn pan experiments. Some appear remarkably similar, while others will appear very distinct.

Fresh

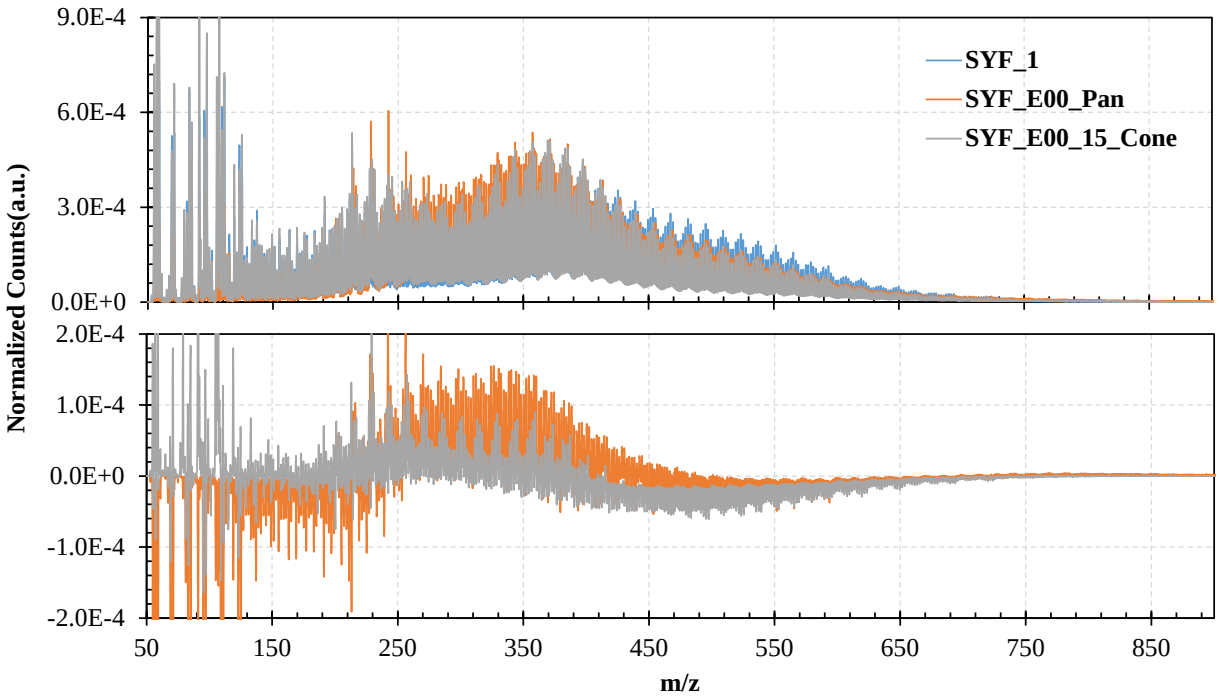

Fig. 49-Comparative MS plots of residues from cone calorimetry and ISB residues from fresh Santa Ynez.

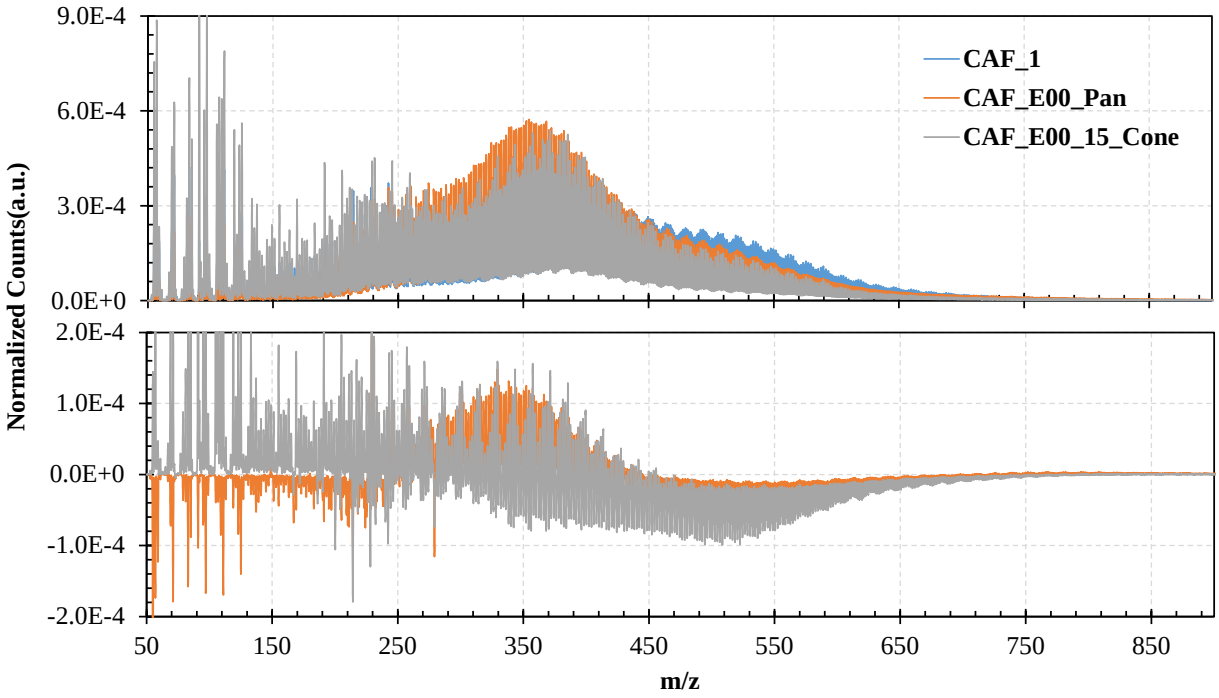

Fig. 50-Comparative MS plots of residues from cone calorimetry and ISB residues from fresh Carpinteria.

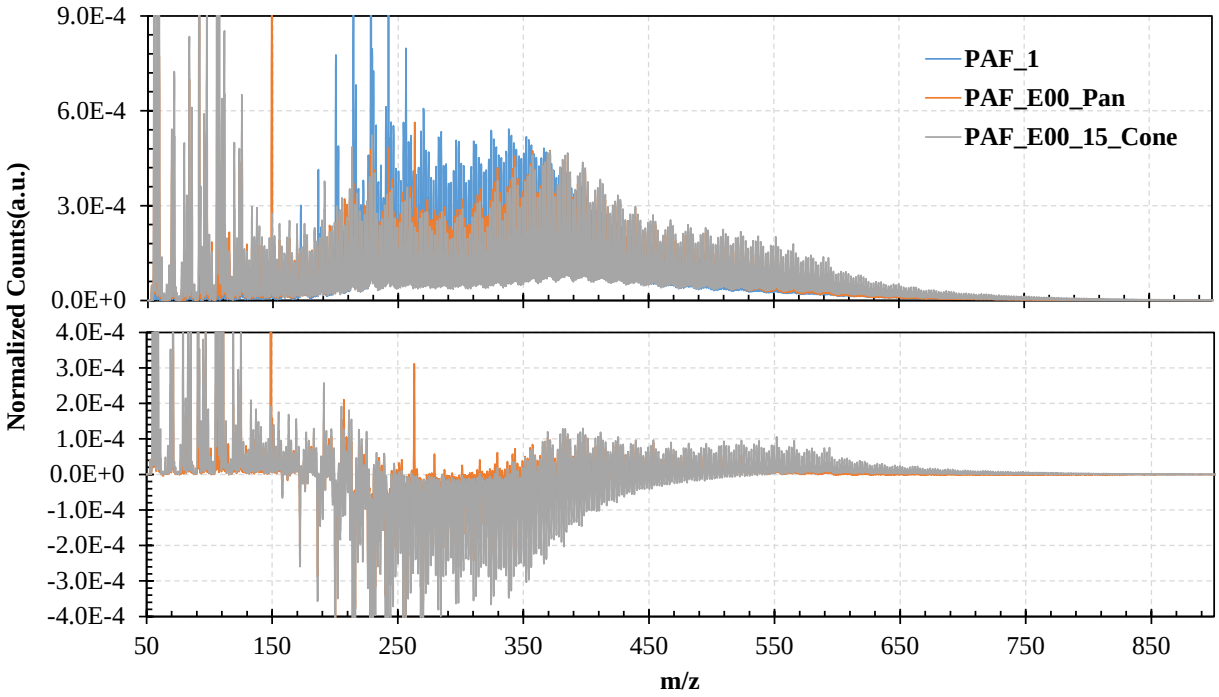

Fig. 51-Comparative MS plots of residues from cone calorimetry and ISB residues from fresh Point Arguello.

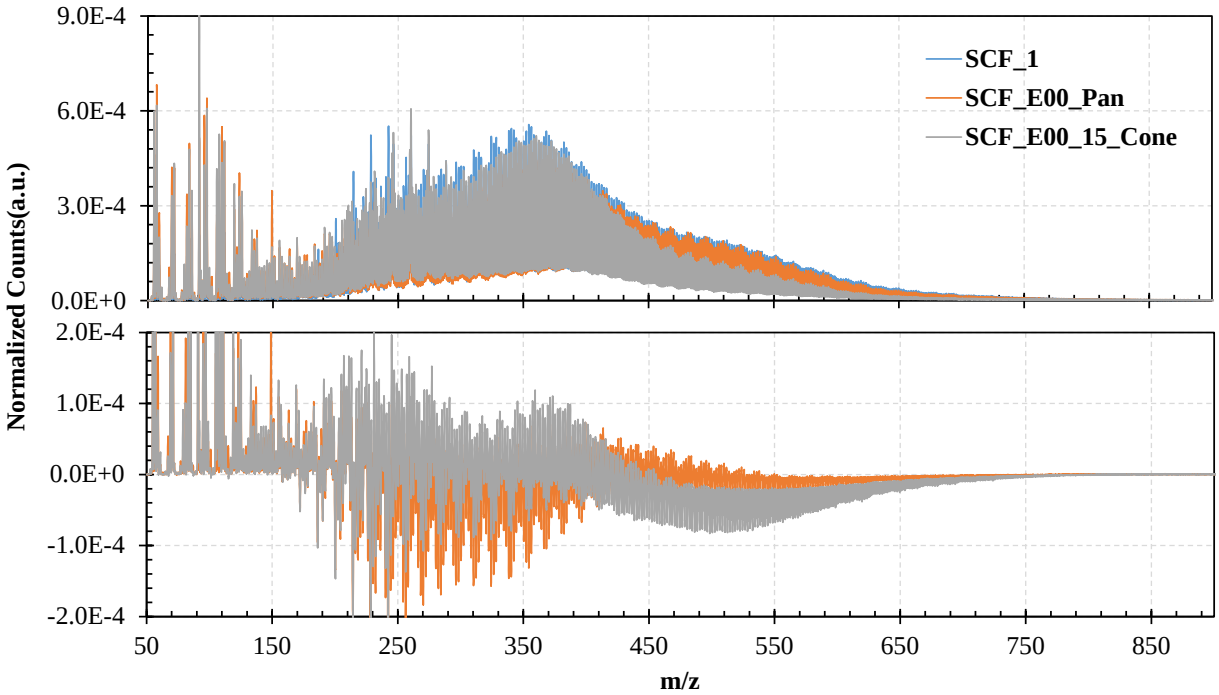

Fig. 52-Comparative MS plots of residues from cone calorimetry and ISB residues from fresh Santa Clara.

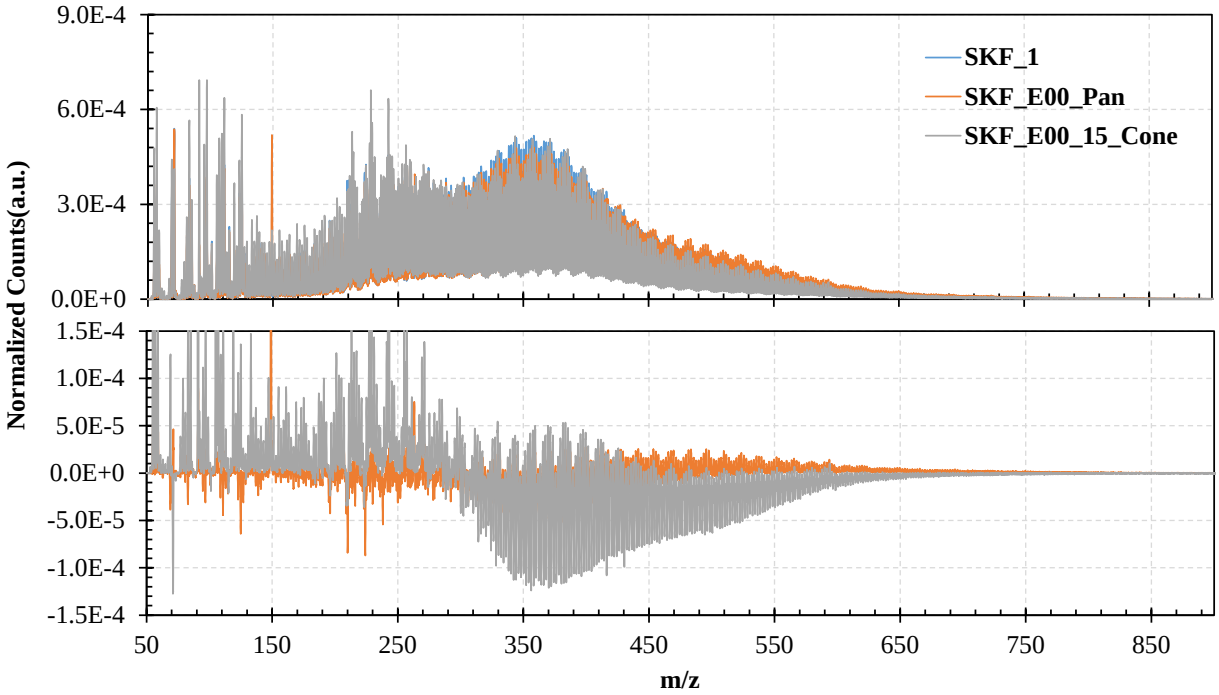

Fig. 53-Comparative MS plots of residues from cone calorimetry and ISB residues from fresh Sockeye.

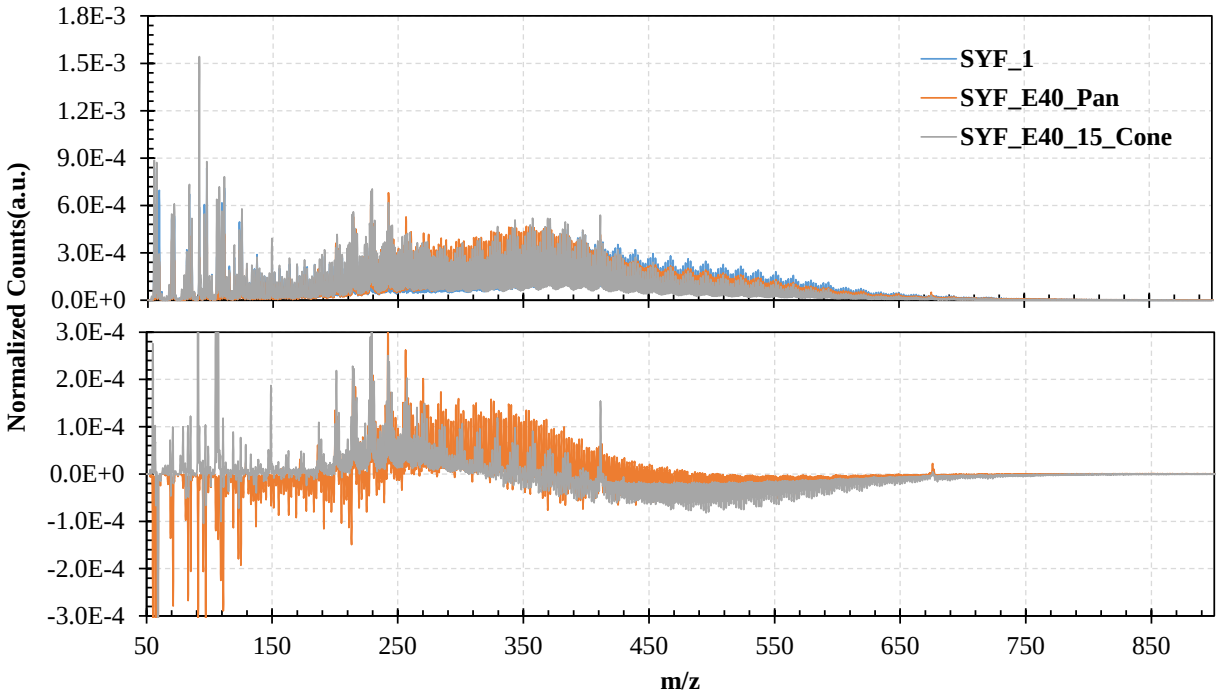

Fig. 54-Comparative MS plots of fresh and ISB residues from emulsions of Santa Ynez.

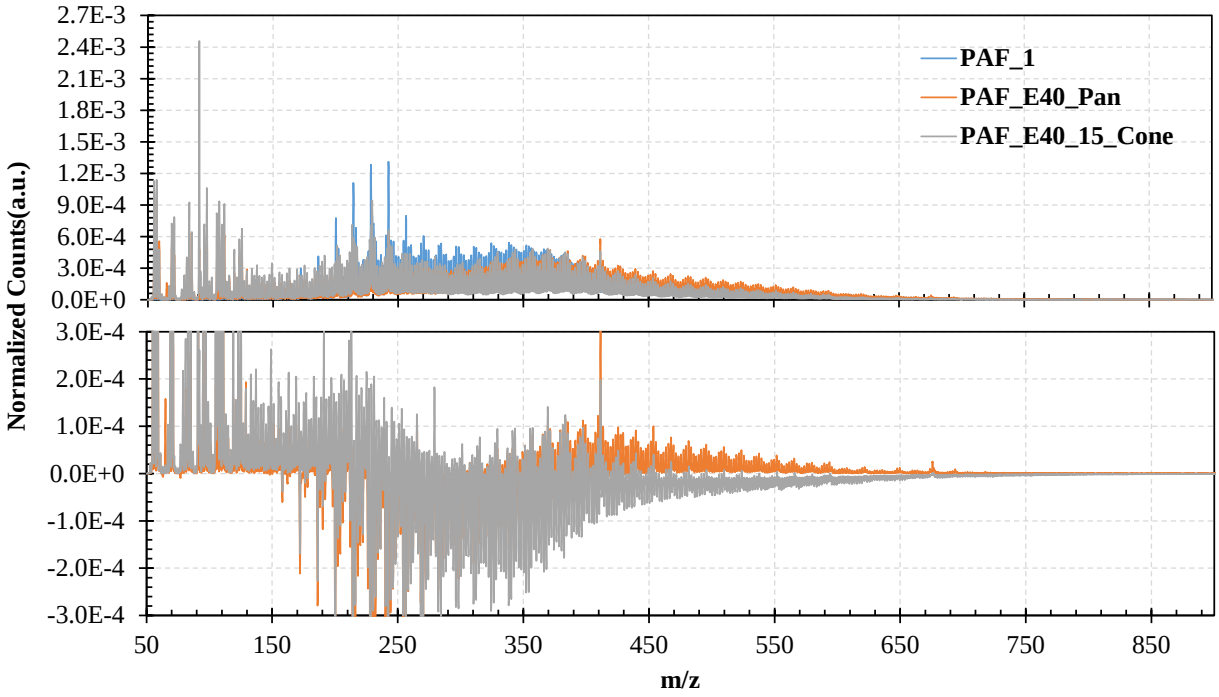

Fig. 55-Comparative MS plots of fresh and ISB residues from emulsions of Point Arguello.

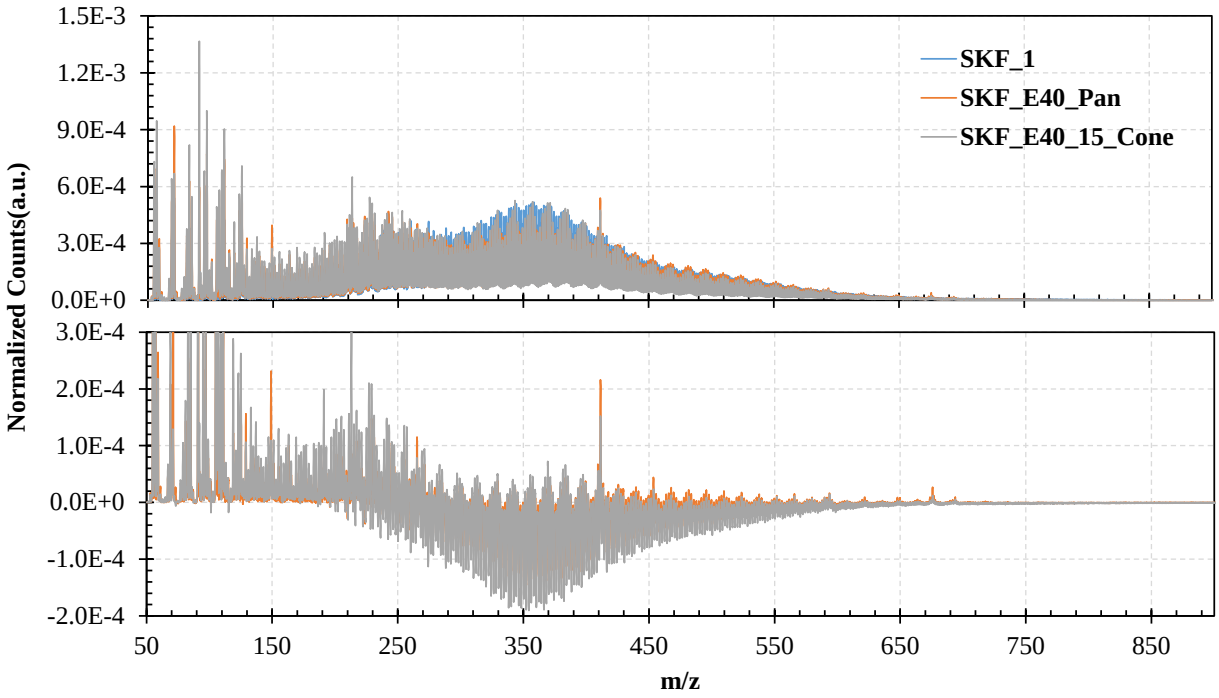

Fig. 56-Comparative MS plots of fresh and ISB residues from emulsions of Sockeye.

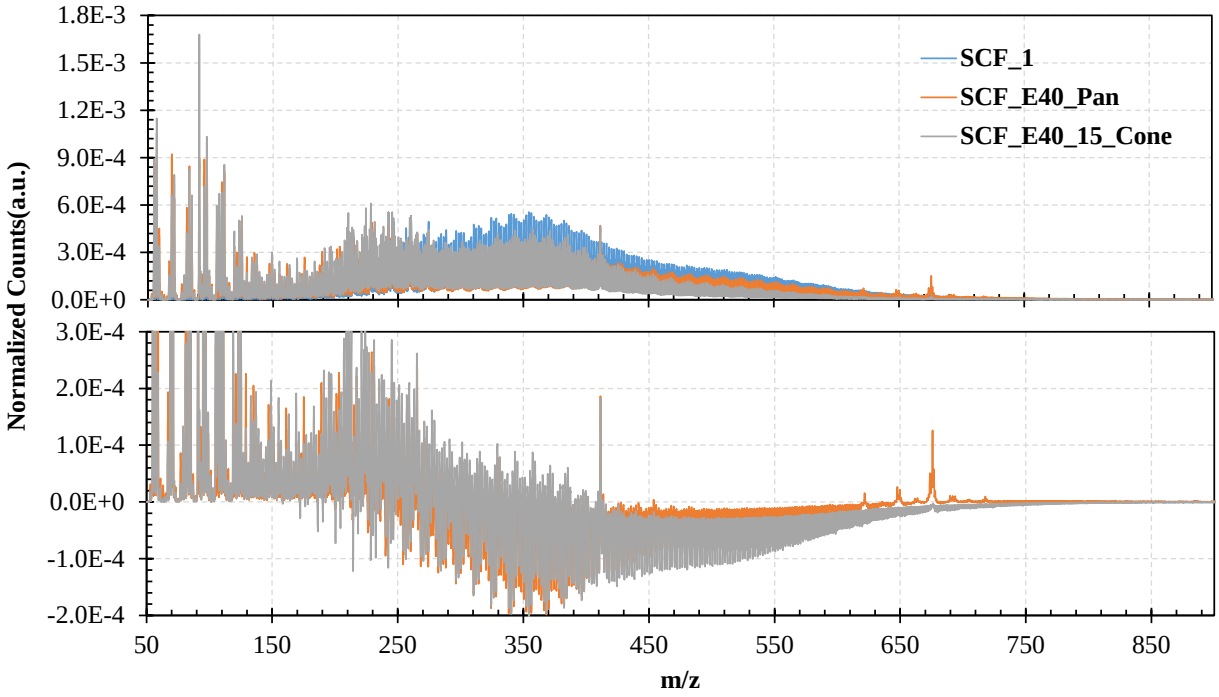

Fig. 57-Comparative MS plots of fresh and ISB residues from emulsions of Santa Clara.

Weathered

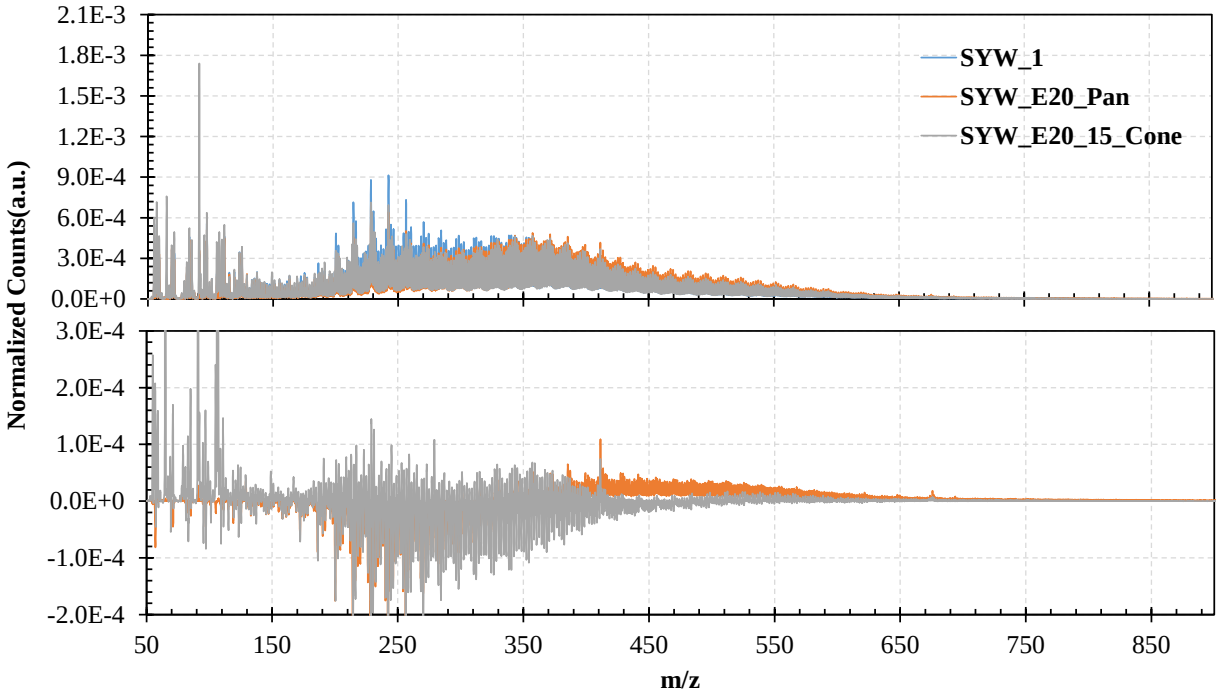

Fig. 58-Comparative MS plots of weathered and ISB residues from 20% emulsions of Santa Ynez.

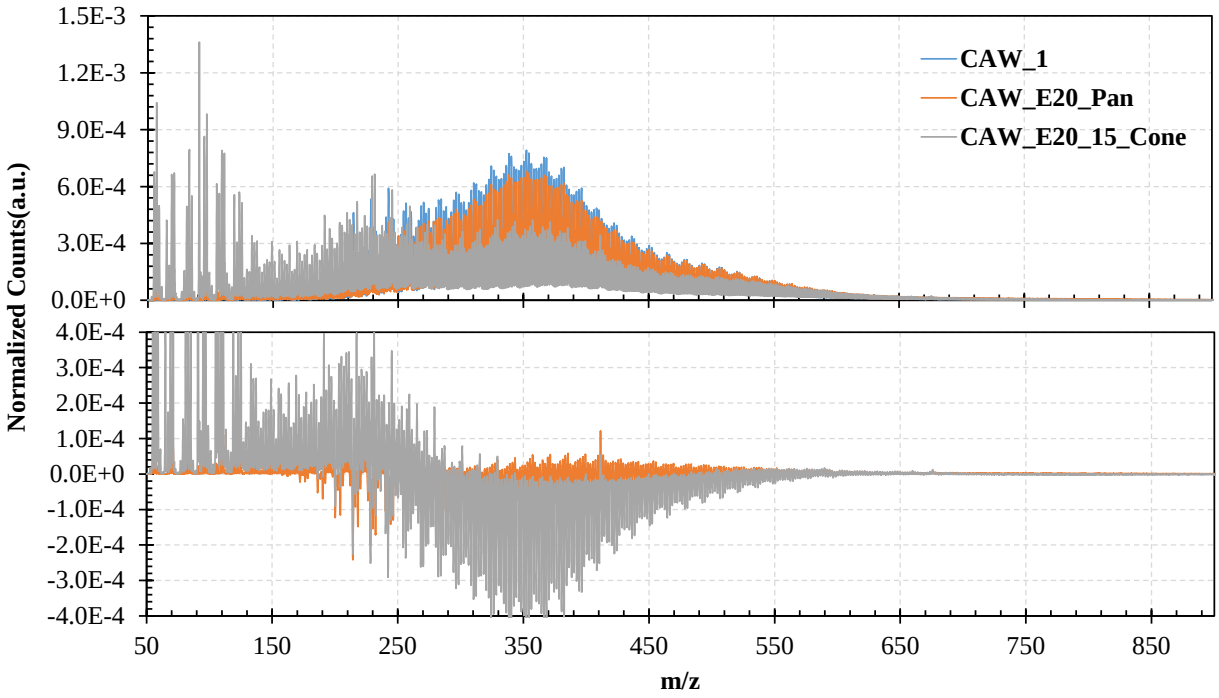

Fig. 59-Comparative MS plots of weathered and ISB residues from 20% emulsions of Carpinteria.

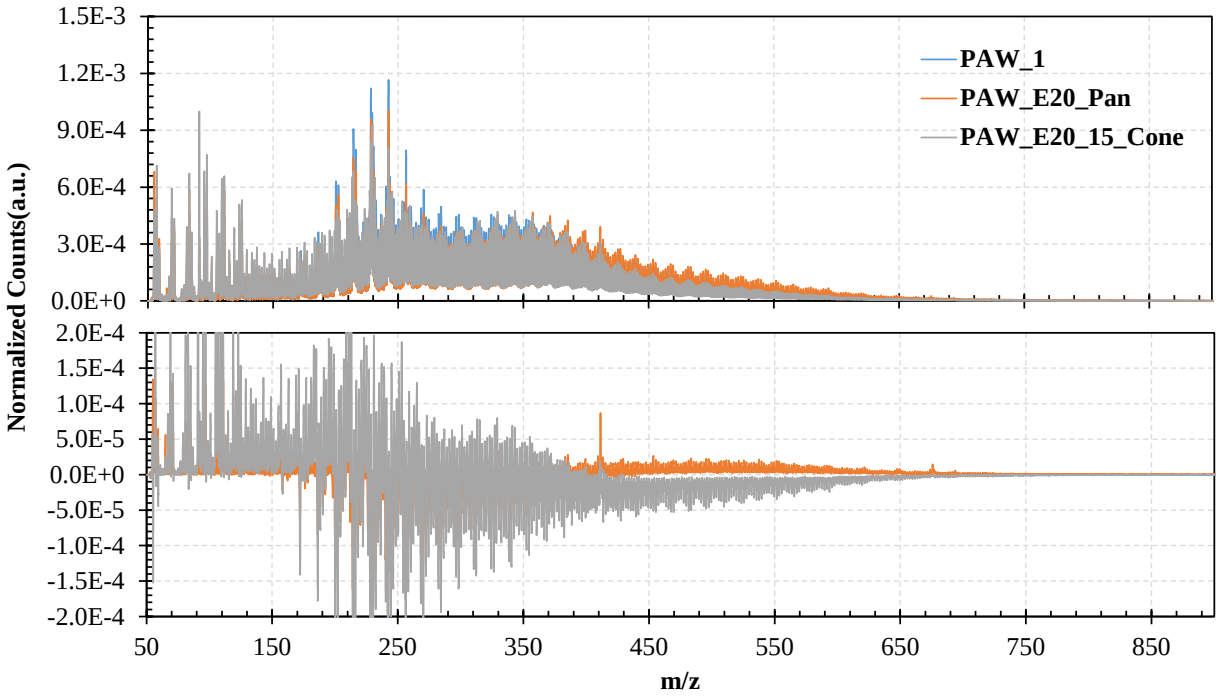

Fig. 60-Comparative MS plots of weathered and ISB residues from 20% emulsions of Point Arguello.

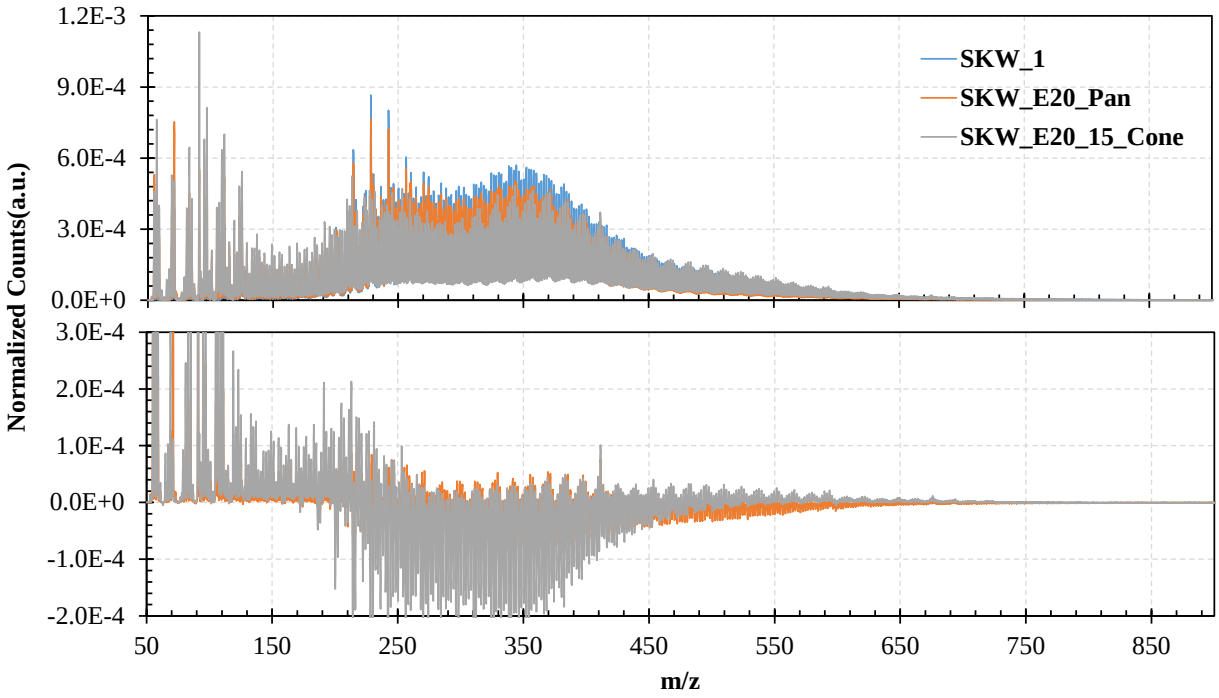

Fig. 61-Comparative MS plots of weathered and ISB residues from 20% emulsions of Sockeye.

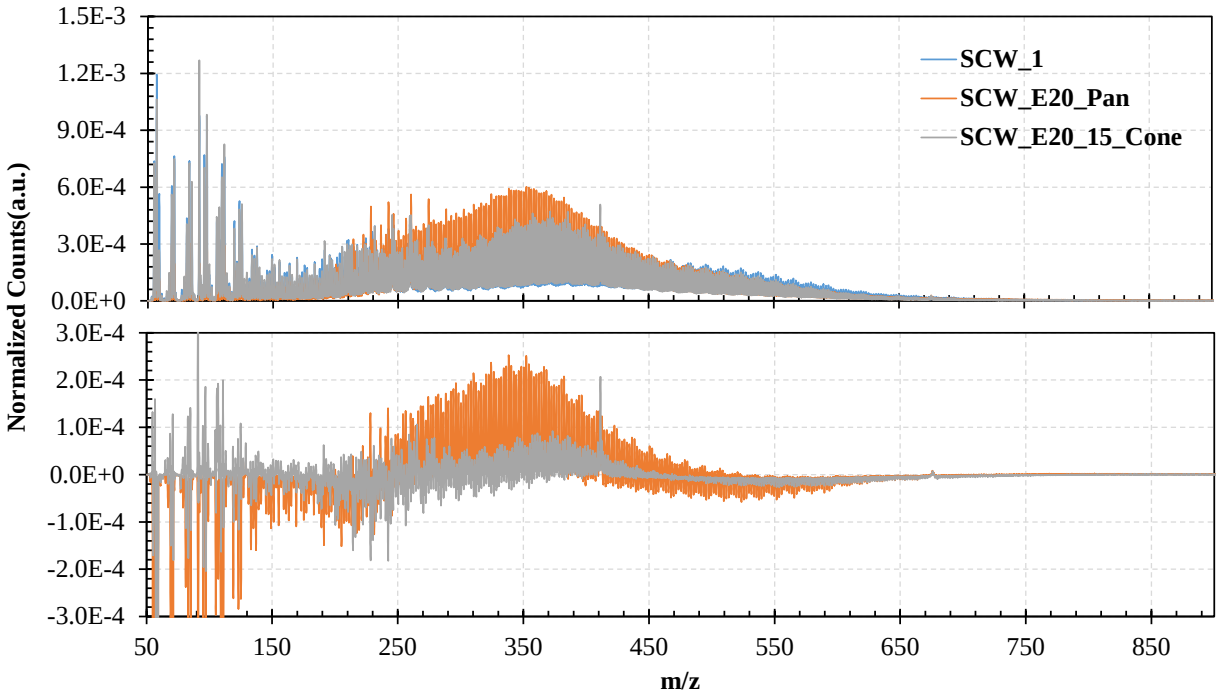

Fig. 62-Comparative MS plots of weathered and ISB residues from 20% emulsions of Santa Clara.

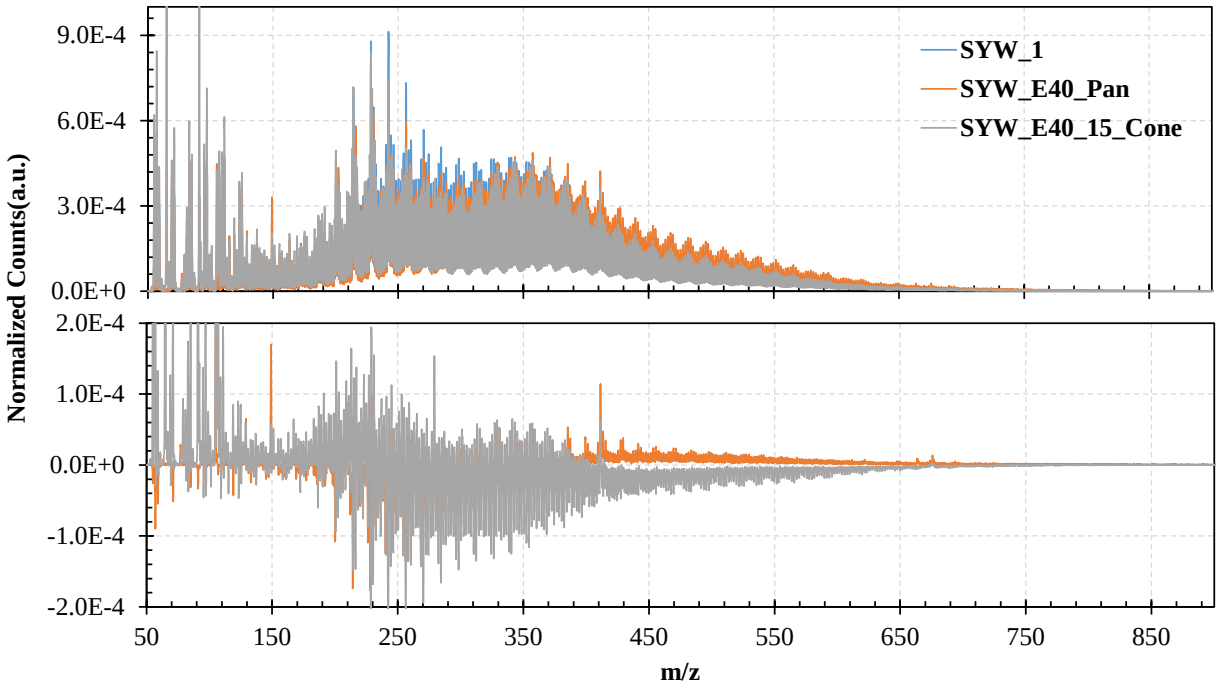

Fig. 63-Comparative MS plots of weathered and ISB residues from 40% emulsions of Santa Ynez.

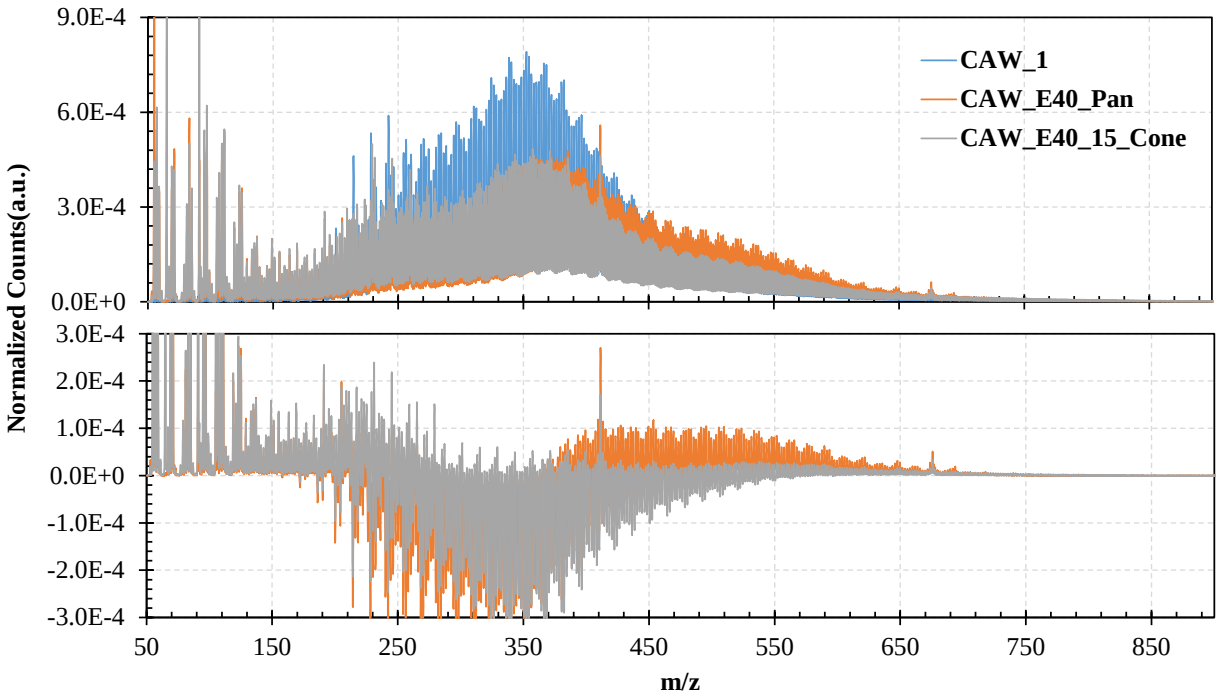

Fig. 64-Comparative MS plots of weathered and ISB residues from 40% emulsions of Carpinteria.

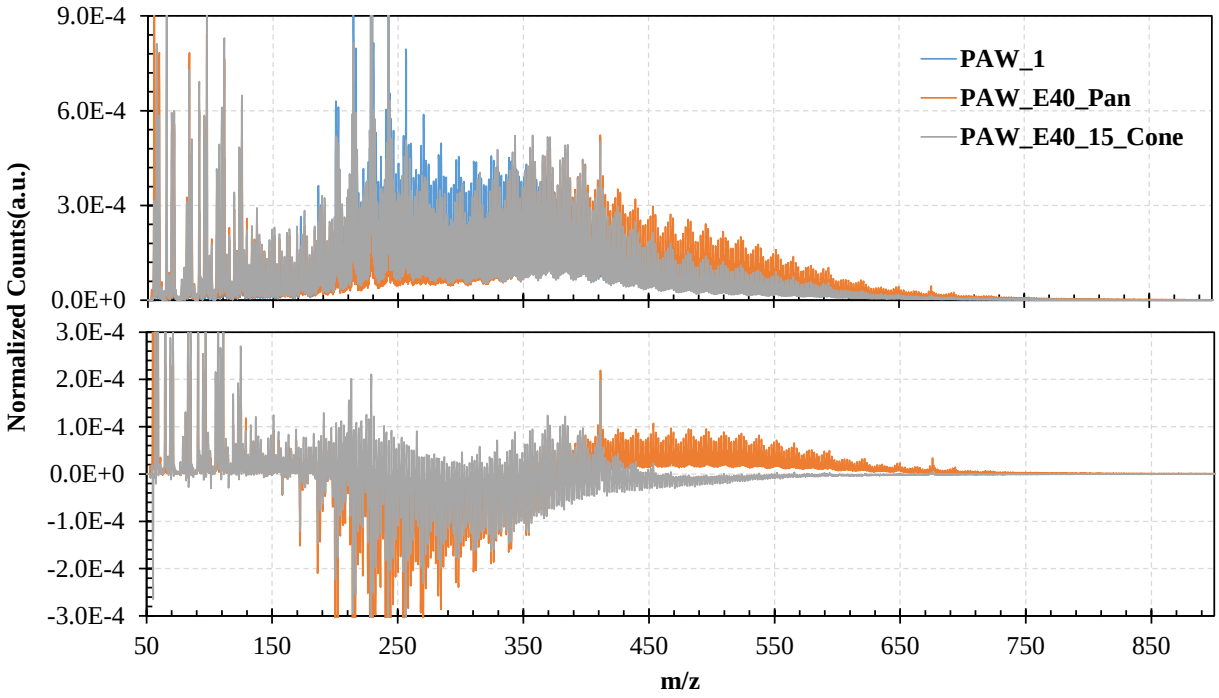

Fig. 65-Comparative MS plots of weathered and ISB residues from 40% emulsions of Point Arguello.

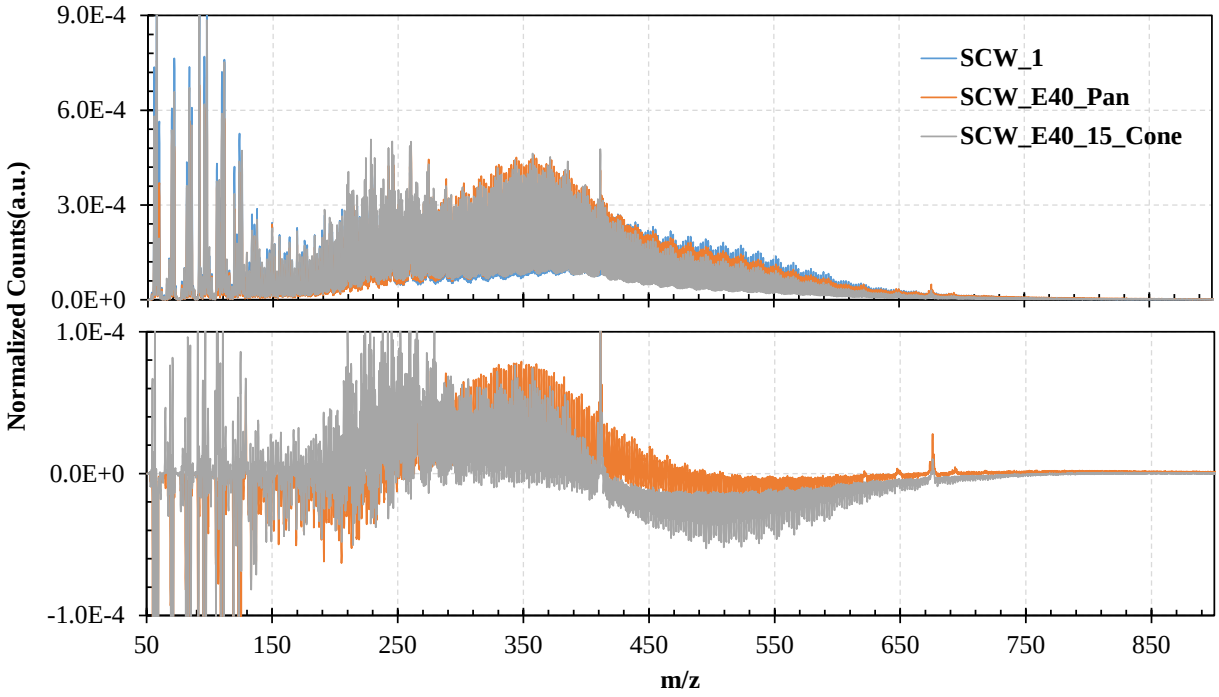

Fig. 66-Comparative MS plots of weathered and ISB residues from 40% emulsions of Saint Clara.

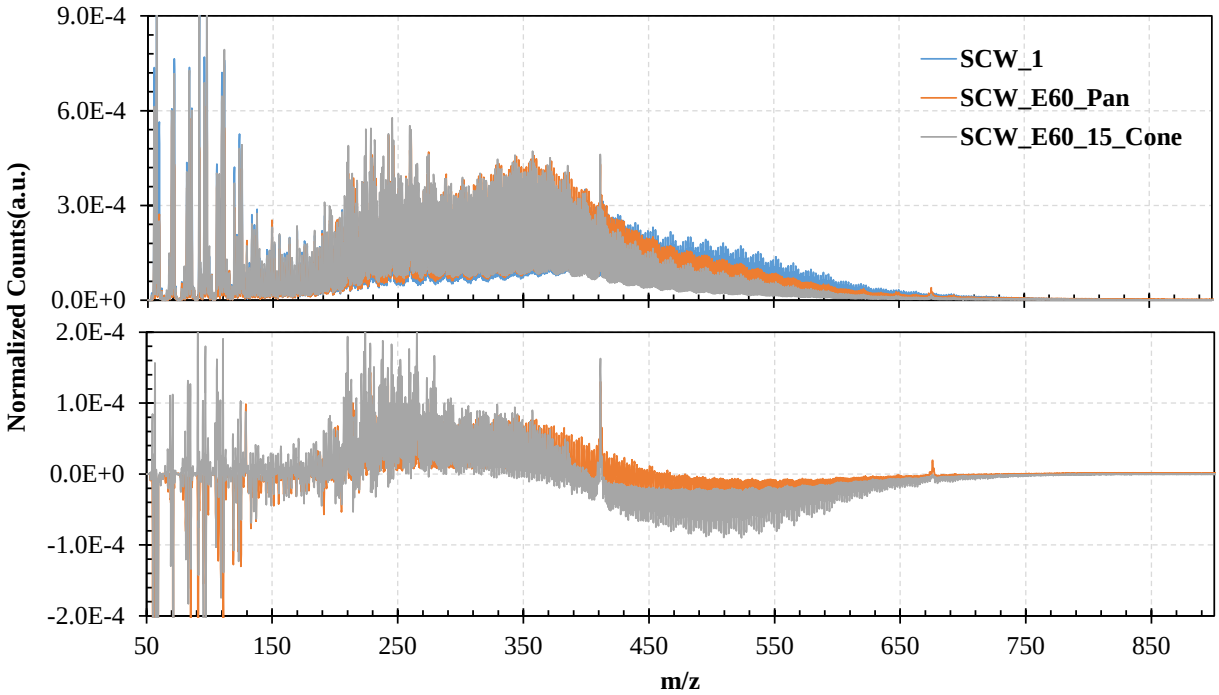

Fig. 67-Comparative MS plots of weathered and ISB residues from 60% emulsions of Santa Clara.